NASA TECHNICAL NOTE

NASA TN D-2697

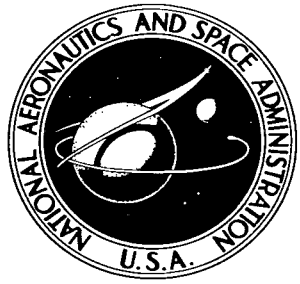

APPLICATION OF STATISTICAL FILTER THEORY TO THE INTERPLANETARY NAVIGATION AND GUIDANCE PROBLEM

by John S. White, George P. Callas, and Luigi S. Cicolani

Ames Research Center
Moffett Field, Calif.

NATIONAL AERONAUTICS AND SPACE ADMINISTRATION • WASHINGTON, D. C. • MARCH 1965

APPLICATION OF STATISTICAL FILTER THEORY TO THE INTERPLANETARY NAVIGATION AND GUIDANCE PROBLEM

By John S. White, George P. Callas,
and Luigi S. Cicolani

Ames Research Center
Moffett Field, Calif.

NATIONAL AERONAUTICS AND SPACE ADMINISTRATION

For sale by the Office of Technical Services, Department of Commerce,
Washington, D.C. 20230 -- Price $3.00

TABLE OF CONTENTS

APPLICATION OF STATISTICAL FILTER THEORY TO THE INTERPLANETARY NAVIGATION AND GUIDANCE PROBLEM

By John S. White, George P. Callas, and Luigi S. Cicolani

Ames Research Center
Moffett Field, Calif.

SUMMARY

This paper presents the results of a study wherein the Kalman filtering technique is applied to Interplanetary Navigation and Guidance. The study considers the number, type, and timing of observations to be made, and the number and timing of velocity corrections. Both fixed time-of-arrival guidance and a periapse-control guidance are considered. The results are presented principally in terms of uncertainty on arrival, miss on arrival, and magnitude of velocity increments required.

It is shown that the observations can be restricted to sextant measurements of the target planet, the launch planet, and the moon (when in the vicinity of the earth), and that daily observations are desirable during the major portion of the flight, with a much more frequent observation schedule at each end. Four velocity corrections should be made which, with a periapse-control guidance law, use a total of 30 m/sec velocity increment for each leg of the mission, resulting in a miss in the radius of periapse of 4 to 5 km.

INTRODUCTION

Preliminary analyses of manned interplanetary missions (e.g., refs. 1 and 2) show that some sort of midcourse navigation and guidance must be considered. It is assumed that this navigation and guidance scheme should probably be self-contained aboard the vehicle, both in terms of data taking and computing, and will provide an estimate of the accuracy in arriving at the target planets, and the amount of midcourse corrective fuel required.

By interplanetary navigation and guidance we mean the process of measuring the space vehicle trajectory and exercising control so as to arrive at the target planet with certain acceptable end conditions. In general, one would like to optimize this process in the sense of selecting the most economical measurement scheme and control policy which will satisfy the end condition requirements.

However, in this paper actual optimization is not attempted because of the great complexity of the problem. Instead, we take the somewhat pragmatic and empirical approach of specifying what seems to be a "good" system with a number of free parameters associated with the observation and correction schedule, and then adjust the parameters until we obtain what seems to be satisfactory performance. In this way we determine the requirements of an on-board guidance scheme and the amount of midcourse fuel required.

To expedite this procedure we divide the problem into its two natural parts, namely, trajectory determination and control. In the first part Kalman filter theory is used as a basis for estimating the trajectory, and in the second part impulsive velocity corrections are assumed which are computed using control laws which will correct estimated end conditions to correspond to those desired.

This same general approach was used in the lunar guidance work previously done at Ames (refs. 3 to 5), and the present paper may be regarded as an extension of the earlier studies. Some of the questions to be considered are: (1) the type of observations and their timing, (2) the number and time of making velocity corrections, and (3) the effect of sighting accuracy and initial condition errors and uncertainties.

Certain ground rules for this study must be stated. First, we are concerned only with the midcourse guidance phase, which is defined, for the purpose of this paper, as starting at the periapse of the departure hyperbola and ending at the vacuum periapse of the arrival hyperbola. Secondly, the midcourse corrective maneuvers which will be required are impulsively applied. Third, by assumption the trajectory estimation scheme is a completely on-board operation; that is, observational data will be obtained by on-board sensors, and the computation will be carried out on-board. This requirement results from the fact that we are considering a manned mission, and we do not want to depend upon the earth-vehicle communication link. Of course, in an actual mission, data gathered from earth-based equipment would undoubtedly also be used, and the computations would be repeated on the ground to provide as much redundancy as possible.

In the first section of the report, the mathematics involved in the trajectory estimation and guidance phases of the problem are given. In the second section, the computations are described which are necessary for computing the statistics of the system performance, the manner in which the computations of planetary and vehicle motion were implemented for the computer program is described, and finally the assumptions made regarding the types and scheduling of observations are outlined. In the final section the results obtained from the computer program are presented in terms of the statistics, or covariance matrices, of the random variables of interest, such as miss at the target, required velocity changes, etc.

SYMBOLS

A	transition matrix relating deviations at the end point to present deviations
A_1, A_2, A_3, A_4	submatrices of A
c	ratio of uncertainty in planet radius to planet radius
E_{miss}	covariance matrix of miss at the end point
E_{unc}	covariance matrix of uncertainty at the end point
E_p	covariance matrix at the end point in perigee coordinate system
$f, \dot{f}, g, \dot{g}$	scalar constants used in updating elliptical motion
G	guidance law matrix relating velocity correction to present deviations
H	matrix of partial derivatives of the observed quantity with respect to the state variables
H_1	submatrix of H
I	identity matrix
K	weighting matrix
P	covariance matrix of present uncertainty
P'	covariance matrix of present uncertainty after an observation
P_1, P_2, P_3, P_4	submatrices of P
PAR	covariance matrix of present deviations
PAR'	covariance matrix of present deviations after a velocity correction
Q	covariance matrix of observation errors
Q_{inst}	covariance matrix of instrument errors
Q_M	covariance matrix of errors in measuring velocity
q^2	element of Q
r	position vector of a body in conic motion

r_R	position vector of a body in conic motion at reference time
S	covariance matrix of errors in making velocity correction
S_4	submatrix of S
t	time
v	velocity vector of a body in conic motion
v_R	velocity vector of a body in conic motion at reference time
V_{CM}	covariance matrix of desired velocity corrections
x	state vector representing position and velocity deviations from reference
$\hat{x}$	state vector of estimated deviation from reference
x_G	corrective velocity vector
γ	half the subtended angle of an observed body
δr_p	rms value of the deviation in radius of periapse
δR_S	uncertainty in position of observed body
ΔV	vector of corrective velocity
$\Sigma\Delta V$	sum of ΔV
$\varphi(t_i,t_j)$	transition matrix relating the state at time t_i to state at time t_j
$(\ )^T$	transpose

Planetary Symbols:

☉	Sun
☿	Mercury
♀	Venus
⊕	Earth
♂	Mars
☾	Moon
♑	Deimos
♇	Phobos

DESCRIPTION OF PROBLEM

As previously mentioned the problem of interplanetary guidance can be conveniently broken down into two parts. First is the navigation problem, in which one observes some variables and estimates the present trajectory. Second is the guidance phase, in which one estimates how far the present trajectory misses the desired end condition, determines, by use of a guidance law, a corrective maneuver which will reduce this miss to zero, and finally performs this maneuver.

Trajectory Estimation

For a navigation scheme based on the Kalman filter theory, observation data are obtained and compared with the expected value of the observation, as computed from the estimated trajectory. The deviation is multiplied by a weighting matrix and then added to the trajectory estimate to provide an improved estimate. The weighting matrix, as derived by the Kalman method, is the optimal filter for a linear problem and thus uses the observed data to maximum advantage insofar as the measured deviations are linear functions of the difference between the estimated and actual trajectories. It is computed by use of the covariance matrix of the error in estimation, the covariance matrix of the errors in making the observation, and the partial derivatives of the observed quantities with respect to the state vector. Thus, in order to compute the weighting matrix, one must first compute these required covariance matrices.

The equations used for the navigation scheme are summarized and described below and referenced to corresponding equations in references 3 and 4 where they are derived.

We assume that we are given $P(t)$, the covariance matrix of errors in the estimated trajectory at some initial time, $t = t_0$, and we desire to process the results of an observation at some later time, $t = t_1$.

We must first update the estimated state vector from time t_0 to time t_1 as follows:

$$\hat{x}(t_1) = \Phi(t_1,t_0)\hat{x}(t_0) \tag{1}$$

(eq. (2), ref. 3) where $\Phi(t_1,t_0)$ is the transition matrix which relates conditions at time 1 to those at time 0. This same transition matrix can be used to update the covariance matrix also, as

$$P(t_1) = \Phi(t_1,t_0)P(t_0)\Phi^T(t_1,t_0) \tag{2}$$

(eq. (15), ref. 3).

At the time of the observation we must compute the H matrix, which is the partial derivative matrix of the observed quantity with respect to the state variables. The H matrix will have the same number of columns as there are variables in the state vector, and will have one row for each different quantity observed simultaneously. If we consider observations which depend only on position and not velocity, as is done in this study, then the H matrix can be partitioned into two matrices of 3 columns each;

$$H = \begin{bmatrix} H_1 & 0 \end{bmatrix}$$

The elements of the H matrix will be given when we consider the types of observations to be made. The P matrix, updated to the time of the observation, can also be partitioned into 3×3 submatrices:

$$P = \begin{bmatrix} P_1 & P_2^T \\ P_2 & P_4 \end{bmatrix}$$

Then the weighting matrix K is given by the following:

$$K = \begin{bmatrix} P_1 \\ P_2 \end{bmatrix} H_1^T \left[H_1 P_1 H_1^T + Q \right]^{-1} \qquad (3)$$

(eq. (17), ref. 3) where Q is the covariance matrix of observation errors. This weighting matrix can then be used to update the P matrix to include the data just obtained by the observation as follows:

$$P' = P - KHP \qquad (4)$$

(eq. (16), ref. 3).

The result of equation (4) is then a new covariance matrix, P', which is used as the initial P matrix in equation (2) when the same sequence of events is repeated for the next observation, and so on.

We also need to derive an additional equation to determine the new value of the P matrix after a velocity correction has been made. It is assumed that the velocity correction is measured by three inertially oriented accelerometers, and that the covariance matrix of measurement errors is given by the 3×3 Q_M matrix. If one assumes that the measurement errors are small, we find that the new P matrix is given as:

$$P' = \begin{bmatrix} P_1' & P_2' \\ P_3' & P_4' \end{bmatrix} = \begin{bmatrix} P_1 & P_2^T \\ P_2 & P_4 + Q_M \end{bmatrix} \qquad (5)$$

Thus, equations (1) through (5) allow the computation of the P matrix at any point along the trajectory, and thus determine the statistics of the difference between the actual and estimated trajectory.

Guidance Laws

The previous discussion has been concerned with the estimation of the vehicle trajectory. We now wish to consider the second part of the control problem, namely, determining and performing some corrective maneuvers which will allow the vehicle to arrive at the target planet with no errors in the specified arrival conditions. The guidance law then relates the corrective maneuver to the information concerning the estimated trajectory.

It is assumed that the vehicle, on arrival at the target planet, will use atmospheric braking to reduce its energy relative to the planet. In order to do this successfully, the vacuum periapse must be low enough that enough energy can be dissipated, and yet high enough that g limits are not exceeded. Thus one has a corridor of acceptable periapse distances.

In order to develop such a guidance law, one must first decide on some method for guaranteeing that the vehicle will arrive within the corridor. One simple overspecified approach is to first determine a nominal trajectory inside the corridor at periapse, and then guide the vehicle so that it arrives at this specified point at the specified time. This is a fixed time-of-arrival guidance scheme, and the miss is the distance from the vehicle to the specified point at that time. An alternate approach, a little more complicated, is to directly control the radius of periapse to the desired value within the corridor with some control of the out-of-plane error, and to do this using a minimum amount of fuel. This is called a radius-of-periapse guidance scheme, and allows the time of arrival to vary. Other approaches could also be used, which would use still other guidance laws. Further, it may be expedient to use different guidance laws during different phases of the mission.

Whichever guidance law is used must relate the corrective maneuver x_G to the present deviation $\hat{x}$, so that the desired end conditions are satisfied; that is,

$$x_G = G\hat{x} \tag{6}$$

(eq. (D6), ref. 4) where the G matrix is the mathematical expression of the guidance law.

The fixed time of arrival guidance law is derived in reference 4, equations (7) and (D7) as

$$G = -\begin{bmatrix} 0 & 0 \\ A_2^{-1}A_1 & I \end{bmatrix} \tag{7}$$

The terms in this equation come from $A = \begin{bmatrix} A_1 & A_2 \\ A_3 & A_4 \end{bmatrix}$, which is the transition matrix relating deviations in position and velocity at the fixed time of arrival to present position and velocity deviations from the reference trajectory.

The radius-of-periapse guidance law is derived in appendix B, equation (B13), which contains the matrix

$$G = \begin{bmatrix} 0 & 0 \\ \bar{U}\bar{W}^T + K\bar{N}\bar{N}^T & -\bar{U}\bar{U}^T - \bar{N}\bar{N}^T \end{bmatrix} \tag{8}$$

The quantities $\bar{U}$, $\bar{W}$, K, and $\bar{N}$ are all functions of the reference trajectory, and are described in the appendix. The terms involving $\bar{N}$ are used to control the out-of-plane error, and the other terms control the periapse error.

DESCRIPTION OF SIMULATION

The equations in the previous section describe, in statistical terms, the required on-board computations. In order to study the performance of this system, we need to determine the statistics of the deviation between the actual and reference trajectories. Also, these statistics are functions of the planetary motions, the vehicle trajectory, and the type and timing of observations made to improve the estimate of the trajectory. These features of the interplanetary navigation and guidance problem will be considered in the next few sections.

Statistics of System Performance

In order to determine the statistics of the final miss, we must first develop the statistics of the deviation between the actual and reference trajectories, the PAR covariance matrix.

This matrix is updated from one time to the next in the same fashion as the P matrix, by use of equation (2). It is not changed by an observation, but will be changed by a velocity correction. The equation for this is given by equation (D11) in reference 4 as

$$PAR' = (I + G)(PAR - P)(I + G)^T + P + S \tag{9}$$

As can be seen from equations (7) and (8), the G matrix can be partitioned as follows:

$$G = \begin{bmatrix} 0 & 0 \\ G_2 & G_4 \end{bmatrix}$$

With this partitioning, the 3×3 covariance matrix of expected velocity corrections can be computed as follows:

$$V_{CM} = (G_2\ G_4)(PAR - P)(G_2\ G_4)^T \tag{10}$$

(eq. (D19), ref. 4).

The S matrix in equation (9) represents the statistics of the errors in making the desired velocity correction and can be represented as

$$S = \begin{bmatrix} 0 & 0 \\ 0 & S_4 \end{bmatrix} \tag{11}$$

(see eq. (D16), ref. 4).

In computing the S matrix it was assumed that: (a) the magnitude of the actual velocity change deviates from the desired magnitude by an unknown amount whose standard deviation is proportional to the correction, and by a random cutoff error, and (b) the direction of the actual correction differs slightly from that of the desired correction because of a pointing error. These three random variables (the constant of proportionality, the cutoff error, and the pointing error) are all assumed to have zero mean and specified standard deviation. An equation for computing the S_4 matrix (which equals $\bar{\eta}\bar{\eta}^T$) is derived in equation (A16).

These equations give a statistical description (second-order statistics) of the estimated and actual trajectories, and of the corrective maneuvers. However, for a clearer picture of what is happening along the trajectory, some additional quantities are desired.

In space navigation, one is not really interested in one's present position per se but, instead, is interested in the miss and the uncertainty in the knowledge of position at some future time, T, when one expects to be at the target point. This can be computed if the transition matrix from now to the final time is given. This matrix can be defined from equation (1) as $A = \Phi(T,t)$. Thus the 6×6 covariance matrix of the miss is

$$E_{miss} = A(PAR)A^T \tag{12}$$

and that of the uncertainty is

$$E_{unc} = A(P)A^T \tag{13}$$

The upper left 3×3 portions of these matrices describe the statistics of the position components of the miss and uncertainty, and the square root of the trace of these 3×3's gives the rms total position miss and uncertainty, r_{miss} and r_{unc}, respectively.

We are also interested in rms values of the altitude, downrange, and crossrange components of miss and uncertainty at the time of reference periapse. These components can be determined by rotating the E matrices from the reference coordinate system into a periapse coordinate system defined as follows: the X axis along the radius vector from the center of the target planet to the periapse of the reference trajectory, the Z axis perpendicular to the X axis and the velocity vector at this periapse, and the Y axis to complete a right-hand orthonormal triad. Let θ represent the rotational matrix relating the two coordinate systems. Then the covariance matrix in the periapse coordinate system is $E_p = \theta E \theta^T$, and the three diagonal elements of E_p represent the variances of altitude, downrange, and crossrange miss (or uncertainty), respectively. Also of interest is δr_p, the rms deviation in the radius of periapse. Equation (B22), derived in appendix B, relates the deviation of the radius of periapse to the present state vector. Taking the expected value of this equation gives

$$\delta r_p^2 = Z^T(PAR)Z$$

where Z is defined in equation (B20).

The square root of the trace of the V_{CM} matrix (eq. (10)) gives the expected value of the magnitude of the individual velocity correction ΔV. In order to find the total velocity correction made, ΔV_T, that is, the sum of the individual velocity corrections, one must combine the expected values for each of the individual corrections. The method of combining these values depends upon the assumptions made regarding their correlation. If one assumes that the individual velocity corrections are perfectly uncorrelated, then one adds the individual ΔV's on a root sum square basis; that is, $\Delta V_T = \sqrt{\Sigma(\Delta V)^2}$. On the other hand, if they are perfectly correlated, then one adds the ΔV on a linear basis; that is, $\Delta V_T = \Sigma \Delta V$. The true situation is somewhere between these two cases, but for this report we have used the more pessimistic linear basis giving

$$\Delta V_T = \Sigma \Delta V \tag{14}$$

We now have the equations which enable us to obtain statistical data concerning the uncertainties in the knowledge of the trajectory, the dispersion of the trajectory, and the midcourse velocity corrections.

Vehicle Motion

The behavior of a vehicle in space can be described by means of conic sections plus minor perturbations due to noncentral force fields. Since, in this study, we are concerned only with relatively small deviations from a reference trajectory, it was felt that the perturbations could be ignored and the conic sections alone used to describe the vehicle trajectory. That is, the conic section approximation should have the same general characteristics

as those of the exact trajectory in regard to deviations. Thus, for the purpose of a study of the navigation scheme, precise n-body trajectories need not be computed.

Since it was desired to study effects from periapse of the departure planet to periapse of the target planet, a patched conic technique was required. In this case, the vehicle traversed sections of three conics, a hyperbola about the departure planet, an ellipse about the Sun, and a hyperbola about the target planet. At the transition points, the position and velocity of the two conics, both expressed in the same coordinate system, were equated to provide the desired match. The transition points were located at the sphere of influence of the appropriate planet, and were computed by the formula $a(m/M)^{2/5}$, where a is the mean Sun-planet distance, m is the mass of the planet, and M is mass of the Sun. The following table lists the radii of the spheres, as given in reference 6 (p. 93).

Venus	616,960 km
Earth	924,820 km
Mars	577,630 km

The reference trajectory of the vehicle was specified by giving the position and velocity of the vehicle at the sphere of influence of the departure planet. These conditions were adjusted so as to give a satisfactory departure periapse and a satisfactory arrival altitude, while holding the inclination of the vehicle orbit with respect to the ecliptic to small values (to take advantage of planetary motion). When it was desired to obtain the vehicle's position and velocity at some other time, the reference values were updated as follows:

$$\left.\begin{aligned} r &= f r_R + g v_R \\ v &= \dot{f} r_R + \dot{g} v_R \end{aligned}\right\} \qquad (15)$$

where $f, g, \dot{f}, \dot{g}$ are functions of the initial position and velocity and the change in eccentric anomaly from the reference position to the desired position. These equations are derived in reference 7.

Planetary Motion

Since the vehicle's trajectory is described by conic sections, it seems reasonable to describe the planetary orbits by conic sections also. The elements of the planetary conics were obtained from the 1964 Nautical Almanac (ref. 8) and the Explanatory Supplement (ref. 9). These reference elements were all expressed in the equinox and ecliptic of Jan. 6.0, 1964, and the variations of these orbits were determined with respect to this fixed ecliptic. This procedure then fixed the reference inertial system for the entire problem as being the equinox and ecliptic of Jan. 6.0, 1964.

The orbital elements were updated by means of their variations to a reference time in the immediate vicinity of the launch date, and then, throughout the flight of the vehicle from the earth out to some planet and

back, the conic elements were considered fixed. At this reference time, the position and velocity of the planet were determined in three coordinates, as $r_{RP} + v_{RP}$. Equation (15) was then used to update the planetary position and velocity as desired.

The positions of the natural satellites of the Earth and Mars are also required so that they can be used as bodies to be observed. Their orbital elements were obtained from the Explanatory Supplement (ref. 9), and treated in exactly the same fashion as the planets. The values used for these elements and their variations are given in table I for each of the planets and satellites.

Observation Types and Schedules

The principal types of measurements that can be made on-board the vehicle are optical determinations of an angle. Theoretically other quantities might also be measured, such as range and range rate from a radar, relative velocity from some velocimeter, and angular velocity of the line of sight, but these all have practical limitations and will not be considered here. There are two optical instruments which can be used, the sextant and the theodolite. In a vehicle the sextant, which would be used to measure the angle between a star and some body in the solar system, is quite convenient to use. The theodolite is more awkward, both from the standpoint of the man who must make two adjustments at once, and from the standpoint of the equipment, since the theodolite must be mounted on a stable platform.

In a general research study such as this, however, the theodolite is easier to consider, since it does not require, as does the sextant, any decision as to which of the many stars should be used to provide the second line of sight. Therefore, for this study we are principally considering theodolite data, although this will be compared with sextant data.

It should also be pointed out that using either instrument one can determine the subtended angle of a planet and, from this, deduce the range to the planet. This is a most inaccurate measurement, useful only at extremely close ranges, and is not considered here.

As mentioned earlier, it is necessary to compute the H matrix associated with each type of observation. For a theodolite, we have

$$H = \begin{bmatrix} \frac{\partial \alpha}{\partial x} & \frac{\partial \alpha}{\partial y} & \frac{\partial \alpha}{\partial z} \\ \frac{\partial \beta}{\partial x} & \frac{\partial \beta}{\partial y} & \frac{\partial \beta}{\partial z} \end{bmatrix} = \begin{bmatrix} \frac{xz}{R^2R'} & \frac{yz}{R^2R'} & \frac{z^2 - R^2}{R^2R'} \\ \frac{-y}{R'^2} & \frac{x}{R'^2} & 0 \end{bmatrix}$$

where α and β are the celestial latitude and longitude of the observed body as seen from the vehicle, x, y, and z are components of the vector from the vehicle to the observed body, $R = \sqrt{x^2 + y^2 + z^2}$, and $R' = \sqrt{x^2 + y^2}$. These equations are derived in appendix C of reference 3.

For a sextant, using the same notation except that α is the measured sextant angle, we have

$$H = \left(\frac{\partial\alpha}{\partial x} \frac{\partial\alpha}{\partial y} \frac{\partial\alpha}{\partial z} \right) = \left[\frac{(x/R)\cos\alpha - x_S}{R \sin\alpha} \quad \frac{(y/R)\cos\alpha - y_S}{R \sin\alpha} \quad \frac{(z/R)\cos\alpha - z_S}{R \sin\alpha} \right]$$

where x_S, y_S, z_S are the components of the unit vector in the direction of the star.

In order to process an observation using this estimation scheme, there must also be available the covariance matrix of errors in making the observation. The observation error can be considered to have three components, all assumed uncorrelated with respect to each other and from one observation to the next. The first component is an instrument error, which is caused by inaccuracies in the observing instrument itself, and in the pilot's ability to use it. The covariance matrix of this instrument error is defined as Q_{inst}, and must be known a priori. The second component is inversely proportional to range, and can be considered as an additional pilot error due to the inability to locate the center of an extended disk, or as an error in the knowledge of the radius of the observed body.[1] Its covariance matrix is $c^2\gamma^2 I$, where c is the rms value of the ratio of the uncertainty in the radius to the radius of the body, γ is one-half the angle subtended by the observed body, and I is the identity matrix. The third component of error is due to the uncertainty in the position of the observed body.[2] If the observed body is the central body for the conic section, this component is zero. If, on the other hand, we are observing a satellite of the central body, then this position error will exist. To account for this correctly, the uncertainty in the orbital elements should be considered individually and appropriately combined to get an uncertainty in the x,y,z coordinates of the satellite. For simplicity in this study, however, it was assumed that the rms error in the observation due to the position error could be specified as $\delta R_S/R$, where δR_S is the rms value of that component of the position uncertainty which affects the observation, and R is the distance to the observed body. The covariance matrix of this error is then $(\delta R_S/R)^2 I$. With these assumptions, the total covariance matrix of observation errors, which is a diagonal matrix with equal elements q^2, becomes

$$Q = Q_{inst} + \left[c^2\gamma^2 + \left(\frac{\delta R_S}{R} \right)^2 \right] I$$

which is then used in equation (3). Figure 1 is a plot of q versus range for several planets and satellites for those representative values of Q_{inst}, c, and δR_S used in the study.

Having discussed the types of observations to be made, we must now discuss what bodies should be observed and when. It seems apparent that in the vicinity of a planet one should observe that planet, and possibly its

---

[1]This error may have a bias type component, which would result in a time correlation that has been ignored for simplicity.

[2]The time correlation, resulting from the bias effects of this error, was ignored for simplicity.

moons, and also perhaps the Sun. In the heliocentric portion of the trajectory, one should consider observing the departure and arrival planets, the Sun, and the other planets.

For the timing of observations, one wants to make more observations at times when the position along the trajectory, and therefore the observed quantity, is changing rapidly, namely, at the beginning and end of the flight, and fewer observations during the central portion of the trajectory when observables are changing slowly. When the uncertainty in the knowledge of final miss has reached some satisfactorily small quantity, then no further observations are required.

The observation schedule is selected to minimize the miss and uncertainty at the end point, and also to minimize the amount of fuel required to make the velocity corrections. Thus, the observation and velocity schedule are interdependent and must be optimized together.

RESULTS OF SIMULATION STUDY

Reference Trajectories

In this section the results of the simulation study are presented. The previous section has defined all the equations used to determine the desired statistics and discussed various considerations concerning observation and velocity correction schedules. To be more specific, we must first specify the reference conditions.

Three different reference trajectories were used as examples for this simulation. The first trajectory is a high-speed round trip from Earth to Mars. This is near the 1971 opposition, with 112-day flight time to Mars, 7-day stay at Mars, and 191-day return flight. The second trajectory is a lower speed round trip from Earth to Mars, also in 1971. The outbound trip is 153 days, with a 6-day stay at Mars. The return flight is 251 days. The third trajectory is also a round trip to Mars, with a swingby of Venus on the return leg. This swingby has the advantage of reducing the entry velocity on return to the Earth, with essentially no additional propulsive requirements. This trajectory is in the 1975 period. The Earth to Mars trip time is 170 days. The stay time at Mars is 30 days, and the return trip is 185 days to Venus and 125 days back to Earth.

These three trajectories will be termed the high speed, low speed, and Venus swingby, respectively. Additional details about them are listed in table II. From this table, it can be seen that the Venus swingby trajectory is not absolutely continuous at Venus. Small changes in the reference condition could be made to make this trajectory continuous. However, for the purpose of this study it was not felt necessary to make this correction. Plots of all three trajectories, projected onto the plane of the ecliptic, are given in figures 2, 3, and 4, along with the motion of the various planets. The orbits relative to the Sun, and relative to the launch and

target planets are shown. On these figures, the time from departure is indicated. For the heliocentric portion, the symbols indicate which departure is referred to.

It can be seen from these plots that in some cases the vehicle passes relatively close to the Moon. The closest approach occurs on the outbound leg of the high speed trajectory (fig. 2(b)). In this case the distance of closest approach to the Moon is over 100,000 km, which is well outside the sphere of influence of the Moon. It seems reasonable to assume, therefore, that for the purpose of this study, the turning effect of the Moon on these trajectories can be neglected.

The effects of close passage on the information content of the observations cannot be neglected, as will be shown later. In order to isolate this effect and to show the effects of launching at different times during the lunar cycle, the mean anomaly of the Moon was changed while keeping all other lunar orbital parameters fixed. This had the effect of moving the Moon in its orbit with respect to the vehicle trajectory. Such a rotation will be denoted as "Moon (θ)" where θ is the angle by which the mean anomaly has been advanced.

Nominal Error Assumptions

This estimation scheme requires an estimate of the error in the knowledge of each piece of information. In particular, we must know the initial covariance matrices, P and PAR, which represent the second-order statistics of the knowledge of the state vector, and of the deviation of the state vector from the nominal. These matrices are assumed diagonal in a launch coordinate system, and the values are listed in table III. These nominal rms errors were used as initial values in both the P and PAR matrices at launch from the Earth and again at launch from Mars. In the swingby trajectory, where the vehicle passes Venus without stopping, the P and PAR matrices are continuous.

Also listed in table III are the nominal values of the errors in making and measuring velocity corrections, and the error associated with making observations. In connection with the observation noise, the "Radius Uncertainty/Planet Radius" was assumed to be 100 times as large for Deimos and Phobos as for the other solar system bodies, and they were also assumed to have a much larger position uncertainty. For certain runs, these nominal error values were changed. These changes are specifically indicated in the appropriate places.

Observation Schedules

In the lunar guidance studies, operational requirements indicated that it would be desirable to take relatively few observations. The flight time

to the Moon is about 2 days, and during this time about 40 observations must be taken to reduce the arrival uncertainty to a desired minimum. Although more observations certainly could be made, they do not seem desirable or necessary.

In the interplanetary mission, however, we have a somewhat different situation. Here we have a long flight of a hundred or more days, and marginal accuracy can be obtained with observations spaced every several days during the major portion of the flight, and a concentration of observations at the beginning and end of the flight. However, operationally, it seems quite reasonable and probably desirable to take at least daily observations so that the astronauts can chart their progress.

If one uses this large amount of information in the navigation problem, it becomes difficult to tell which type of observation is useful and which is not. On the other hand, if one uses a minimum observation schedule, the usefulness of individual observations becomes much more apparent. Therefore, in considering what type of observations should be made, we have used a near minimum observation schedule, but have also included the results of daily observation schedules for comparison.

The lunar work has also shown (ref. 5) that it is desirable to make observations of quantities which are changing fairly rapidly. This implies that one should observe the departure (or arrival) planet fairly often when in its immediate vicinity, and that in the long period of heliocentric flight, observations need not be made too often. In considering the types of observations to be made, we will discuss first the heliocentric phase and then the departure and arrival planetocentric phases.

Observations during heliocentric phase.- During the heliocentric phase of the trajectory, there are many bodies which one might observe. These are the departure and arrival planets, the Sun, other planets, and planetary satellites. Considering the distances involved, one would expect that there would be no information obtainable from the planetary satellites that could not be obtained also from the mother planet, and therefore these bodies have not been considered in this phase. In order to show the effect of various observations, we will present a series of figures on which are plotted curves of position uncertainty at arrival, r_{unc}, vs time, and also an uncertainty ratio, which shows the effect of changing the observation schedule. It should be noted that the time scale for these plots is expanded at the start of the trajectory.

To show the effect of observing the Sun, we have plotted in figure 5(a) the results of two different observation schedules used during the outbound leg of the high speed trip. These two schedules are the same until the time of the first velocity correction at 2.4 days. This particular initial observation schedule is a minimum schedule, with a large residual uncertainty, which thus shows better the effects during the heliocentric phase. Subsequent to the first correction, the schedule associated with the reference schedule consists of theodolite measurements of both the Earth and Mars at 8-day intervals, with several daily observations of Mars at the end. It should be noted that this plot stops about 5 days short of periapse. The Sun-added

schedule uses the same schedule, except that the Sun is observed every 8 days in addition to Earth and Mars. As expected, the additional information from the extra solar observations did decrease the uncertainty a little, by about 6 percent at 43 days. However, by 106 days the uncertainty ratio has returned to unity.

In figure 5(b) we have shown a similar effect for the return leg of the same mission. In this case observations were made every 6 days of only one body, and several observations of a given body were made before observations were made of a different body. In the figure the same total number of observations were taken for the two cases, but solar observations were substituted for some of the Mars and Earth observations, as indicated. It can be seen from the figure that the run with solar observations has at times a higher uncertainty, indicating that there is not as much information in the solar observations as there is in the combination Mars-Earth observations, although the difference is small. Again, at 186 days, 5 days before periapse, the difference has decreased to a negligible amount. These data lead one to the conclusion that there is no great need to observe the Sun.

Similar data were taken of observations of other planets, specifically Mercury, Venus, Jupiter, and Saturn. These results are shown in figures 6(a) and 6(b). In figure 6(a) on the outbound leg, we have shown the uncertainty using the same reference schedule as in figure 5(a), but have added Venus observations for the other schedule. The plot of the uncertainty ratio shows that the added observations of Venus had very little effect. If similar uncertainty ratios were plotted for the other planets, the deviation from unity would be even less. In figure 6(b), we have substituted into the reference schedule of figure 5(b) some Mercury and Venus observations. This substitution gives higher uncertainties prior to 150 days, but after that time the uncertainties are equal.

These data imply that during the heliocentric portion of the trajectory, one can obtain all the information required by observations of the launch and target planets, and that the Sun and other planets need not be observed, although substitution of the Sun for some of the planetary observations is allowable.

The data shown on these curves is also tabulated in table IV, along with similar data for the other planets which were not shown on the curve. Since observations of Jupiter and Saturn showed virtually no effect on the outbound leg, they were not considered as observable bodies on the return leg. The predicted uncertainty at arrival is tabulated for several values of time along the trajectory with the last point being a few days before periapse and reinforces the conclusion that there is no need to observe any bodies but the departure and arrival planets, and that what small differences do exist in the middle of the trajectory have virtually vanished near the end.

Now consider a daily observation schedule. In figure 7(a) we have shown the uncertainty from the Sun-added schedule of figure 5(a). We have also shown the curve for daily observations of the same bodies. It can be seen that, as expected, the daily schedule shows considerable improvement.

A daily observation schedule for the return leg is shown in figure 7(b), along with the comparable curve from the reference schedule of figure 5(b). Again, we have a sizable improvement during the heliocentric portion of the trajectory. Table IV includes the data from these runs also.

A similar comparison of daily versus minimum schedules is presented in table V for the Venus swingby case. For the minimum observation case, there were single observations every 5 days from Earth to Mars, every 6 days from Mars to Venus, and every 4 days from Venus to Earth. These spacings were chosen to make the number of observations in each leg roughly equal. These observations were of either the arrival planet, the departure planet, or the Sun. In the daily observation case, observations of all three bodies were used each day. Again, the last point is several days before periapse. The initial observation schedule is identical for the two cases on leaving the Earth, but there are a few extra observations in the daily case on leaving Mars, which gives the small difference in the uncertainty at 3 days. The uncertainty on arrival at Venus was carried over and used as the initial uncertainty for the Venus departure leg, so that the initial uncertainty on leaving Venus is different for the two cases. There were a large number of observations made near Venus and, after completing these observations, the effect of the change of the initial uncertainty on arriving at Venus has been virtually cancelled. From this table we again conclude that daily observations will appreciably reduce the predicted uncertainty during the latter portion of the heliocentric trajectory. Thus, we conclude that the effect of daily observations, over observations spaced more widely in time, is to reduce the uncertainty more quickly. This is desirable, since it will result in more accurate velocity corrections as will be discussed later. Thus, during the heliocentric phase, it is apparent that it is desirable to make daily observations of the departure and arrival planets only. Observations of the Sun or other planets will provide virtually no benefit.

Observations during planetary phases.- In the near vicinity of the departure planet, it is necessary to take a large number of observations to get a good determination of the departure trajectory so that an early correction of the insertion errors may be made. Also, on arrival at the target planet it is necessary to take a large number of observations to reduce the periapse uncertainty to a satisfactorily low level (since this cannot be done in the heliocentric portion of the trajectory). Thus at each end of the trajectory, we must take a large number of observations. Since we are concerned here with the trajectory with respect to the nearby planet, it seems reasonable to observe only the nearby planet and its satellite(s), if any. We still must ask, however, whether we should observe both the planet and its satellite(s), or whether only the planet should be observed. In this report we have considered only the natural satellites, but the conclusions should be applicable to man-made satellites as well.

Consider first the Moon when leaving the Earth. The previous data for the heliocentric phase have had observations of only the Earth during the launch phase. The first 3 days of the reference schedule from figure 5(a) is repeated in figure 8. If we now substitute Moon observations for about half the Earth observations, there is a greater than 10:1 reduction in uncertainty as indicated by the lowest curve in the figure. Referring back to figure 2(b),

we can see that the vehicle, for the high speed trajectory, passes very close to the Moon, and thus we get a large amount of very good data concerning the downrange position. If the launch were at other times of the lunar cycle, this beneficial effect is not as great, as is indicated by the other two curves, where the Moon is considered to be 90° and 180° away from its true position.

These curves show that there is always some benefit to be gained by making some of the early observations of the Moon, and the closer the trajectory comes to the Moon, the more the benefit. It can be seen that the benefit of Moon observations extends throughout the entire mission, although the effect is decreasing towards the end of the trip. The reason for this benefit is that a close passage of the Moon gives excellent information about downrange travel and total velocity, while if there is not a close passage then the combination of Moon and Earth measurements have a large base line which gives better range data. Such range data are not available from observations of the Earth only.

Most of the other data presented in the remainder of the report have used the unfavorably located Moon on the basis that if we can get satisfactory arrival conditions with the unfavorable Moon, then we will still be all right with a favorable Moon and the Moon's position has provided no additional constraints on the launch window.

We also need to know the desirability of observing the Moon on the return mission. This is shown in figure 9(a) for the high speed trajectory, where we have considered the case of no Moon observations at all, some Moon observations, and some observations of Moon (180). Referring back to figure 2(e), it can be seen that the Moon is located in a fairly favorable position, and therefore Moon (180) will be unfavorably located. Figure 9(a) shows that there is a large difference in the three cases, and that observing Moon (180) is quite beneficial, with considerable additional benefit gained by observing the Moon, and that this benefit occurs even though the number of observations has been decreased. The components of the predicted uncertainty at arrival, as predicted at 190.5 hours, the time of the last velocity correction, are tabulated below.

1σ Predicted Uncertainty, km

	Altitude	Downrange	Crossrange
Earth only	8	329	4
Moon (180)	6	63	4
Moon	4	7	2

It can be seen that the principal effect of observing the Moon is to reduce the downrange component of the uncertainty, with an attendant minor reduction in the altitude component. If the Moon is favorably located, there will be a greater reduction in the downrange miss.

The effect of observing the Moon during the approach to the Earth is also shown in figure 9(b) for the Venus swingby trajectory. In this trajectory, the Moon position on approach is reasonably favorable as shown by figure 4(f). The curves in figure 9(b) show again that observing the Moon is helpful in reducing the uncertainty, and that a near passage of the Moon is even more desirable.

Now consider the situation at Mars, which is not quite the same as at Earth. At Mars there are two satellites, Deimos and Phobos, whose positions may not be very well known and which have orbits fairly close to Mars. Of these two, it is assumed that Deimos, the outermost satellite, will prove to be the most useful observational body because, in essence, this gives a larger base line for the measurements.

The position uncertainty of the satellites has been assumed to be 100 km, in that direction which will affect the measurement, and this error has been included as a component in the sighting error. The effect of observing these planets on arriving at Mars is shown for the high speed trajectory in figure 10(a). The uncertainty which is plotted for the Mars only case is a continuation of the Moon (180) case shown in figure 8. When the number of Mars only observations during the last 4 days is more than doubled (to a 15-minute interval), the accuracy is improved by about 13. To study the effect of observing Deimos, the extra observation schedule was used as a base, and each set of three observations was made of Mars, Mars and Deimos. This substitution had very little effect on the over-all uncertainty. If, in addition, the second Mars observation was changed to Phobos, the resulting uncertainty ratio was essentially the same,[3] and one would conclude that there is not much point in observing these satellites. If, however, the accuracy with which the position of these satellites is known is considerably greater, say 1 km, the conclusion would be somewhat different.

The uncertainty for the Mars only case is replotted in figure 10(b). Also shown is the uncertainty for the 2 Mars and Deimos case with the 1 km position accuracy. Here the substitution of Deimos observations has considerable effect. This is quite reasonable, since (see fig. 1) the error in observing Deimos for this case is considerably less than the error in observing Mars. Substitution of Phobos for the second Mars observation had little effect, as is shown by the uncertainty ratio curve. The components of the uncertainty at 112.3 days, the time of the last velocity correction, for these runs and also the extra Mars case are listed in the following table.

[3]A study of the detailed data showed, as assumed, that Deimos had the greater contribution to the knowledge of the trajectory.

1σ Uncertainty, km
Deimos and Phobos Uncertainty, 1 km

	Altitude	Downrange	Crossrange
Mars only	24	270	19
Extra observations of Mars	21	176	17
Mars and Deimos	7	14	6
Mars and Deimos and Phobos	7	14	6

The principal effect of the observations of Deimos is a reduction in the downrange uncertainty of about 8:1. There is also an improvement in the altitude and crossrange components, although this is a considerably smaller effect.

In conclusion, the question as to whether or not to observe Deimos is a function of the knowledge of its position. With the present knowledge, it is probably not worthwhile. There seems to be little advantage in observing both satellites over just Deimos.

Sextant observations.- In order to make a comparison between sextant and theodolite type observations, the timing of the observations was kept the same but each theodolite observation was replaced by a pair of sextant observations. The stars for these observations were chosen so that the angle between the two measurement planes was nearly a right angle. It was felt that this doubling of the number of observations was justified, since there is a lot of time available during the interplanetary flight. The results are presented in figure 11. The theodolite case in figure 11(a) is the same as that shown in figure 8 with Moon observations. The sextant gives essentially identical results up to 0.7 day. The sextant case becomes slightly worse from 0.7 day to about 1 day, after which the difference remains essentially constant. This trajectory has a close passage by the Moon just prior to 1 day, and it appears that it is difficult for the sextant case to gain as much information during this interval as does the theodolite case, principally because it may be difficult to get properly located stars in a limited star catalog.

For cases where there is no close passage, the sextant data are equally as good as the theodolite data throughout the trajectory. This is shown in figure 11(b), where the Moon observations of figure 11(a) were replaced by Moon (180) observations (as in fig. 8).

Sighting Accuracy

The previous data have been presented assuming that the observation instrument has a basic sighting accuracy of 10 seconds of arc, and that as one approaches the observed body this noise increases, as indicated in figure 1.

We would like to consider the effect of changing the basic accuracy of the sighting instrument to 5 seconds of arc. Accordingly, two runs were made using identical observation schedules. For one run the basic sighting was the regular 10 seconds of arc, and for the other it was 5 seconds of arc. All other parameters were the same, including the noise increase for nearby objects. The predicted uncertainty was determined at each point, and the predicted uncertainty ratio was computed by dividing the uncertainty for the 5 seconds run by the uncertainty for the 10 seconds run. The results are plotted in figure 12.

The uncertainty ratio started out at 1.0, since the initial uncertainty is not dependent on the sightings. The uncertainty ratio dropped fairly quickly to about 0.6, where it remained until the very end of the trajectory, when the ratio rapidly increased. Theoretically, the intermediate level should be 0.5 after sufficient sightings to work out the effect of the initial conditions, and should increase to near 1.0 at the end of the trajectory, when the dominant noise on the observations is the uncertainty in the planet radius. We have no explanation as to why the theoretical value of 0.5 is not reached.

The effect of using a more accurate sighting instrument would be to provide a proportionate decrease in the final miss, since the uncertainty at the time of the last velocity correction (marked in fig. 12) is still approximately 0.6. There also will be an approximately proportional reduction in the fuel used, except for the first correction which will remain the same.

Velocity Corrections

Having considered various parameters associated with observations and their effect on the uncertainty in the estimate of arrival conditions, we will now turn to the question of the velocity correction schedule and its effect on arrival error conditions. As mentioned previously, the principal requirement is that the actual radius of periapse falls within the entry corridor. At Mars, for a ballistic entry with entry speeds shown in table II, the corridor is about 30 to 50 km. At Earth, the corridor for a lifting vehicle is about 30 km (refs. 1 and 2).

Before specific results are discussed, a few general comments on the velocity correction schedules are in order. There are two requirements placed on this schedule. Firt and foremost it must be such that arrival conditions at the target are satisfactory, and secondly, the fuel used should be minimized.

The first of these requirements implies that there must be a correction made after the accuracy of trajectory estimation is adequate to guarantee safe arrival. For the observation schedule previously discussed, this means that there must be a correction two or three hours prior to arrival periapse. This also allows adequate time for preparations for the terminal maneuver.

The second of these requirements implies that there must be a correction fairly early in the trajectory to correct injection errors. This correction must be delayed, however, until sufficient information has been obtained about the specific injection errors which have occurred. After making this first correction, there will still be some residual error, caused in part by the uncertainty in the knowledge of the estimated trajectory correction when the correction was made and in part due to errors in making the correction. In order to minimize the fuel requirements, one or more additional corrections may be required.

The error in making the correction also gives further justification to the requirement for additional corrections. If the last correction is large, then the error in making the correction, a part of which is proportional to the correction itself, will also be large, perhaps causing an intolerably large miss. This can be reduced by making additional intermediate corrections.

In general, it is desirable to make a given correction as soon as possible in order to minimize the fuel. However, then the trajectory estimate is not as accurate so that the fuel used to make the corrective maneuver will not be efficiently used, and subsequent corrections will be larger. In summary, there is an optimum correction schedule which will minimize the fuel used and still allow safe arrival, and which is also a function of the number of corrections made.

In this study, an effort was made to be sure that the velocity corrections were somewhere near their optimum locations, but the true optimum schedule was not determined. It was found, however, that the optimum is fairly flat, and that the corrections could be moved around somewhat without seriously affecting the amount of fuel used. In terms of time, more movement is allowed of the early corrections and less of the later corrections.

There was no detailed study of the effects of varying the number of corrections. For the fixed-time-of-arrival scheme it was assumed that either three or four corrections would be required, with four preferred. If only three were used, the last correction was undesirably large resulting in too much error on arrival as will be shown later. For the radius-of-perigee control scheme, four corrections were used to give a good comparison with the fixed-time-of-arrival scheme.

One further comment should be made on the location of velocity corrections. There may be points on the trajectory at which it is very undesirable to make a correction. To demonstrate this, consider the adjacent sketch. If the vehicle is at point A, directly opposite the target, then there is no (small) maneuver which will allow the vehicle to correct any out-of-plane errors. Therefore, one should not try to make a correction at a point such as A (or any point which is an integral

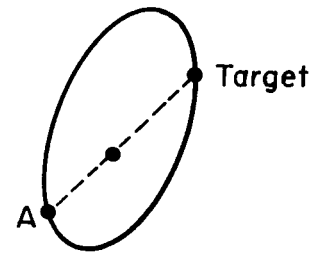

multiple of 180° away from the target) but should wait about 1/8 of an orbit until a small correction can be effective.[4]

Thus the amount of fuel used for the midcourse corrections is dependent on the observation schedule as well as on the velocity correction schedule. If a lot of information is collected early, then the early corrections will be made more accurately and the later corrections will be smaller. This is illustrated in table VI, where two trajectories from figure 8 are compared in terms of fuel requirements as well as uncertainty. It can be seen that for the trajectory in which the Moon was observed, as opposed to Moon (180), the uncertainty is much smaller at the time of the first velocity correction. This does not affect the size of the first velocity correction, which is principally used to correct the injection errors. However, this first correction is made more accurately so that the second correction is considerably smaller. The second correction, in turn, is also made more accurately so that the third correction is smaller. Thus, if the observation schedule can be adjusted so as to reduce the uncertainty at the time of nth velocity correction, there will be very little effect on the size of the nth correction, but there will be a reduction in the size of the n plus first correction.

Another effect can be noticed in connection with this table. The uncertainty at the time of the last velocity correction is nearly the same for the two cases and, therefore, one would expect the miss at arrival also to be nearly equal. This is true of the downrange component, which is the largest. However, the other two components of error are roughly proportional to the size of the velocity correction. To understand this, one must realize that both the predicted uncertainty and the predicted miss vectors lie principally along the trajectory, with the downrange component of these vectors varying from 4 to 200 times the other two components. This means that most of each correction is being used to reduce the downrange miss. Any error in the direction in which the correction is applied will principally affect the crossrange and vertical components of the miss, and have very little effect on the downrange miss. Such an application error is, of course, proportioned to the magnitude of the correction so that as the correction gets larger the vertical miss gets larger also, as shown in table VI.

There are three ways to reduce the size of the last velocity correction. First, one can increase the information content at the time of the next to the last correction so that it can be made more accurately. Second, one can make an additional correction sometime after the second correction. Then, in order to minimize the total fuel used, the second velocity correction should be moved somewhat earlier. Thirdly, one can change the guidance law and not correct the downrange component at all. This will be discussed in a later section.

Fixed-time-of-arrival guidance.- If one applies all of the considerations previously discussed, both as to observations and corrections, one would use

---

[4]There is an additional singularity beyond one orbit, which is not of interest here. A fairly detailed discussion of these singularities is given in appendix O of reference 10.

an observation schedule with observations of both the Moon and the Earth in the vicinity of the Earth, daily observations of the Earth and Mars during the heliocentric portion of the trajectory, and Mars only in the vicinity of that planet. There would be a concentration of observations near the launch planet to quickly reduce the predicted uncertainty, and also near the target planet so that safe arrival within the desired corridor could be guaranteed. There would be four velocity corrections in each leg. Such an observation and velocity correction schedule is shown in table VII for each of the three trajectories discussed, and the 1σ values of the velocity corrections and of the miss are shown in table VIII. Also included is the allowable corridor width for the expected entry conditions. For each trajectory, the Moon was placed in a relatively unfavorable location. This corresponds to departure (or arrival) at the time of the month when the Moon provides the least information. If the vehicle departs (or arrives) at other times of the month, better results will be obtained.

In order that the actual trajectory will pass within the corridor with some satisfactory degree of probability, the radius of periapse rms miss, being a 1σ value, should be multiplied by an approximate safety factor before being compared with the corridor width. If one uses a factor of 5 or 6, then the arrival conditions at the Earth are satisfactory, while the arrival conditions at Mars are marginal to unsatisfactory. The fuel required for the midcourse corrections is about 90 m/sec, 1σ, for the outbound leg, and 30-50 m/sec for (each of) the return leg(s). It should be noted that the last correction on approaching Mars is quite large, which tends to cause the large miss.

Radius-of-periapse guidance.- As mentioned earlier, one method of reducing the size of the final correction is to correct only the vertical and crossrange errors, and not the downrange error. This should also have the beneficial effect of reducing the miss at Mars. This was done by using the radius-of-periapse guidance law. This guidance law could only be used when inside the sphere of influence of the target planet, since otherwise the assumptions made in the derivation would not be valid. Therefore, the early corrections were made using the same fixed-time-of-arrival correction.

To see the effect of this guidance law, the same observation and velocity correction schedule listed in table VII was used, with the exception that the last one or two corrections (inside the sphere of influence) used the radius of perigee guidance law (as indicated by footnote b in table VII). The results are tabulated in table VIII b.

As expected, this guidance law has markedly reduced the size of the velocity correction where it was used at the expense of increasing the downrange miss. The resultant total fuel required is then about 30 m/sec, 1σ, for each leg, and the arrival conditions at Mars, as well as at the Earth, are now satisfactory.

There is an interesting additional effect on the Venus swingby mission. In this case the fourth correction on approaching Venus has been reduced, and also the first correction on leaving Venus is reduced. This can be explained as follows. The fixed-time-of-arrival correction on approaching Venus not

only reduces the periapse miss, but also the downrange miss. It does this, however, at the expense of an increased deviation of the downrange velocity error. The sensitivities of final error as a function of initial error for the Venus-Earth trajectory are such that the net result is a larger predicted error for the fixed-time-of-arrival scheme than for the periapse control scheme, resulting in a larger first correction for the fixed-time-of-arrival scheme.

Initial Deviations

In this report we have assumed a specific value for the initial covariance of the deviation from reference. This is listed in table III. If this initial dispersion is changed, the rms velocity corrections will also change. To show this effect, the initial dispersion was increased by a factor of 5, and the results are compared with the reference case in table IX.

As one would expect, the change in the first correction is directly proportional to the change in the deviation. This first velocity correction is designed to remove all the known errors at the time of the correction, and if this correction was made accurately, the second correction would be independent of the size of the first. However, there are errors in making the first correction which are proportional to the size of the correction, and these errors cause the size of the second error to increase with the initial deviation and, therefore, the second correction increases. From table IX, one can see that this increase is considerably less than proportional to the increase in the initial deviation.

By the time of the third correction (and subsequent corrections if they were to be made) the effect of the larger initial deviation has been essentially wiped out, since the size of the third correction for both cases is essentially the same as is the miss at arrival.

Thus the effect of the size of the initial deviation is to cause a proportional change in the size of the first correction, a minor change in the size of the second correction, and virtually no change to subsequent corrections nor to the arrival miss.

Initial Uncertainties

We are also concerned with the effect of changes in the rms initial uncertainty. To study this effect, the rms initial uncertainties listed in table III were multiplied by a factor of 5. Since it is unreasonable to expect that the initial dispersion would be smaller than the rms uncertainty, the initial dispersion was also multiplied by a factor of 5, as in the previous section. The resulting rms predicted uncertainty is compared with the reference case in figure 13. By the time of the first velocity correction, at 2.4 days, the rms predicted uncertainty ratio is nearly unity and, at 106 days, when the second correction is made, the ratio is even closer to unity.

The rms velocity corrections for this case are given in table IX, using the same reference as for the increased initial dispersion. The velocity corrections should be compared with those of the increased initial dispersion case, since the rms uncertainty and dispersion were both increased. The increased initial rms uncertainty had only a minor effect on the size of the velocity corrections.

CONCLUDING REMARKS

This report shows that a self-contained on-board navigation system for interplanetary flights is feasible from a performance point of view. Such a system can use a sextant which is accurate to 10 seconds of arc for obtaining data. During the major portion of the flight, observations every day are satisfactory but, at the start and end of each flight, observations spaced 15 minutes apart may be required. During the initial and final phases, these observations should be only of the nearby planet and its satellites. However, the position of the Martian satellites has to be known more accurately than at present for them to be of use. During the heliocentric trajectory, observations of only the launch and target planets are satisfactory, with observations of the Sun or the other planets then contributing very little additional information.

The scheme studied uses four midcourse velocity requirements for each leg of the trip, and uses a radius-of-periapse guidance law inside the sphere of influence of the target planet with a fixed-time-of-arrival law elsewhere. The fuel requirement is about 30 m/sec for each leg of the mission, and the rms miss in the radius of periapse at arrival is 4 to 5 km, which will satisfy the corridor requirements of 30 km with a fairly high degree of probability.

Ames Research Center
National Aeronautics and Space Administration
Moffett Field, Calif., Nov. 23, 1964

APPENDIX A

DERIVATION OF S MATRIX

To evaluate the performance of a space vehicle which undergoes velocity maneuvers, the covariance matrix of the uncertainty vector in applying the velocity maneuvers must be evaluated. Battin in reference 11 has derived an expression which assumes that the inaccuracy in establishing a commanded velocity vector is due to random errors in orientation and thrust magnitude. Although this error model is satisfactory for large velocity maneuvers, a third random error becomes predominant for small velocity corrections. This third error which must be considered is engine cutoff. The purpose of this appendix is to derive the covariance matrix for the uncertainty in applying a velocity correction when this cutoff term is included. Battin's derivation and notation (ref. 11) will be used as the format for this derivation.

The vector uncertainty $\underline{\eta}$ in establishing a commanded velocity correction $\Delta\hat{\underline{v}}$ is due to errors in cutoff, thrust magnitude, and orientation. These errors are assumed to be independent random errors with zero mean.

Consider a coordinate system chosen such that the commanded velocity correction vector is along the Z axis. Then if M is the transformation matrix which relates this selected axis system and the original reference system, the commanded velocity vector $\Delta\hat{\underline{v}}$ is

$$\Delta\hat{\underline{v}} = \Delta\hat{v}\, M \begin{bmatrix} 0 \\ 0 \\ 1 \end{bmatrix} \tag{A1}$$

Define K as an error proportional to the thrust magnitude, and ϵ as the thrust cutoff error, where K and ϵ are random variables with zero mean. The applied velocity magnitude is given by

$$\Delta v = (1 + K)\Delta\hat{v} + \epsilon \tag{A2}$$

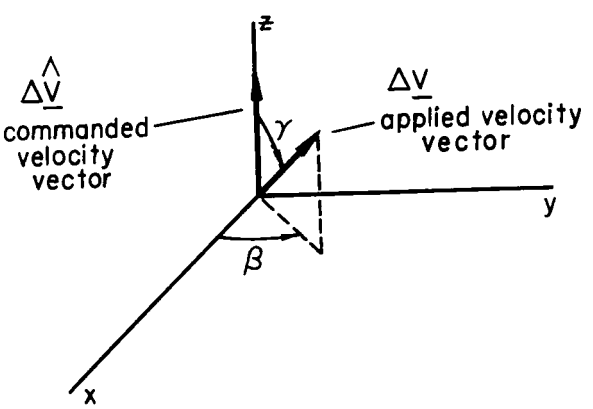

Sketch (a)

Let γ be a random angle between the commanded velocity vector, $\Delta\hat{\underline{v}}$, and the applied velocity vector, Δv. Furthermore, let β be a uniformly distributed angle over the interval $0 \leq \beta \leq 2\pi$, which represents the rotation of $\Delta\underline{v}$ about the Z axis as shown in sketch (a). Now, if γ is small so that $\sin\gamma \cong \gamma$ and $\cos\gamma = 1$, then the applied velocity vector is given by

$$\Delta\underline{v} = [(1 + K)\Delta\hat{v} + \epsilon]M \begin{bmatrix} \gamma\cos\beta \\ \gamma\sin\beta \\ 1 \end{bmatrix} \tag{A3}$$

the uncertainty vector $\underline{\eta}$ is the difference between the commanded and applied velocity vectors

$$\underline{\eta} = \Delta\hat{\underline{v}} - \Delta\underline{v} \tag{A4}$$

and the covariance matrix of the uncertainty vector $\underline{\eta}$ is defined as the expected value of $\underline{\eta}\underline{\eta}^T$ which is written as

$$\overline{\underline{\eta}\underline{\eta}^T} = \overline{\Delta\hat{\underline{v}}\,\Delta\hat{\underline{v}}^T} + \overline{\Delta\underline{v}\,\Delta\underline{v}^T} - \overline{\Delta\hat{\underline{v}}\,\Delta\underline{v}^T} - \overline{\Delta\underline{v}\,\Delta\hat{\underline{v}}^T} \tag{A5}$$

Performing each of the above operations separately we have for the first term

$$\Delta\hat{\underline{v}}\,\Delta\hat{\underline{v}}^T = \Delta\hat{v}^2 M \begin{bmatrix} 0 & 0 & 0 \\ 0 & 0 & 0 \\ 0 & 0 & 1 \end{bmatrix} M^T \tag{A6}$$

Performing the expected value operation this becomes

$$\overline{\Delta\hat{\underline{v}}\,\Delta\hat{\underline{v}}^T} = E\left\{ \Delta\hat{v}^2 M \begin{bmatrix} 0 & 0 & 0 \\ 0 & 0 & 0 \\ 0 & 0 & 1 \end{bmatrix} M^T \right\} \tag{A7}$$

Expanding the second term of equation (A5), we have

$$\Delta\underline{v}\,\Delta\underline{v}^T = [(1 + K^2 + 2K)\Delta\hat{v}^2 + \epsilon^2 + 2\epsilon K\Delta\hat{v} + 2\epsilon\Delta\hat{v}]M \begin{bmatrix} \gamma^2\cos^2\beta & \gamma^2\sin\beta\cos\beta & \gamma\cos\beta \\ \gamma^2\sin\beta\cos & \gamma^2\sin^2\beta & \gamma\sin\beta \\ \gamma\cos\beta & \gamma\sin\beta & 1 \end{bmatrix} M^T \tag{A8}$$

which has the expected value

$$\overline{\Delta\underline{v}\,\Delta\underline{v}^T} = E\left\{ \left[(1 + K^2)E\,\Delta\hat{v}^2 + \epsilon^2\right] M \begin{bmatrix} \overline{\frac{\gamma^2}{2}} & 0 & 0 \\ 0 & \overline{\frac{\gamma^2}{2}} & 0 \\ 0 & 0 & 1 \end{bmatrix} M^T \right\} \tag{A9}$$

The third term of equation (A5) may be expanded to obtain

$$\overline{\Delta\hat{\underline{v}}\,\Delta\underline{v}^T} = [(1 + K)\Delta\hat{v}^2 + \epsilon\Delta\hat{v}]M \begin{bmatrix} 0 & 0 & 0 \\ 0 & 0 & 0 \\ \gamma\cos\beta & \gamma\sin\beta & 1 \end{bmatrix} M^T \tag{A10}$$

which has the expected value

$$\overline{\Delta\hat{\underline{v}}\,\Delta\underline{v}^T} = E\left\{ \Delta\hat{v}^2 M \begin{bmatrix} 0 & 0 & 0 \\ 0 & 0 & 0 \\ 0 & 0 & 1 \end{bmatrix} M^T \right\} \tag{A11}$$

In equation (A5) the last term is as the transpose of the third term; therefore,

$$\overline{\Delta\underline{v}\ \Delta\underline{\hat{v}}^T} = E\left\{\Delta\hat{v}^2 M \begin{bmatrix} 0 & 0 & 0 \\ 0 & 0 & 0 \\ 0 & 0 & 1 \end{bmatrix} M^T\right\} \tag{A12}$$

Combining equations (A7), (A9), (A11), and (A12) with equation (A5), and noting that equations (A7) and (A12) cancel yields

$$\overline{\underline{\eta\eta}^T} = E\left\{\left[(1 + \overline{K^2})\Delta\hat{v}^2 + \overline{\epsilon^2}\right] M \begin{bmatrix} \frac{\overline{\gamma^2}}{2} & 0 & 0 \\ 0 & \frac{\overline{\gamma^2}}{2} & 0 \\ 0 & 0 & 1 \end{bmatrix} M^T - \Delta\hat{v}^2 M \begin{bmatrix} 0 & 0 & 0 \\ 0 & 0 & 0 \\ 0 & 0 & 1 \end{bmatrix} M^T\right\} \tag{A13}$$

Rearranging terms, we have

$$\overline{\underline{\eta\eta}^T} = E\left\{\overline{K^2}\ \Delta\hat{v}^2 M \begin{bmatrix} \frac{\overline{\gamma^2}}{2} & 0 & 0 \\ 0 & \frac{\overline{\gamma^2}}{2} & 0 \\ 0 & 0 & 1 \end{bmatrix} M^T + \overline{\epsilon^2} M \begin{bmatrix} \frac{\overline{\gamma^2}}{2} & 0 & 0 \\ 0 & \frac{\overline{\gamma^2}}{2} & 0 \\ 0 & 0 & 1 \end{bmatrix} M^T + \Delta\hat{v}^2 M \left\{ \begin{bmatrix} \frac{\overline{\gamma^2}}{2} & 0 & 0 \\ 0 & \frac{\overline{\gamma^2}}{2} & 0 \\ 0 & 0 & 1 \end{bmatrix} - \begin{bmatrix} 0 & 0 & 0 \\ 0 & 0 & 0 \\ 0 & 0 & 1 \end{bmatrix} \right\} M^T \right\} \tag{A14}$$

Recognize that K^2 is negligible compared to unity and note that if the velocity is large compared to the cutoff error so that the product $\overline{\epsilon^2\gamma^2}/2$ is small compared to $E(\Delta\hat{v}^2\overline{\gamma^2}/2)$, then we can approximate equation (A14) by

$$\overline{\underline{\eta\eta}^T} = E\left\{\overline{K^2}\ \Delta\hat{v}^2 M \begin{bmatrix} 0 & 0 & 0 \\ 0 & 0 & 0 \\ 0 & 0 & 1 \end{bmatrix} M^T + \overline{\epsilon^2} M \begin{bmatrix} 0 & 0 & 0 \\ 0 & 0 & 0 \\ 0 & 0 & 1 \end{bmatrix} M^T + \frac{\overline{\gamma^2}}{2} \Delta\hat{v}^2 M \left\{ [I] - \begin{bmatrix} 0 & 0 & 0 \\ 0 & 0 & 0 \\ 0 & 0 & 1 \end{bmatrix} \right\} M^T \right\} \tag{A15}$$

where [I] is the unit matrix. Using equation (A7) we can reduce equation (A15) to

$$\overline{\underline{\eta\eta}^T} = \overline{K^2}\ \overline{\Delta\underline{\hat{v}}\ \Delta\underline{\hat{v}}^T} + \frac{\overline{\gamma^2}}{2}\left[\overline{\Delta\hat{v}^2} I - \overline{\Delta\underline{\hat{v}}\ \Delta\underline{\hat{v}}^T}\right] + \overline{\epsilon^2} E\left[\frac{\Delta\underline{\hat{v}}\ \Delta\underline{\hat{v}}^T}{\Delta\hat{v}^2}\right] \tag{A16}$$

If $\Delta\hat{v}$ were spherically distributed (i.e., no preferred direction), then equation (A16) would reduce to the easily computed form

$$\overline{\underline{\eta\eta}^T} = \overline{K^2}\ \overline{\Delta\underline{\hat{v}}\ \Delta\underline{\hat{v}}^T} + \frac{\overline{\gamma^2}}{2}\left[\overline{\Delta\hat{v}^2} I - \overline{\Delta\underline{\hat{v}}\ \Delta\underline{\hat{v}}^T}\right] + \overline{\epsilon^2}\ \frac{\overline{\Delta\underline{\hat{v}}\ \Delta\underline{\hat{v}}^T}}{\overline{\Delta\hat{v}^2}} \tag{A17}$$

Actually $\Delta\hat{v}$ is not in general spherically distributed, but in this study it has been so assumed so that a simple computation could be employed in the S_4 matrix in equation (11).

APPENDIX B

TERMINAL PHASE PERIAPSE GUIDANCE LAW

Consider a vehicle on an interplanetary flight approaching its target planet. The vehicle will be on an orbit with respect to the target which is assumed close to some hyperbolic reference orbit, and which can be described by deviations $\delta\bar{r}(t)$, $\delta\bar{V}(t)$ from that reference orbit. The reference orbit and deviations are the basic information from which the guidance correction is computed, and it is assumed that the deviations are small enough to allow a linearized approximation of the guidance correction.

The objective of the variable arrival time guidance is to adjust the velocity of the vehicle so that

(a) the orbit has the desired periapse range, r_p, and

(b) periapse is located in the reference plane of motion.

No attempt is made to arrive at periapse at some reference time.

DEFINITIONS

$\bar{r},\bar{V}$	vehicle state relative to the target planet
$\bar{U}_r,\bar{U}_h,\bar{N}$	unit vectors in the radial, horizontal, and normal directions where $\bar{U}_r = \frac{\bar{r}}{\lvert\bar{r}\rvert}$; $N = \frac{\bar{r}x\bar{V}}{\lvert\bar{r}x\bar{V}\rvert}$; and $\bar{U}_h = \bar{N}x\bar{U}_r$
r_p	desired value of periapse range
t_c	time at which a guidance correction is made
$\overline{\Delta V}$	the guidance correction
$\dot{r},V_h$	range rate and horizontal speed; $\dot{r} = \bar{V}.\bar{U}_r$, $V_h = \bar{V}.\bar{U}_h$
μ	gravitational constant of the target planet
$(\ )_c$	quantities associated with the reference orbit at t_c
$(\ )_a$	quantities associated with the actual orbit at t_c

THE GUIDANCE CORRECTION

From two-body theory the following relation among $r, r_p, \dot{r}, V_h$ occurs:

$$\left.\begin{aligned} V_h^2 &= \frac{\rho^2}{1-\rho^2}\,\dot{r}^2 + \frac{2\mu}{r}\,\frac{\rho}{1+\rho} \\ \rho &= \frac{r_p}{r} \end{aligned}\right\} \qquad \text{(B1)}$$

If the range, r, and periapse range, r_p, are given, then a hodograph of velocity components $(\dot{r}, V_h)$ which satisfy equations (B1) can be plotted, as in sketch (b).

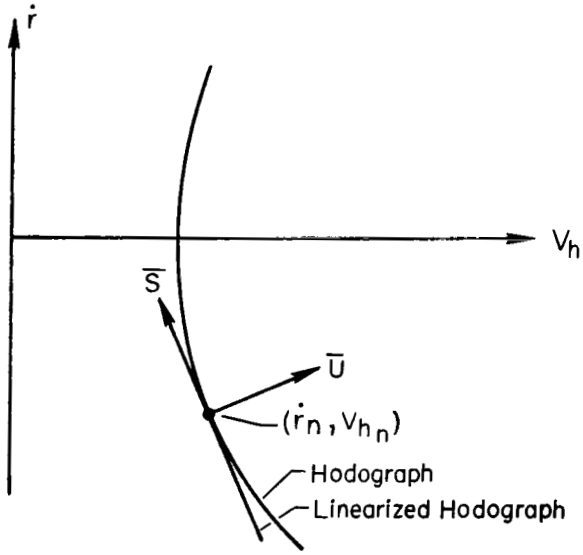

Sketch (b)

At the time of correction, t_c, the vehicle has some state:

$$\left.\begin{aligned} \bar{r}_a &= \bar{r}_c + \delta\bar{r}(t_c) \\ \bar{V}_a &= \bar{V}_c + \delta\bar{V}(t_c) \end{aligned}\right\} \qquad \text{(B2)}$$

The guidance law must correct the state $\bar{r}_a, \bar{V}_a$ to some state $\bar{r}_a, \bar{V}_a + \Delta\bar{V}$ which satisfies equations (B1) for the desired periapse range; that is, the actual velocity vector must be corrected to some point on the hodograph. The directions associated with the velocity components of the hodograph are $\bar{U}_{r_a}$ and $\bar{U}_h$, where $\bar{U}_h$ is to be determined such that it is in the desired plane of motion and the correct sense of orbital rotation about the target is maintained.

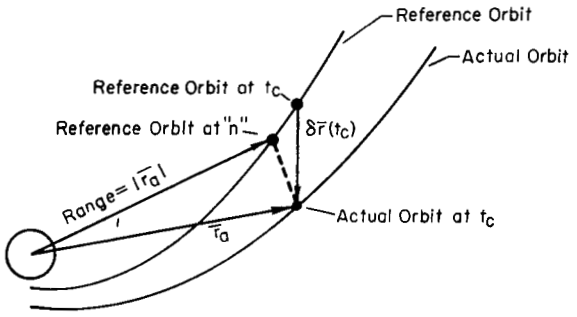

Sketch (c)

The hodograph will be approximated by its slope in the region of interest, that is, by its slope at the point $(\dot{r}_n, V_{h_n})$ which is taken to be the range rate and horizontal speed on the reference orbit at the range r_a (see sketch (c)). These components satisfy equations (B1) for the range r_a since the reference orbit has the desired periapse range. Their values, to a first-order approximation, are given by:

$$\left.\begin{aligned} \dot{r}_n &\cong \dot{r}_c + \left(\frac{d\dot{r}}{dr}\right)_c \Delta r \\ V_{h_n} &\cong V_{h_c} + \left(\frac{dV_h}{dr}\right)_c \Delta r \\ \Delta r &= r_a - r_c \cong \delta\bar{r}\cdot\bar{U}_{r_c} \end{aligned}\right\} \qquad \text{(B3)}$$

where

The derivatives in equations (B3) are taken along the reference orbit at t_c.

$$\left.\begin{aligned} \left(\frac{d\dot{r}}{dr}\right)_c &= \frac{1}{\dot{r}_c r_c}\left(V_{h_c}^2 - \frac{\mu}{r_c}\right) \\ \left(\frac{dV_h}{dr}\right)_c &= -\frac{V_{h_c}}{r_c} \end{aligned}\right\} \qquad \text{(B4)}$$

Let $\bar{U}_{r_a}, \bar{U}_h$ be the radial and horizontal unit vectors in the desired plane of motion, and let $\bar{U}, \bar{S}$ be the unit normal and tangent vectors to the hodograph at $(\dot{r}_n, V_{h_n})$. The unit vectors $\bar{U}, \bar{S}$ may be obtained by substituting equations (B3) and (B4) into (B1), giving

$$\left.\begin{aligned} \bar{U} &= (-\alpha_n \bar{U}_{r_a} + \bar{U}_h)/\sqrt{1 + \alpha_n^2} \\ \bar{S} &= (\bar{U}_{r_a} + \alpha_n \bar{U}_n)/\sqrt{1 + \alpha_n^2} \end{aligned}\right\} \qquad \text{(B5)}$$

where

$$\alpha_n = \frac{\rho_a^2}{1 - \rho_a^2}\tan\gamma_n$$

$$\tan\gamma_n = \frac{\dot{r}_n}{V_{h_n}}, \qquad \rho_a = \frac{r_p}{r_a}$$

All velocity vectors on the linearized hodograph are then of the form

$$\left.\begin{aligned} \bar{V} &= \bar{V}_n + C\bar{S} \\ \bar{V}_n &= \dot{r}_n \bar{U}_{r_a} + V_{h_n}\bar{U}_h \\ C &= \text{arbitrary constant} \end{aligned}\right\} \qquad \text{(B6)}$$

where

The optimum correction (minimum distance from $\bar{V}_a$ to the linearized hodograph) is the one which just cancels out the part of the vector $\bar{V}_a - \bar{V}_n$ which is perpendicular to the hodograph; that is, the guidance correction is

$$\Delta\bar{V} = (\bar{V}_n - \bar{V}_a) - [(\bar{V}_n - \bar{V}_a).\bar{S}]\bar{S} \tag{B7}$$

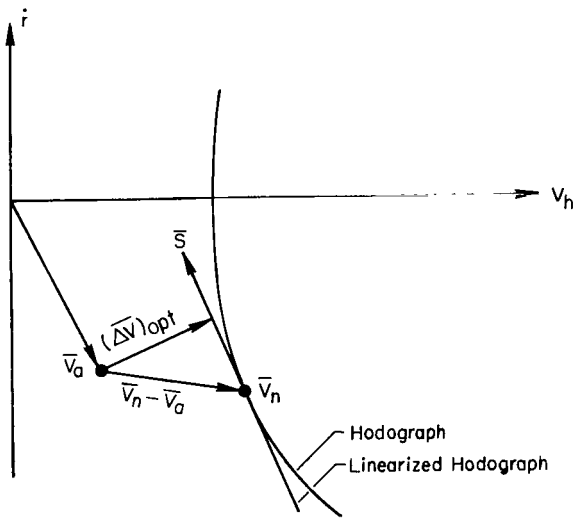

Sketch (d)

Sketch (d) illustrates a case in which the actual velocity, $\bar{V}_a$, lies in the desired plane of motion. A change in velocity to any point on the linearized hodograph will give the desired periapse range to a first-order approximation, but the smallest correction is the one which cancels only the deviation of $\bar{V}_a$ normal to the vector, $\bar{S}$.

PLANE OF MOTION

All the quantities involved in equation (B7) are known except $\bar{U}_h$, the unit horizontal vector in the plane of the corrected orbit. This vector is determined so that periapse is located in the plane of the reference orbit and that the corrected orbit has the same sense of rotation around the target planet as the reference orbit. It may be noted that the reference approach orbit may be very nearly radial at entrance to the sphere of influence of the target so that the deviated orbit may have a sense of rotation opposite to the reference orbit even for small deviations $\delta\bar{r}, \delta\bar{V}$.

Let

θ = true anomaly on the corrected orbit at t_c

$$\bar{U}_{r_a} = \bar{U}_{r_c} + \Delta\bar{U}_r \tag{B8}$$

then

$$\Delta\bar{U}_r = \frac{\bar{r}_a}{r_a} - \frac{\bar{r}_c}{r_c} \cong \frac{1}{r_c}\left[\delta\bar{r} - (\delta\bar{r}.\bar{U}_{r_c})\bar{U}_{r_c}\right]$$

Assume that θ and $\bar{U}_h$ differ from θ_c and $\bar{U}_{h_c}$ by small quantities

$$\theta = \theta_c + \Delta\theta$$

$$\bar{U}_h = \bar{U}_{h_c} + \Delta\bar{U}_h$$

This form of $\bar{U}_h$ gives the correct sense of rotation - the assumption $\bar{U}_h = -\bar{U}_{h_c} + \Delta\bar{U}_h$ would reverse the rotation. The periapse position on the corrected orbit is

$$\bar{U}_p = \cos\theta\bar{U}_{r_a} + \sin\theta\bar{U}_h$$

Since we require that $\bar{U}_p$ be in the reference plane of motion (see sketch (e)), then

$$\bar{U}_p\cdot\bar{N}_c = 0 = \cos\theta\,\Delta\bar{U}_r\cdot\bar{N}_c + \sin\theta\,\Delta\bar{U}_h\cdot\bar{N}_c$$

Second-order quantities in this equation are neglected and, assuming θ is not near zero, the normal component of $\Delta\bar{U}_h$ is found to be

$$\Delta\bar{U}_h\cdot\bar{N}_c = -\text{ctn}\,\theta_c\,\frac{\delta\bar{r}\cdot\bar{N}_c}{r_c}$$

Similarly, $\bar{U}_h$ is perpendicular to $\bar{U}_{r_a}$, so

$$\bar{U}_h\cdot\bar{U}_{r_a} = 0 = \bar{U}_{h_c}\cdot\Delta\bar{U}_r + \bar{U}_{r_c}\cdot\Delta\bar{U}_h$$

After the expression for $\Delta\bar{U}_r$ in equation (B8) is introduced, this yields the radial component of $\Delta\bar{U}_h$ as:

$$\Delta\bar{U}_h\cdot\bar{U}_{r_c} = -\frac{\delta\bar{r}\cdot\bar{U}_{h_c}}{r_c}$$

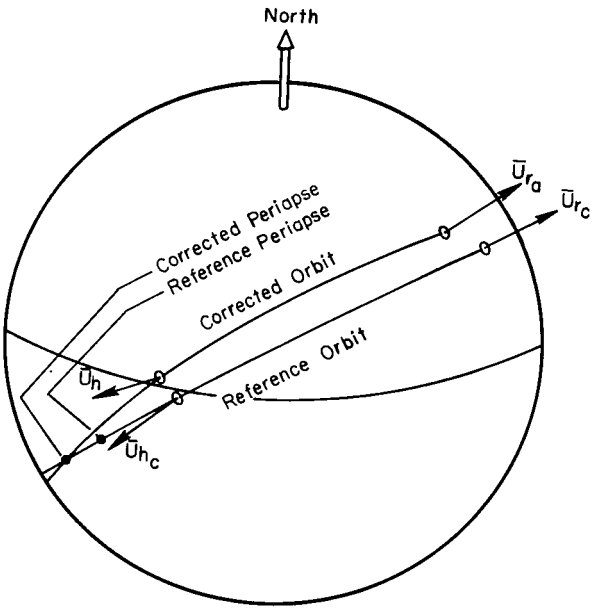

Sketch (e)

Finally, $\Delta\bar{U}_h\cdot\bar{U}_{h_c}$ is negligible. The vector $\bar{U}_h$ is therefore

$$\bar{U}_h \cong \bar{U}_{h_c} - \text{ctn}\,\theta_c\,\frac{\delta\bar{r}\cdot\bar{N}_c}{r_c}\,\bar{N}_c - \frac{\delta\bar{r}\cdot\bar{U}_{h_c}}{r_c}\,\bar{U}_{r_c} \qquad \text{(B9)}$$

GUIDANCE LAW

The guidance law, equation (B7), can now be reduced to final form. The vector $\bar{V}_n$ differs from the reference velocity, $\bar{V}_c$, by a small quantity and hence can be written as,

$$\bar{V}_n = \bar{V}_c + \Delta\bar{V}_n$$

where $\Delta\bar{V}_n$ can be obtained by introducing the expressions in equations (B3), (B8), and (B9) into equation (B6)

$$\Delta\bar{V}_n = \left[\left(\frac{d\dot{r}}{dr}\right)_c \delta\bar{r}.\bar{U}_{r_c} - \frac{V_{h_c}}{r_c}\,\delta\bar{r}.\bar{U}_{h_c}\right]\bar{U}_{r_c}$$

$$+ \left[\left(\frac{dV_h}{dr}\right)_c \delta\bar{r}.\bar{U}_{r_c} + \frac{\dot{r}_c}{r_c}\,\delta\bar{r}.\bar{U}_{h_c}\right]\bar{U}_{h_c}$$

$$+ \left(\frac{\dot{r}_c}{r_c} - \frac{V_{h_c}}{r_c}\,\text{ctn}\,\theta_c\right)(\delta\bar{r}.\bar{N}_c)\bar{N}_c + \text{second-order quantities} \qquad \text{(B10)}$$

By use of equations (B2), the factor $\bar{V}_n - \bar{V}_a$ which appears in the guidance law becomes

$$\bar{V}_n - \bar{V}_a = \Delta\bar{V}_n - \delta\bar{V}$$

The unit vector, $\bar{S}$, differs from $\bar{S}_c$ by a small quantity, so that the guidance equation, to first order in small quantities, is

$$\Delta\bar{V} \cong (\Delta\bar{V}_n - \delta\bar{V}) - [(\Delta\bar{V}_n - \delta\bar{V}).\bar{S}_c]\bar{S}_c \qquad \text{(B11)}$$

where

$$\bar{S}_c = (\bar{U}_{r_c} + \alpha_c\bar{U}_{h_c})/\sqrt{1 + \alpha_c{}^2}$$

$$\bar{U}_c = (-\alpha_c\bar{U}_{r_c} + \bar{U}_{h_c})/\sqrt{1 + \alpha_c{}^2}$$

$$\alpha_c = \frac{\rho_c{}^2}{1 - \rho_c{}^2}\tan\gamma_c, \qquad \tan\gamma_c = \frac{\dot{r}_c}{V_{h_c}}, \qquad \rho_c = \frac{r_p}{r_c}$$

and equation (B11), after utilizing (B10), reduces to

$$\Delta\bar{V} \cong \bar{U}_c(\bar{W}.\delta\bar{r} - \bar{U}_c.\delta\bar{V}) + \bar{N}_c(K\delta\bar{r}.\bar{N}_c - \delta\bar{V}.\bar{N}_c) \qquad \text{(B12)}$$

where

$$\bar{W} = \left\{\left[-\alpha_c\left(\frac{d\dot{r}}{dr}\right)_c + \left(\frac{dV_h}{dr}\right)_c\right]\bar{U}_{r_c} + \frac{1}{1 - \rho_c{}^2}\,\frac{\dot{r}_c}{r_c}\,\bar{U}_{h_c}\right\}\Big/\sqrt{1 + \alpha_c{}^2}$$

$$K = \frac{\dot{r}_c}{r_c} - \frac{V_{h_c}}{r_c}\,\text{ctn}\,\theta_c$$

The derivatives which appear in $\bar{W}$ have already been given in equations (B4). The coefficient of $\bar{N}_c$ in the guidance law adjusts the plane of motion and depends only on the components of $\delta\bar{r},\delta\bar{V}$ normal to the reference orbital plane. The coefficient of $\bar{U}_c$ adjusts the velocity vector to obtain the desired periapse range and depends only on the components of $\delta\bar{r},\delta\bar{V}$ in the reference orbital plane. The response to a velocity deviation, $\delta\bar{V}$, is to cancel all of $\delta\bar{V}$ except for the part along $\bar{S}_c$ which does not, to first order, affect the periapse range.

In the notation of the text, let x be the deviation state vector. Equation (B12) then has the form:

$$\Delta\bar{V} = [(\bar{U}_c\bar{W}^T + K\bar{N}_c\bar{N}_c{}^T) \quad -(\bar{U}_c\bar{U}_c{}^T + \bar{N}_c\bar{N}_c{}^T)]x \tag{B13}$$

The following form can also be obtained (refer to eq. (B11))

$$\Delta\bar{V} = (I-\bar{S}_c\bar{S}_c{}^T)(B \quad -I)x \tag{B14}$$

where

$$B = \left(\frac{d\dot{r}}{dr}\right)_c \bar{U}_{r_c}\bar{U}_{r_c}{}^T - \frac{V_{h_c}}{r_c}\left(\bar{U}_{r_c}\bar{U}_{h_c}{}^T + \bar{U}_{h_c}\bar{U}_{r_c}{}^T\right) + \frac{\dot{r}_c}{r_c}\bar{U}_{h_c}\bar{U}_{h_c}{}^T + K\bar{N}_c\bar{N}_c{}^T$$

Equation (B14) may be compared to the fixed-time-of-arrival guidance law in which the factor $(A_2{}^{-1}A_1 \quad -I)$ is analogous to the factor $(B \quad -I)$ of (B14). The factor $(I-\bar{S}_c\bar{S}_c{}^T)$ is the effect of optimizing the guidance correction, since, if the correction were not optimized, then the guidance law would be

$$\Delta\bar{V} = \bar{V}_n - \bar{V}_a = \Delta\bar{V}_n - \delta\bar{V} = (B \quad -I)x$$

PERIAPSE MISS DISTANCE

The goal of the terminal guidance system is to obtain the desired value of periapse. A quantity of special interest to the statistical analysis of the text is, therefore, the error in achieving this goal.

The hodograph equations (B1) can be inverted to obtain an expression for r_p as follows:

$$r_p = \frac{\mu}{V^2 - 2(\mu/r)}\left[\sqrt{1 + \frac{V_h^2}{\mu/r}\left(\frac{V^2}{\mu/r} - 2\right)} - 1\right] \tag{B15}$$

where equation (B15) assumes hyperbolic orbits $[V^2/(\mu/r) > 2]$. This expression gives the periapse range as a function of the independent variables, r, V_h^2, V^2, whose values on the actual orbit differ from their reference values by small amounts. Hence, the periapse miss distance can be computed from the linear approximation:

$$\Delta r_p = \left(\frac{\partial r_p}{\partial r}\right)_c \Delta r + \left(\frac{\partial r_p}{\partial V_h^2}\right)_c \Delta V_h^2 + \left(\frac{\partial r_p}{\partial V^2}\right)_c \Delta V^2 \tag{B16}$$

The derivatives in this equation are obtained from equation (B15):

$$\left.\begin{aligned}
\left(\frac{\partial r_p}{\partial r}\right)_c &= \rho_c \frac{V_{h_c}^2 - \rho_c^2 \frac{\mu}{r_c}}{V_{h_c}^2 - \rho_c \frac{\mu}{r_c}} \\
\left(\frac{\partial r_p}{\partial V_h^2}\right)_c &= \frac{1}{2} \frac{r_p}{V_{h_c}^2 - \rho_c \frac{\mu}{r_c}} \\
\left(\frac{\partial r_p}{\partial V^2}\right)_c &= -\rho_c^2 \left(\frac{\partial r_p}{\partial V_h^2}\right)_c
\end{aligned}\right\} \tag{B17}$$

The deviations of the independent variables, Δr, ΔV^2, ΔV_h^2, are related to the state deviations, to first order, by

$$\left.\begin{aligned}
\Delta r &\cong \delta\bar{r} \cdot \bar{U}_{r_c} \\
\Delta V_h^2 &\cong 2V_{h_c} \bar{U}_{h_c} \cdot \left(\delta\bar{r} - \frac{\dot{r}_c}{r_c} \delta\bar{r}\right) \\
\Delta V^2 &\cong 2\bar{V}_c \cdot \delta\bar{r}
\end{aligned}\right\} \tag{B18}$$

Substituting equations (B18) into (B16) gives

$$\begin{aligned}
\Delta r_p \cong & \left[\left(\frac{\partial r_p}{\partial r}\right)_c \bar{U}_{r_c} - 2 \frac{\dot{r}_c V_{h_c}}{r_c} \left(\frac{\partial r_p}{\partial V_h^2}\right)_c \bar{U}_{h_c} \right] \cdot \delta\bar{r} \\
& + \left\{ 2\dot{r}_c \left(\frac{\partial r_p}{\partial V^2}\right)_c \bar{U}_{r_c} + 2V_{h_c} \left[\left(\frac{\partial r_p}{\partial V_h^2}\right)_c + \left(\frac{\partial r_p}{\partial V^2}\right)_c \right] \bar{U}_{h_c} \right\} \cdot \delta\bar{V} \\
\cong & \bar{Z}_1 \cdot \delta\bar{r} + \bar{Z}_2 \cdot \delta\bar{V}
\end{aligned} \tag{B19}$$

where $\bar{Z}_1, \bar{Z}_2$ are substitute symbols for the expressions in the brackets. By use of equations (B17) the vectors, $\bar{Z}_1, \bar{Z}_2$, become

$$\left.\begin{aligned}
\bar{Z}_1 &= \rho_c \frac{H_c^2}{H_c^2 - \mu r_p}\left[\left(1 - \rho_c \frac{\mu r_p}{H_c^2}\right)\bar{U}_{r_c} - \tan\gamma_c \bar{U}_{h_c}\right] \\
\bar{Z}_2 &= \frac{H_c r_p r_c}{H_c^2 - \mu r_p}\left[-\rho_c^2 \tan\gamma_c \bar{U}_{r_c} + (1 - \rho_c^2)\bar{U}_{h_c}\right]
\end{aligned}\right\} \qquad \text{(B20)}$$

where H_c is the reference angular momentum $r_c V_{h_c}$.

Finally, in the notation of the text, let Z,x be sextuples of periapse derivatives (given by eqs.(B20)) and state deviations

$$\left.\begin{aligned}
Z^T &= \left[\left(\frac{\partial r_p}{\partial x}\right)_c, \left(\frac{\partial r_p}{\partial y}\right)_c, \ldots, \left(\frac{\partial r_p}{\partial \dot{z}}\right)_c\right] \\
x^T &= (\delta x, \delta y, \ldots, \delta \dot{z})
\end{aligned}\right\} \qquad \text{(B21)}$$

and then equation (B19) has the form

$$\Delta r_p = Z^T x \qquad \text{(B22)}$$

REFERENCES

1. Jones, A. L., et al.: Manned Mars Landing and Return Mission Study. Vol. 1 - Condensed Summary (SID 64-619-1); Vol. 2 - Operational Considerations (SID 64-619-2); Vol. 3 - Subsystems Technologies (SID 64-619-3); Vol. 4 - System Integration Design and Evaluation (SID 64-619-4). North American Aviation, Inc., Space and Information Systems Div., April 1964.

2. Sohn, R. L., et al.: Manned Mars Mission Study. Vols. I and II (8572-6011-RU-000), Thompson Ramo Wooldridge, Inc., Space Technology Labs., March 1964.

3. Smith, Gerald L.: Schmidt, Stanley F.; and McGee, Leonard A.: Application of Statistical Filter Theory to the Optimal Estimation of Position and Velocity On Board a Circumlunar Vehicle. NASA TR R-135, 1962.

4. McLean, John D.; Schmidt, Stanley F.; and McGee, Leonard A.: Optimal Filtering and Linear Prediction Applied to a Midcourse Navigation System for the Circumlunar Mission. NASA TN D-1208, 1962.

5. Smith, Gerald L.: Secondary Errors and Off-Design Conditions in Optimal Estimation of Space Vehicle Trajectories. NASA TN D-2129, 1964.

6. Martin Marietta Corp.: Design Guide to Orbital Flight. McGraw-Hill, 1962.

7. Herget, Paul: The Computation of Orbits. Published privately by the author, Cincinnati, 1948.

8. The American Ephemeris and Nautical Almanac, U.S. Government Printing Office, Washington, D.C., 1964.

9. Explanatory Supplement to the Astronomical Ephemeris and the American Ephemeris and Nautical Almanac. London, Her Majesty's Stationery Office, 1961.

10. Stern, Robert G.: Interplanetary Midcourse Guidance Analysis. Experimental Astronomy Laboratory, Massachusetts Institute of Technology Rept. TE-5, May 1963.

11. Battin, Richard H.: A Statistical Optimizing Navigation Procedure for Space Flight. Instrumentation Laboratory, Massachusetts Institute of Technology Rept. R-341, Sept. 1961.

TABLE I.- PLANETARY AND SATELLITE REFERENCE ORBITAL ELEMENTS;
EQUINOX AND ECLIPTIC OF JANUARY 6.0, 1964

Planet or satellite	Inclination		Longitudinal node		Longitudinal periapse		Major axis	Eccentricity	Mean anomaly	Mean motion
Mercury	7.00406	+1	47.90470	-58	76.89552	+43	0.387099	0.205627	23.10500	4.092339
Venus	3.39427	0	76.35583	-136	131.06475	+2	.723332	.006790	231.20800	1.602130
Earth	0	0	0	0	102.32127	+87	1.000000	.016724	2.30280	.985600
Mars	1.84991	0	49.27997	-172	335.39657	+121	1.523691	.093372	331.39700	.524033
Jupiter	1.30480	0	100.06194	-105	13.75575	+59	5.202800	.048452	189.58047	.083091
Saturn	2.48947	0	113.31120	-137	92.37681	+154	9.538840	.055647	310.54525	.033460
Moon	5.14540	0	101.09490	+529900	59.00840	+1114000	60.266500	.054900	285.62430	13.064992
Deimos	37.41647	-111	49.57362	-173	324.50357	+174800	7.040000	.003100	312.48000	285.16196
Phobos	37.71684	-112	49.30517	-167	87.69350	+4326000	2.815000	.017000	184.32000	1128.8441

Variations are specified per 100 days in units of the fifth decimal place with respect to the fixed equinox. Angles are in degrees; major axis is in AU for the planets and in planet radii for the satellites.

TABLE II.- TRAJECTORY CONDITIONS

Trajectory and leg	Departure conditions				Arrival conditions		
	Date	Velocity, km/sec	Altitude, km	Trip time, days	Date	Velocity, km/sec	Altitude, km
High speed Earth to Mars	May 31.57, 1971	11.761	160.00	112.43	Sept. 21.00, 1971	8.49	-3.54
High speed Mars to Earth	Sept. 27.22, 1971	9.813	300.32	190.77	April 4.98, 1972	14.26	-2.96
Low speed Earth to Mars	June 1.95, 1971	11.469	159.79	153.02	Nov. 1.97, 1971	6.25	16.14
Low speed Mars to Earth	Nov. 7.97, 1971	8.053	299.62	251.02	July 15.99, 1972	15.49	4.49
Venus swingby Earth to Mars	Sept. 9.49, 1975	12.020	159.27	170.01	Feb. 26.49, 1976	7.76	26.43
Venus swingby Mars to Venus	March 27.55, 1976	7.097	499.90	185.54	Sept. 29.10, 1976	14.69	3363.59
Venus swingby Venus to Earth	Sept. 28.54, 1976	14.992	3349.96	124.94	Jan. 31.48, 1977	13.91	-11.06

Velocity and altitude are at periapse of the vacuum hyperbola. Dates are given in universal time.

TABLE III.- NOMINAL RMS ERROR VALUES, 1σ

Initial Deviation and Uncertainty

Altitude	3.2187 km	or	2 miles
Downrange	4.8285 km	or	3 miles
Crossrange	1.60935 km	or	1 mile
Vertical velocity	4.47 m/sec	or	10 miles/hr
Downrange velocity	1.788 m/sec	or	4 miles/hr
Crossrange velocity	1.341 m/sec	or	3 miles/hr

Errors in Making Velocity Correction

Magnitude	1 percent
Direction	1 degree
Cutoff	0.2 m/sec

Errors in Measuring Velocity Correction

1 cm/sec, equally likely in all directions

Observation Noise

Instrument Error, Q_{inst}	10 seconds of arc
Radius uncertainty/planet radius, c	0.001 (Sun, Mercury, Venus, Earth, Mars, Jupiter, Saturn, Moon)
	0.01 (Deimos, Phobos)
Position uncertainty, δ_{rs}	1 km (Sun, Mercury, Venus, Earth, Mars, Jupiter, Saturn, Moon)
	100 km (Deimos, Phobos)

TABLE IV.- EFFECT OF OBSERVING THE SUN OR OTHER PLANETS IN ADDITION TO THE DEPARTURE AND TARGET PLANETS

High-speed mission

Predicted uncertainty at arrival, km

Other observed bodies	Time, days - outbound leg				
	3	35	67	106	
None	18,812	16,585	8,863	1,740	
Sun	18,812	15,757	8,610	1,734	
Mercury	18,812	16,186	8,540	1,738	
Venus	18,812	16,015	8,696	1,736	
Jupiter	18,812	16,535	8,819	1,738	
Saturn	18,812	16,585	8,862	1,740	
Sun[a]	18,812	10,861	4,140	931	
	Time, days - return leg				
	2	69	135	171	189
None	130,425	33,862	5,358	1,534	686
Sun	130,425	32,812	7,545	1,474	682
Mercury, Venus	130,425	30,720	8,759	1,526	689
Sun[a]	130,425	9,592	1,790	584	336

[a]Daily observations of Earth, Mars, and Sun.

TABLE V.- EFFECT OF DAILY OBSERVATION SCHEDULE, VENUS SWINGBY MISSION OBSERVING THE DEPARTURE AND TARGET PLANETS, AND THE SUN

Predicted uncertainty at arrival, km

Observation schedule	Earth-Mars leg			
	3 days	53 days	108 days	161 days
Minimum	3,797	3,738	3,070	1,053
Daily	3,797	3,466	1,639	506
	Mars-Venus leg			
	3	63	123	179
Minimum	105,695	71,565	19,992	1,154
Daily	101,587	21,376	7,936	493
	Venus-Earth leg			
	2	39	79	118
Minimum	2,568	2,468	2,003	599
Daily	2,610	2,043	935	437

TABLE VI.- EFFECT OF EARLY REDUCTION OF UNCERTAINTY ON FUEL USED
(rms values)

	Time, days	Observations: Moon (high early accuracy)	Observations: Moon (180) (low early accuracy)
First ΔV	2.4	11.29	11.26
Uncertainty		676.37	13,282.54
Second ΔV	106.0	7.04	22.08
Uncertainty		534.43	2,138.30
Last ΔV	112.3	39.19	161.63
Uncertainty		240.41	271.33
Total corrective velocity[a]		57.53	195.01
Arrival miss: Vertical		8.10	23.85
Arrival miss: Downrange		240.42	272.29
Arrival miss: Crossrange		4.84	18.66

[a]Velocity corrections in meters/sec. Uncertainties and miss in km.

TABLE VII.- OBSERVATION SCHEDULE

(a) High-speed mission, outbound leg

Time, days		Observations	
Initial time	Increment	Number	Body
0.04	0.01	10	Earth
.14	.01	10	Moon (180)
.3	.1	4	Earth
.7	.1	6	Moon (180)
1.3	.1	6	Earth
1.9	.1	5	Moon (180)
2.4	Velocity correction		
3.0	1.0	98[a]	Earth and Mars
100.5	Velocity correction		
101.0	1.0	10[a]	Earth and Mars
110.1	.1	14	Mars
111.5	.05	8	Mars
111.9	Velocity correction[b]		
111.95		1	Mars
112.0	.01	29	Mars
112.3	Velocity correction[b]		
112.32	.01	9	Mars
112.43			Periapse (Mars)

[a]Each observation is of two bodies.

[b]This correction was either fixed time of arrival, or radius of periapse control, depending on the guidance law under study.

TABLE VII.- OBSERVATION SCHEDULE - Continued

(b) High-speed mission, return leg

Time, days			Observations
Initial time	Increment	Number	Body
0.1	0.1	20	Mars
3.0	1.0	85[a]	Mars and Earth
87.5	Velocity correction		
88.0	1.0	79[a]	Mars and Earth
166.5	Velocity correction		
167.0	1.0	12[a]	Mars and Earth
179.0	.5	19[a]	Earth and Moon (180)
188.5	.1	4	Earth
188.9	.1	4	Moon (180)
189.3	.1	3	Earth
189.6	Velocity correction[b]		
189.7	.1	3	Moon (180)
190.0	.02	5	Earth
190.1	.02	5	Moon (180)
190.2	.01	9	Earth
190.3	.01	9	Moon (180)
190.4	.01	9	Earth
190.5	Velocity correction[b]		
190.55	.05	4	Earth
190.77			Perigee

[a]Each observation is of two bodies.

[b]This correction was either fixed time of arrival, or radius of periapse control, depending on the guidance law under study.

TABLE VII.- OBSERVATION SCHEDULE - Continued

(c) Low-speed mission, outbound leg

Time, days			Observations
Initial time	Increment	Number	Body
0.04	0.01	10	Earth
.14	.01	10	Moon (180)
.3	.1	4	Earth
.7	.1	6	Moon (180)
1.3	.1	6	Earth
1.9	.1	5	Moon (180)
2.4	Velocity correction		
3.0	1.0	139[a]	Mars and Earth
141.5	Velocity correction		
142.0	1.0	9[a]	Mars and Earth
150.5	.1	15	Mars
152.0	.05	9	Mars
152.45	Velocity correction[b]		
152.50	.01	34	Mars
152.85	Velocity correction[b]		
152.87	.01	9	Mars
153.02			Periapse (Mars)

[a]Each observation is of two bodies.

[b]This correction was either fixed time of arrival, or radius of periapse control, depending on the guidance law under study.

TABLE VII.- OBSERVATION SCHEDULE - Continued

(d) High-speed mission, return leg

Time, days			Observations
Initial time	Increment	Number	Body
0.1	0.1	20	Mars
3.0	1.0	90[a]	Mars and Earth
92.5	Velocity correction		
93.0	1.0	135[a]	Mars and Earth
227.5	Velocity correction		
228.0	1.0	12[a]	Mars and Earth
240.0	.5	18[a]	Earth and Moon
248.6	.1	4	Earth
249.0	.1	4	Moon
249.4	.1	4	Earth
249.8	.1	4	Moon
250.2	Velocity correction[b]		
250.3	.01	9	Earth
250.4	.01	9	Moon
250.5	.01	9	Earth
250.6	.01	9	Moon
250.7	.01	9	Earth
250.8	Velocity correction[b]		
250.85	.05	3	Earth
251.02			Perigee

[a]Each observation is of two bodies.

[b]This correction was either fixed time of arrival, or radius of periapse control, depending on the guidance law under study.

TABLE VII.- OBSERVATION SCHEDULE - Continued

(e) Venus swingby mission, outbound leg

Time, days			Observations
Initial time	Increment	Number	Body
0.04	0.01	10	Earth
.14	.01	10	Moon (180)
.24	.01	6	Earth
.30	.1	4	Earth
.70	.1	4	Moon (180)
1.10	.1	4	Earth
1.50	.1	4	Moon (180)
1.90	.1	4	Earth
2.30	Velocity correction		
3.0	1.0	159[a]	Earth and Mars
160.5	Velocity correction		
161.0	1.0	15[a]	Earth and Mars
168.5	.1	10	Mars
169.5	.02	8	Mars
169.66	Velocity correction[b]		
169.68	.02	10	Mars
169.88	Velocity correction[b]		
169.90	.02	4	Mars
170.01			Periapse (Mars)

[a]Each observation is of two bodies.

[b]This correction was either fixed time of arrival, or radius of periapse control, depending on the guidance law under study.

TABLE VII.- OBSERVATION SCHEDULE - Continued

(f) Venus swingby mission, Mars-Venus leg

Time, days			Observations
Initial time	Increment	Number	Body
0.1	0.02	10	Mars
.3	.1	27	Mars
3.0	1.0	48[a]	Mars and Venus
50.5	Velocity correction		
51.0	1.0	99[a]	Mars and Venus
149.5	Velocity correction		
150.0	1.0	10[a]	Mars and Venus
160.0	.5	38[a]	Mars and Venus
179.0	Velocity correction		
179.5	.5	8[a]	Mars and Venus
183.5	.1	10	Venus
184.5	.05	10	Venus
185.0	.02	10	Venus
185.2	Velocity correction[b]		
185.22	.02	17	Venus
185.54			Periapse (Venus)

[a]Each observation is of two bodies.

[b]This correction was either fixed time of arrival, or radius of periapse control, depending on the guidance law under study.

TABLE VII.- OBSERVATION SCHEDULE - Concluded
(g) Venus swingby mission, return leg

Time, days		Observations	
Initial time	Increment	Number	Body
0.02	0.02	30	Venus
.62	Velocity correction		
.7	.1	13	Venus
2.0	1.0	80[a]	Venus and Earth
82.5	Velocity correction		
83.0	1.0	17[a]	Venus and Earth
100.0	.5	46[a]	Venus and Earth
123.0	Velocity correction		
123.5	.05	3	Moon (180)
123.65	.05	3	Earth
123.8	.05	3	Moon (180)
123.95	.05	3	Earth
124.1	.05	2	Moon (180)
124.2	.01	9	Earth
124.3	.01	9	Moon (180)
124.4	.01	9	Earth
124.5	.01	9	Moon (180)
124.6	.01	9	Earth
124.7	Velocity correction[b]		
124.72	.01	16	Earth
124.94			Perigee

[a]Each observation is of two bodies.

[b]This correction was either fixed time of arrival, or radius of periapse control, depending on the guidance law under study.

TABLE VIII.- FUEL REQUIREMENTS AND MISS

(a) Fixed-time-of-arrival guidance

Mission	Leg	Size of midcourse corrections, m/sec					Radius of periapse miss, km	Downrange miss, km	Allowable corridor, km
		First	Second	Third	Fourth	Total			
High speed	Outbound	11.27	10.77	17.20	53.64	92.88	8.8	181	30-50
	Return	10.51	2.83	7.33	11.13	31.80	4.7	61	30
Low speed	Outbound	13.29	12.57	23.87	42.55	92.30	8.1	108	30-50
	Return	11.47	7.37	9.60	10.14	38.58	4.6	67	30
Venus swingby	Outbound	10.29	20.18	16.08	24.23	70.78	5.4	157	30-50
	Mars-Venus	9.40	15.00	4.57	12.66	41.63	9.4	359	---
	Return	25.20	3.41	7.98	16.81	53.42	5.0	33	30
(b) Radius-of-periapse guidance									
High speed	Outbound	11.27[a]	10.77[a]	5.68	1.14	28.86	4.8	1173	30-50
	Return	10.51[a]	2.83[a]	6.07	1.43	20.84	5.0	741	30
Low speed	Outbound	13.29[a]	12.57[a]	4.97	1.07	31.93	4.2	1981	30-50
	Return	11.47[a]	7.37[a]	8.83	1.52	29.19	4.8	457	30
Venus swingby	Outbound	10.29[a]	20.18[a]	10.32	.79	41.61	4.6	590	30-50
	Mars-Venus	9.40[a]	15.00[a]	4.57[a]	5.33	34.30	9.6	540	---
	Return	16.79[a]	2.62[a]	7.92[a]	2.41	29.75	4.2	518	30

[a]Fixed time of arrival guidance was used for these corrections.

TABLE IX.- EFFECT OF INITIAL DISPERSION AND RMS UNCERTAINTY
(rms values)

High-speed mission, outbound leg

	Size of midcourse corrections, m/sec				Radius of periapse miss, km	Downrange miss, km
	First	Second	Third	Total		
Reference case	11.27	22.08	161.66	195.01	23.8	272
5 times initial dispersion	56.45	30.33	162.91	249.69	24.0	273
5 times initial dispersion and 5 times initial rms uncertainty	56.44	32.93	174.31	263.68	25.6	273

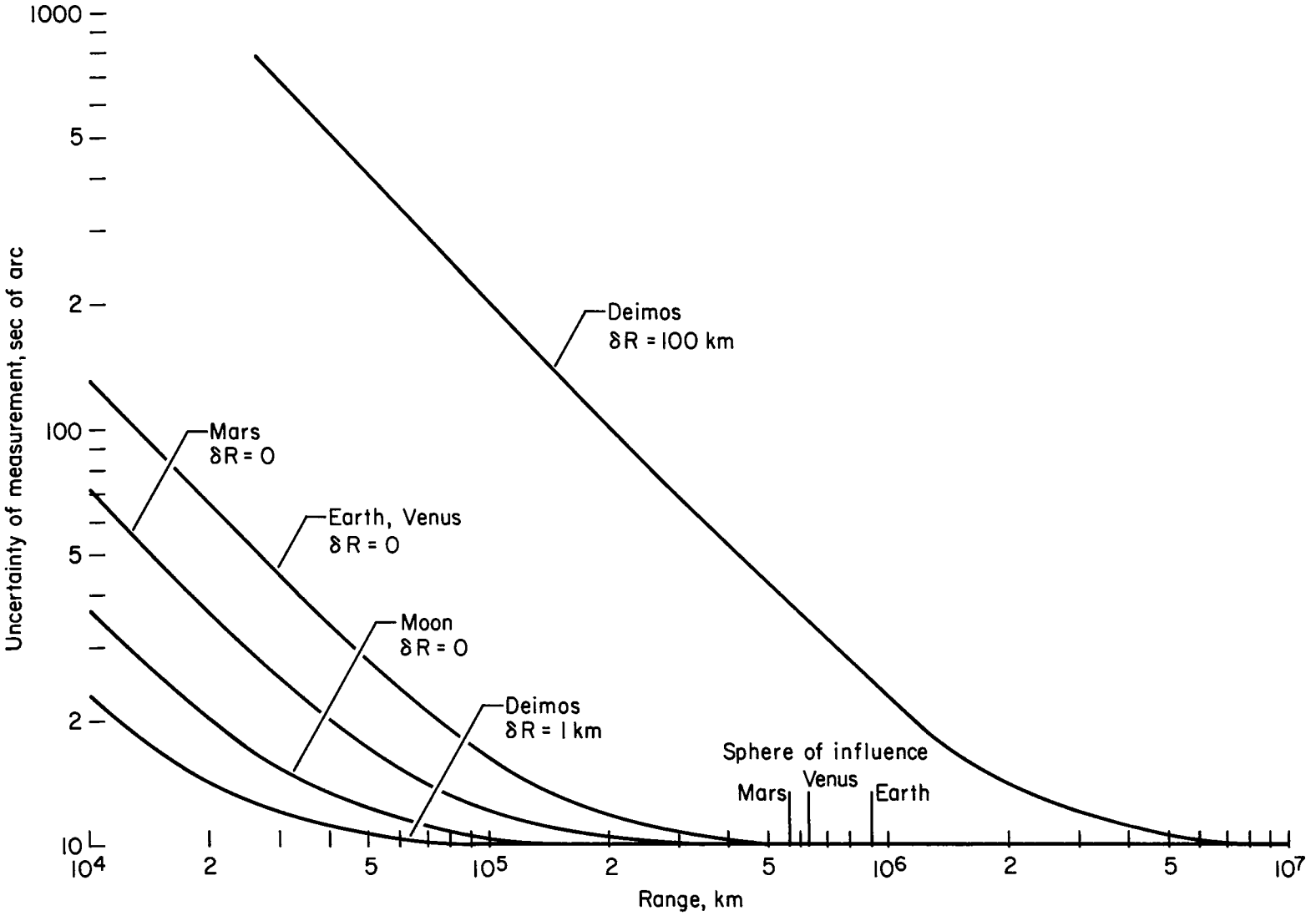

Figure 1.- Observation noise for several bodies.

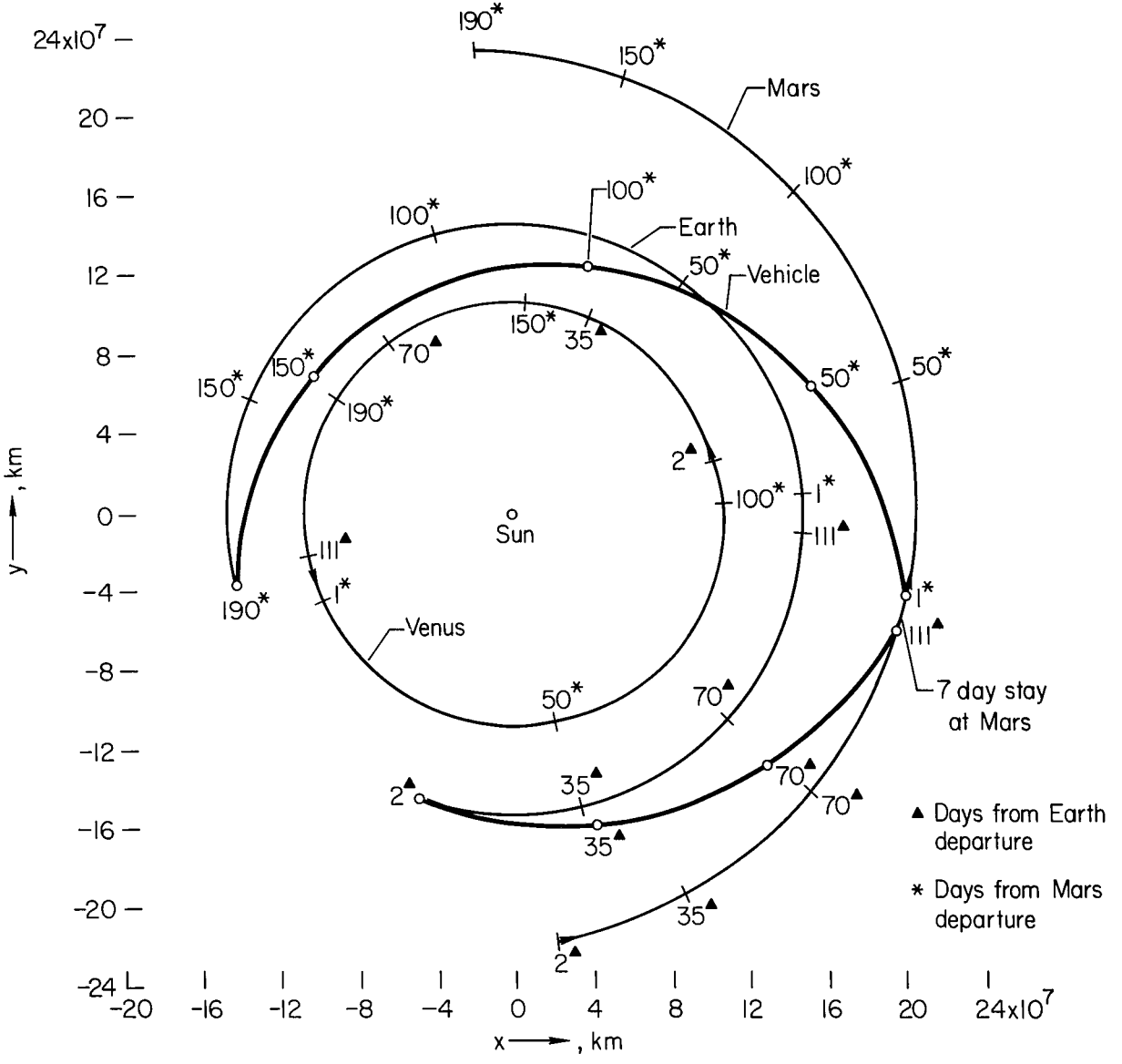

(a) Heliocentric orbit phase.

Figure 2.- Ecliptic projection of planetary and vehicle motion - high-speed trajectory.

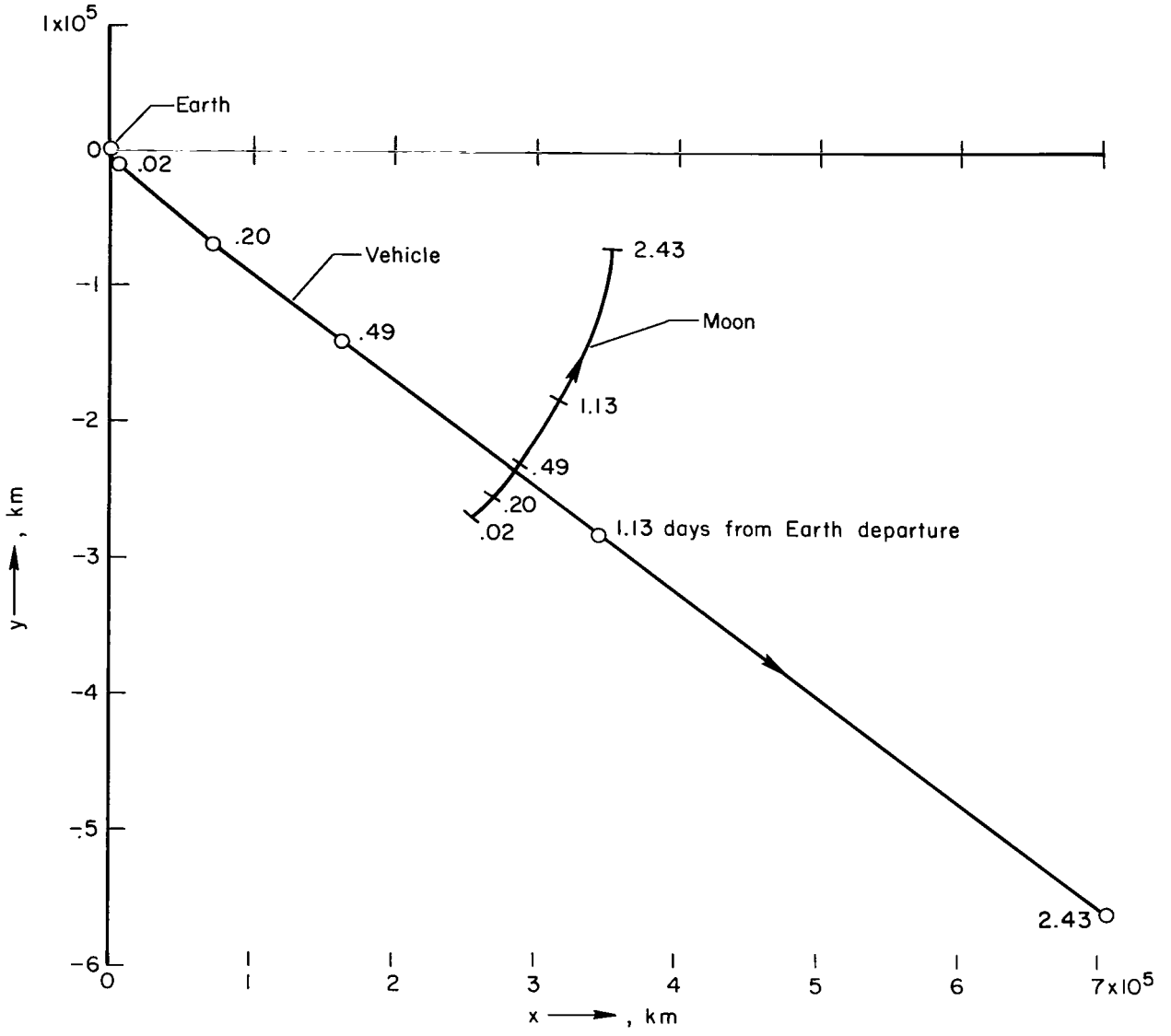

(b) Earth departure phase.

Figure 2.- Continued.

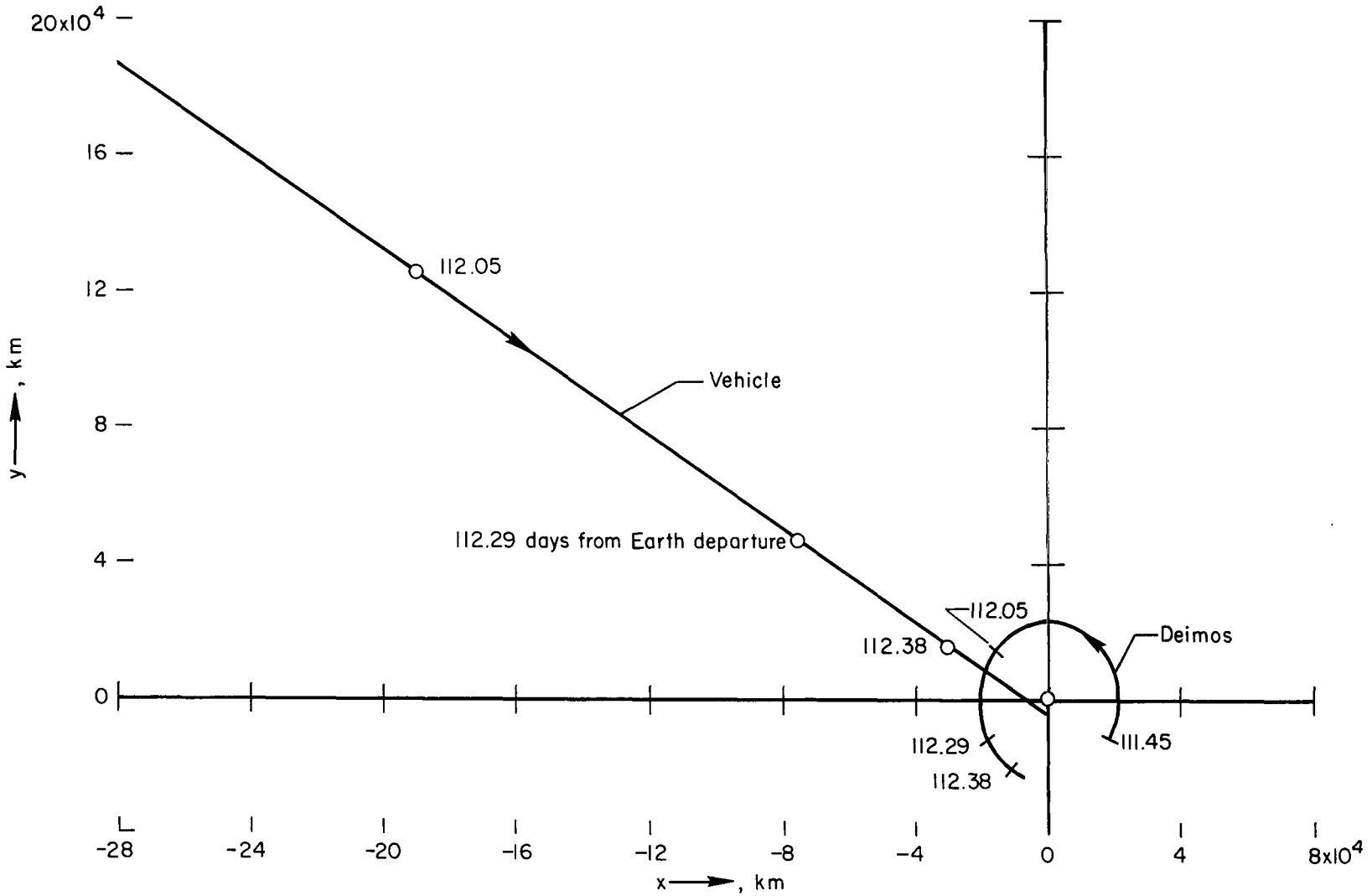

(c) Mars arrival phase.

Figure 2.- Continued.

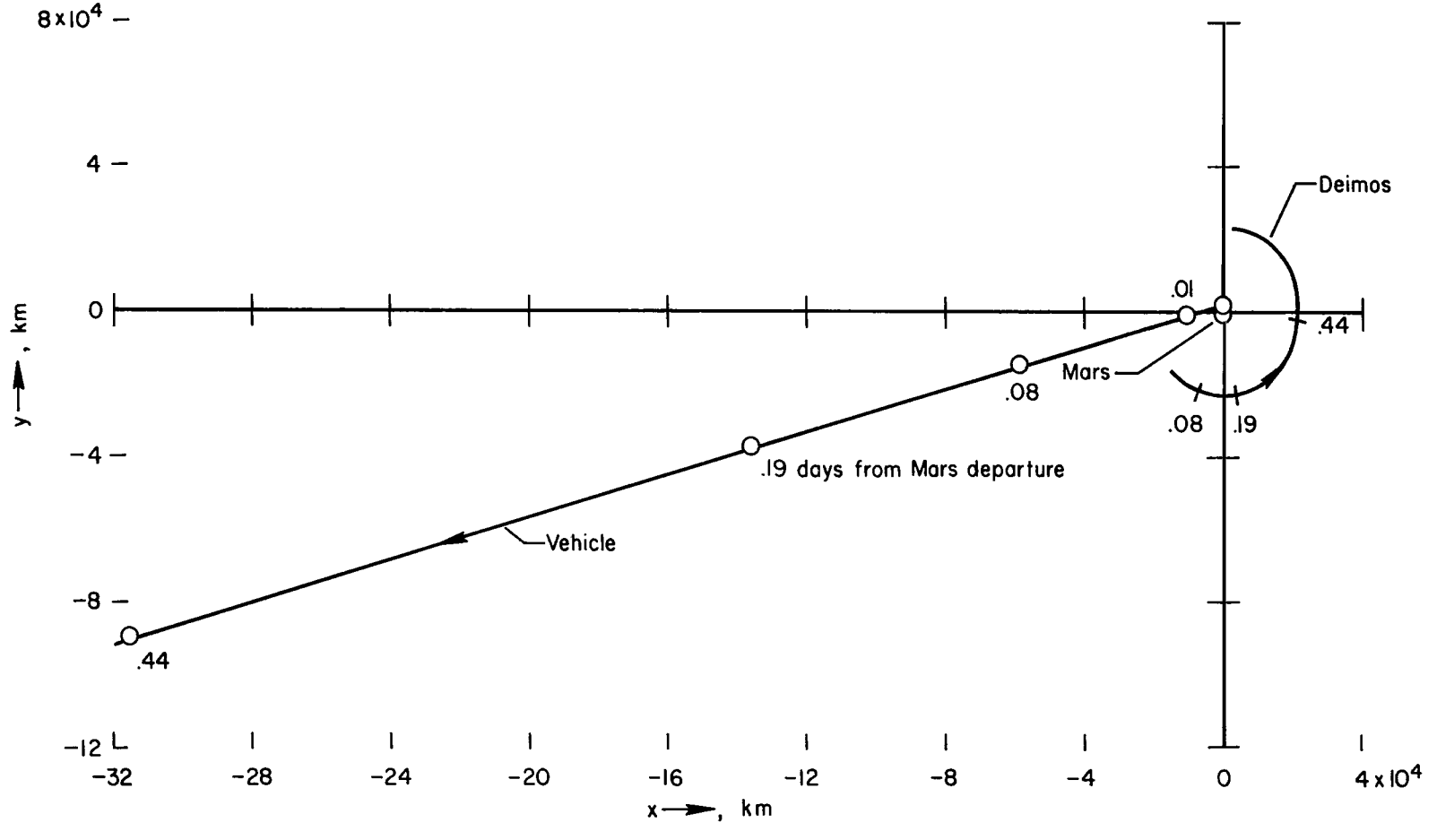

(d) Mars departure phase.

Figure 2.- Continued.

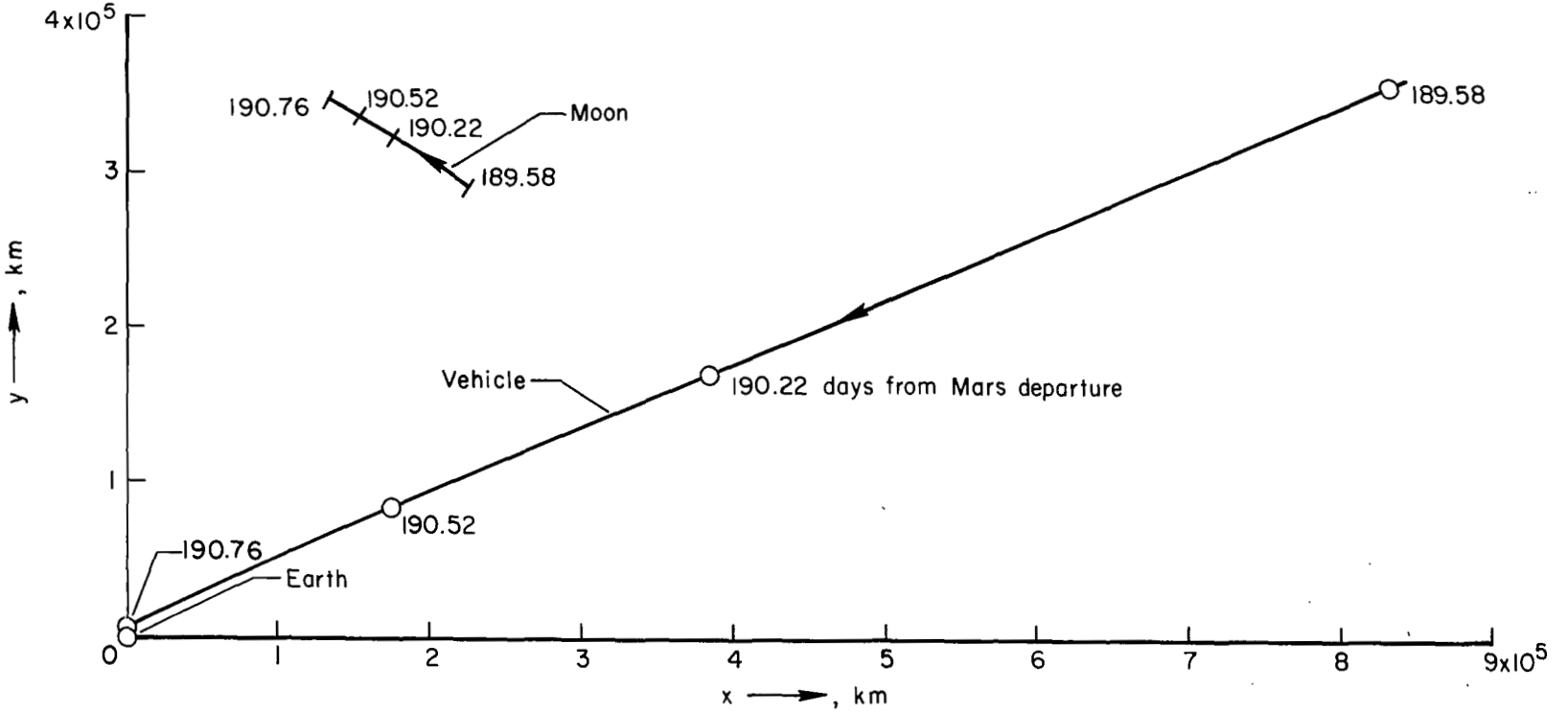

(e) Earth arrival phase.

Figure 2.- Concluded.

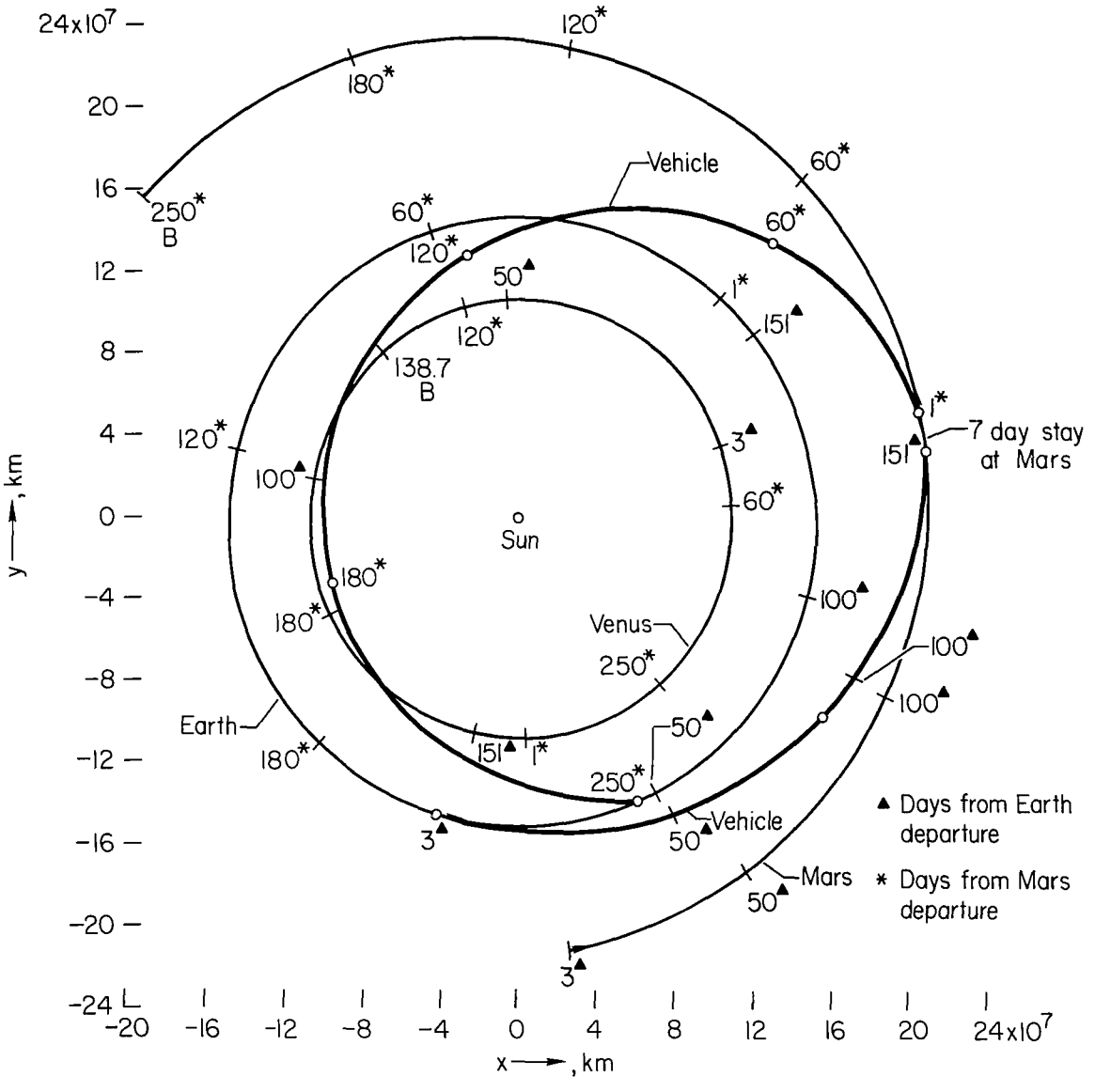

(a) Heliocentric orbit phase.

Figure 3.- Ecliptic projection of planetary and vehicle motion - low-speed trajectory.

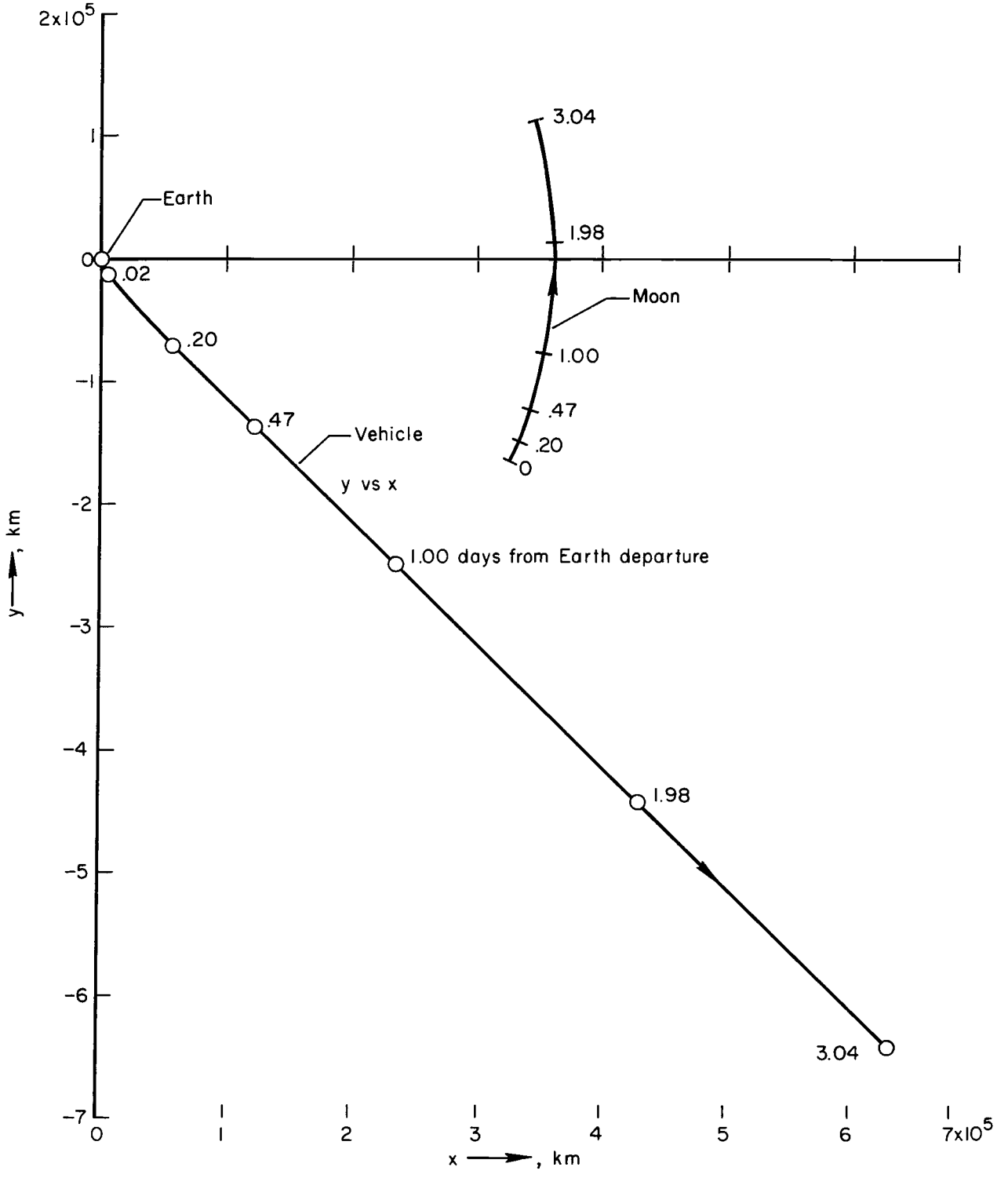

(b) Earth departure phase.

Figure 3.- Continued.

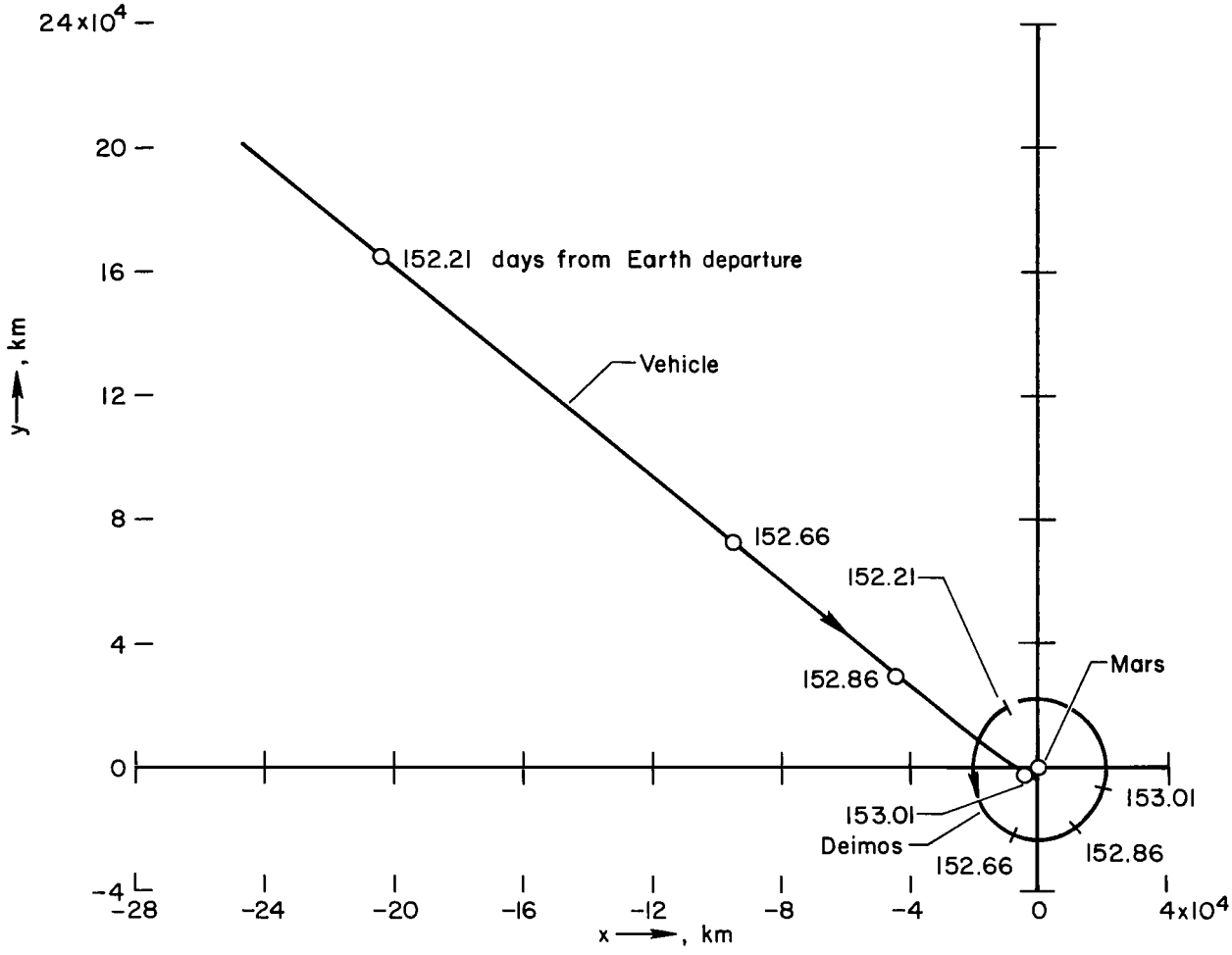

(c) Mars arrival phase.

Figure 3.- Continued.

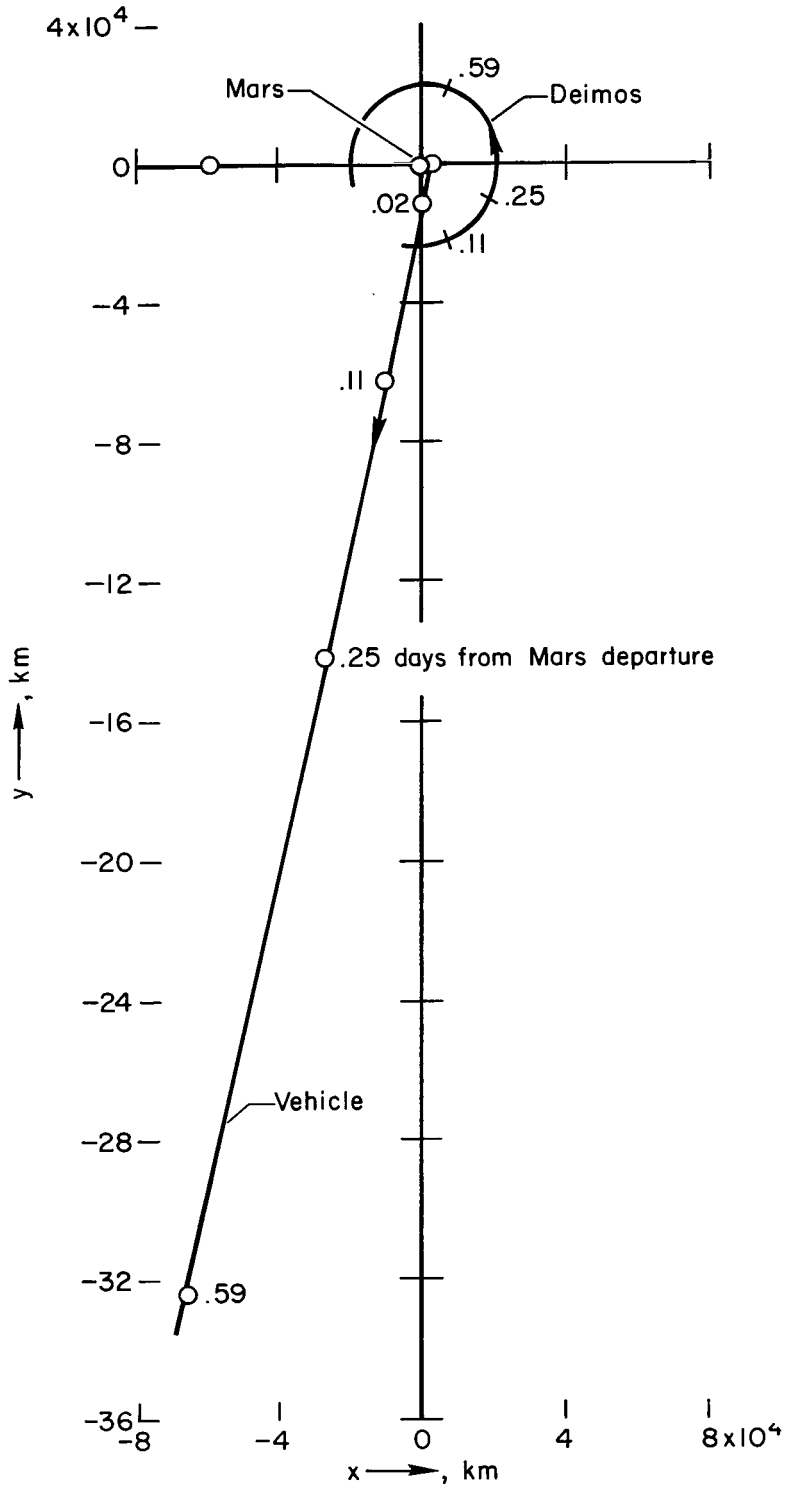

(d) Mars departure phase.

Figure 3.- Continued.

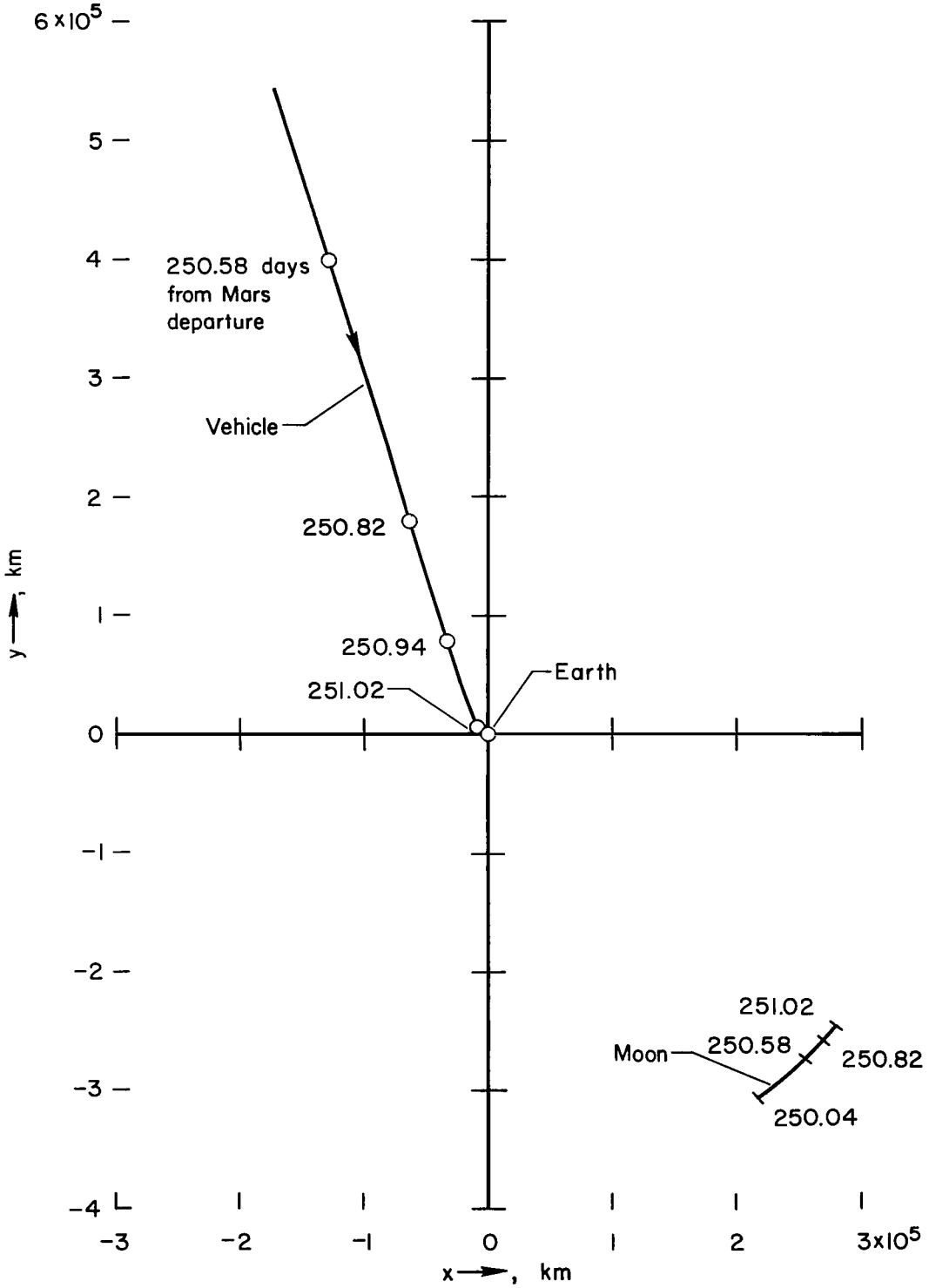

(e) Earth arrival phase.

Figure 3.- Concluded.

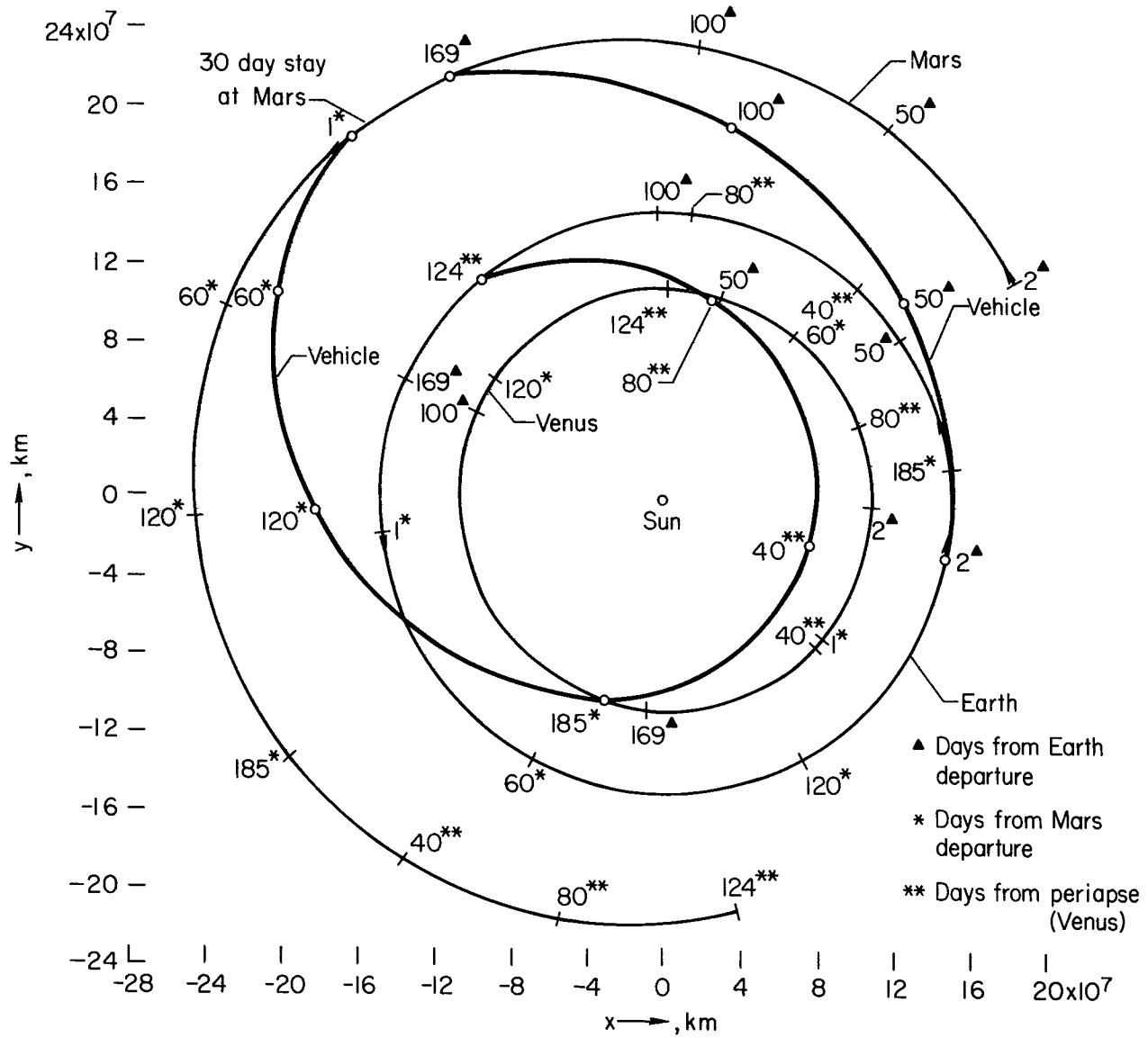

(a) Heliocentric orbit phase.

Figure 4.- Ecliptic projection of planetary and vehicle motion - Venus swingby trajectory.

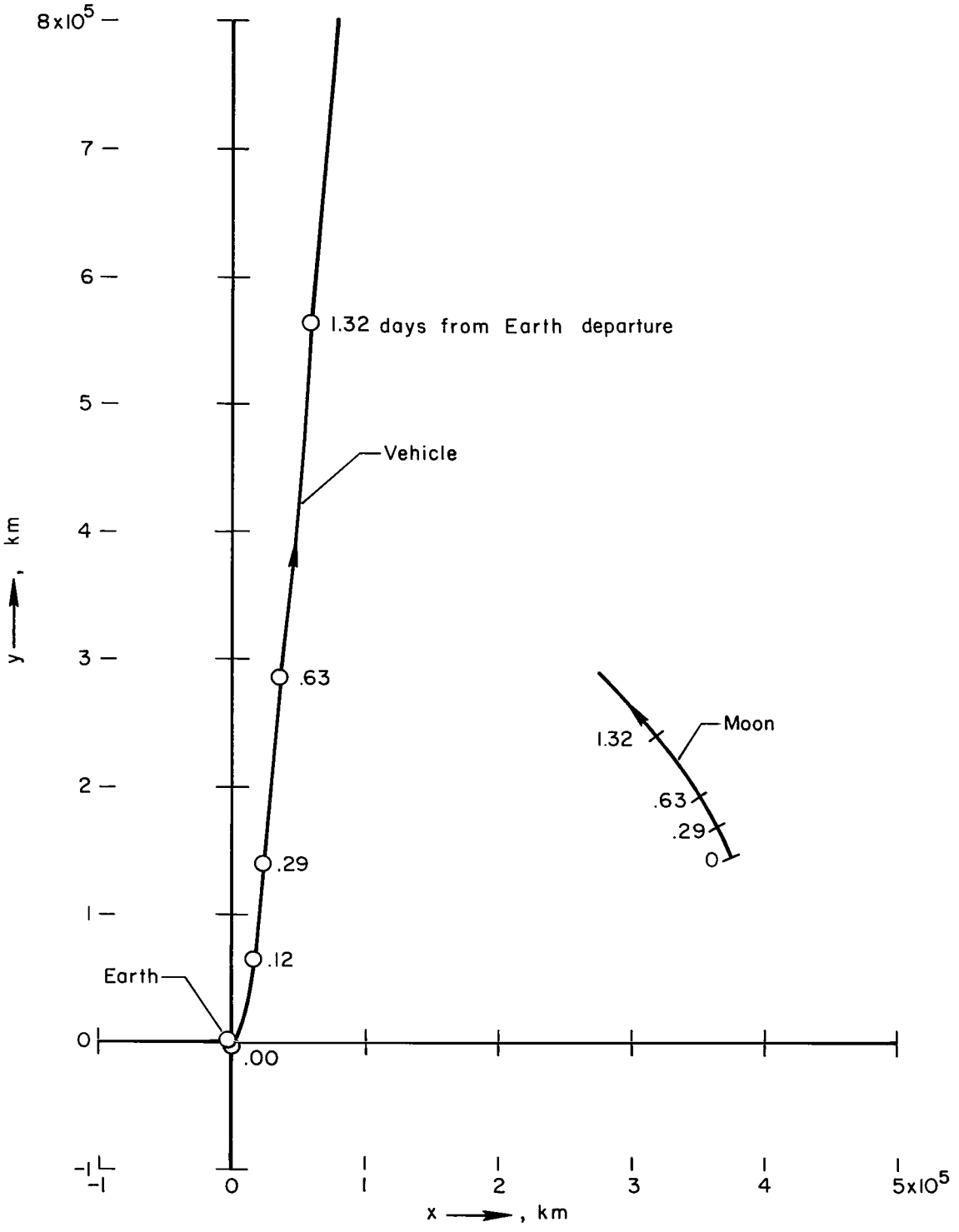

(b) Earth departure phase.

Figure 4.- Continued.

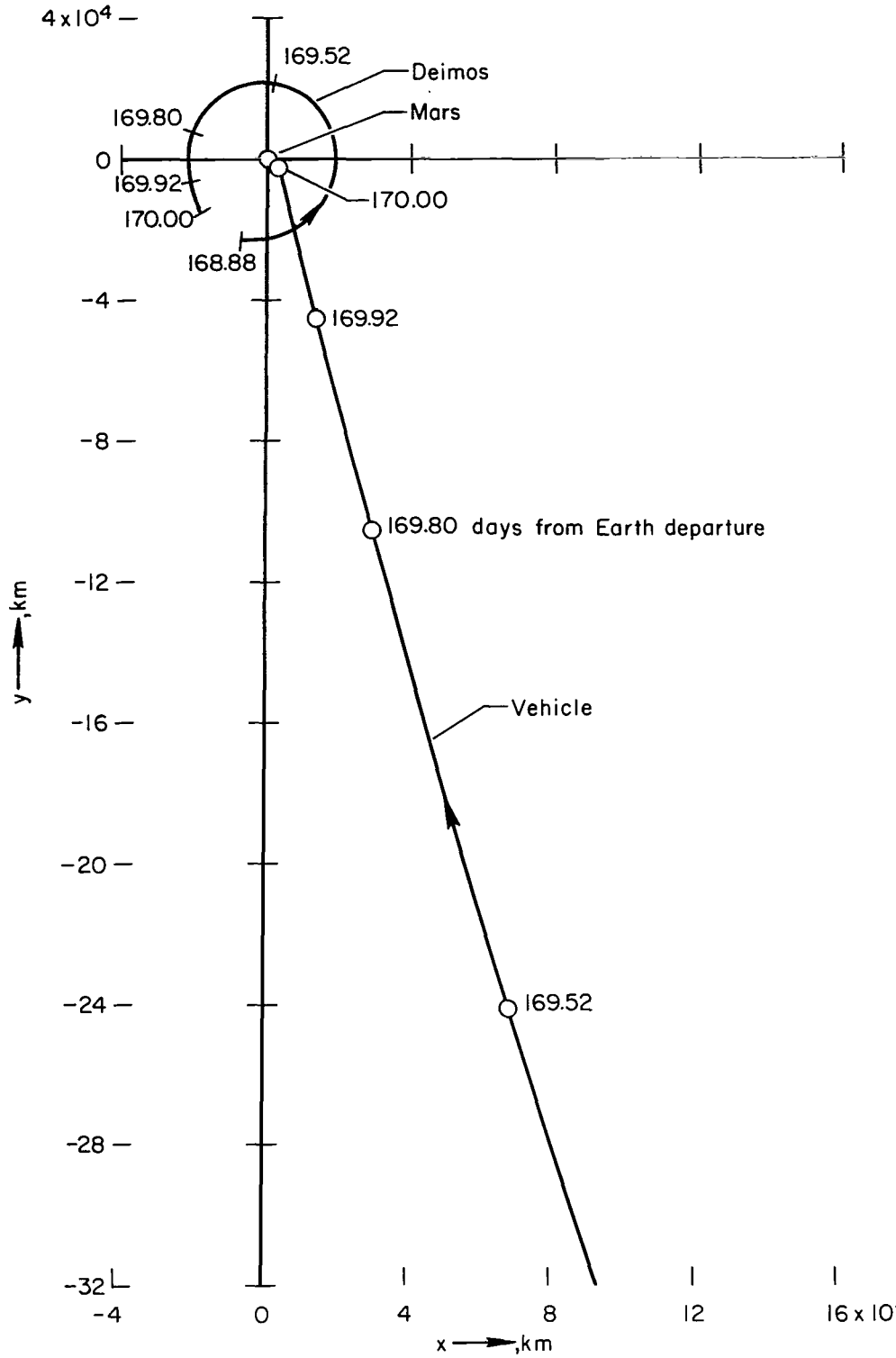

(c) Mars arrival phase.

Figure 4.- Continued.

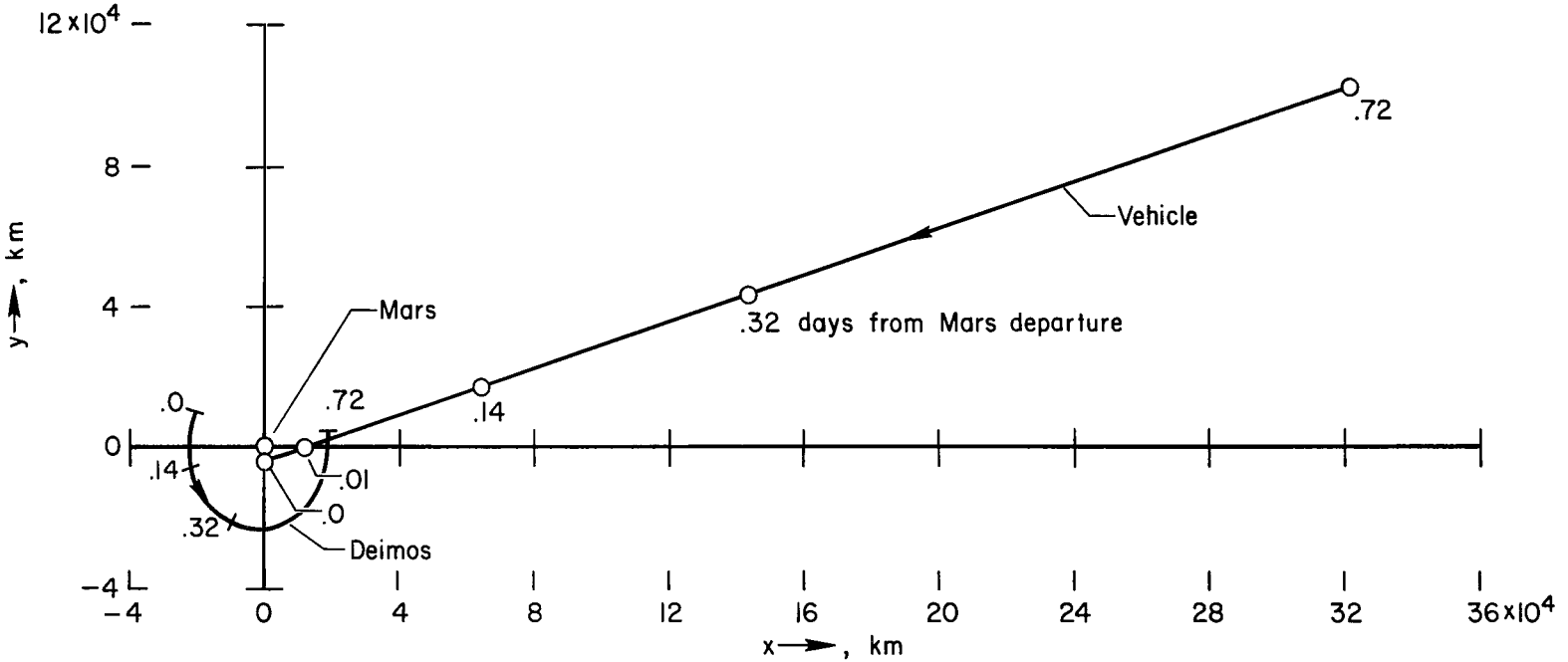

(d) Mars departure phase.

Figure 4.- Continued.

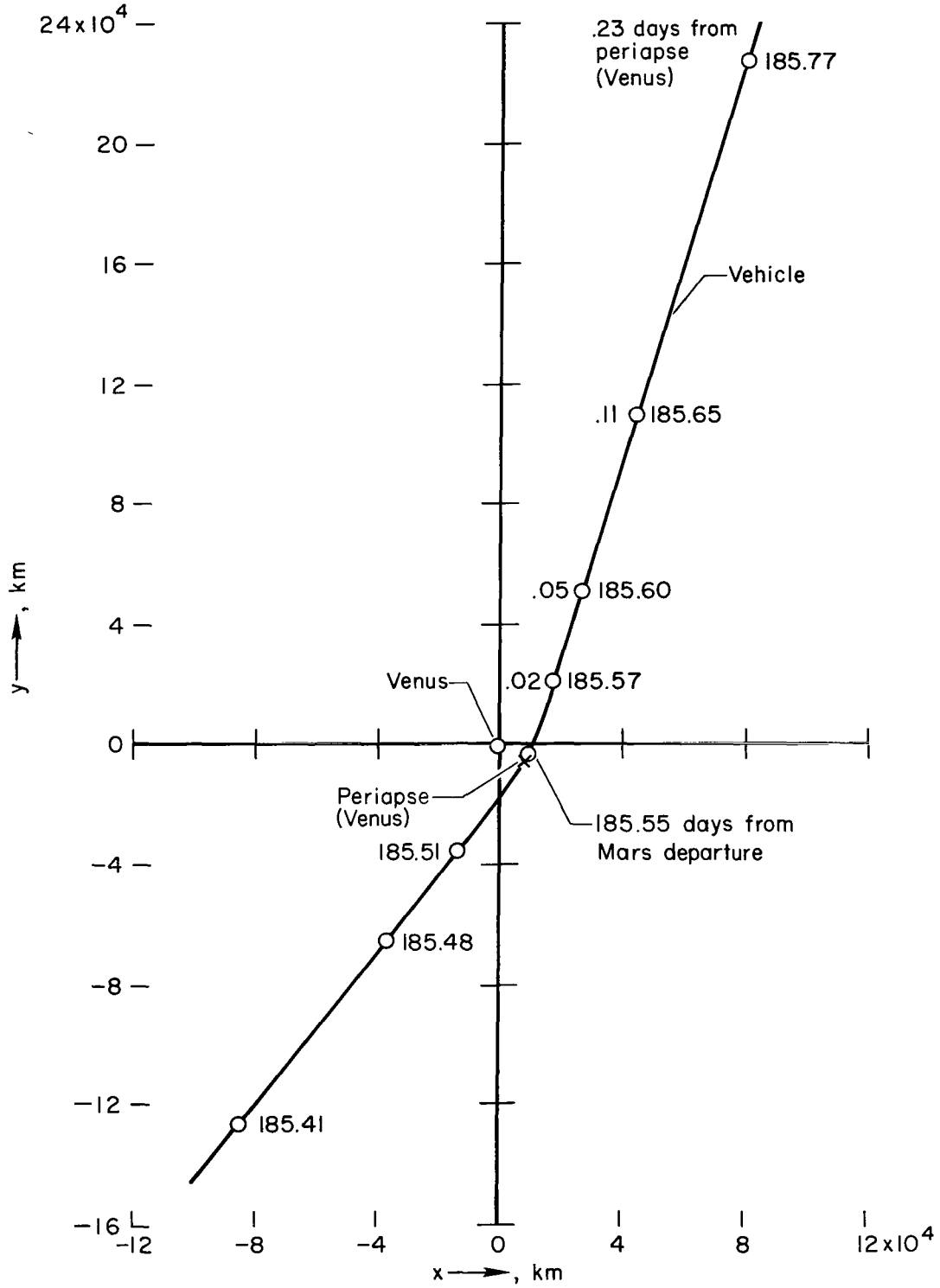

(e) Venus passage phase.

Figure 4.- Continued.

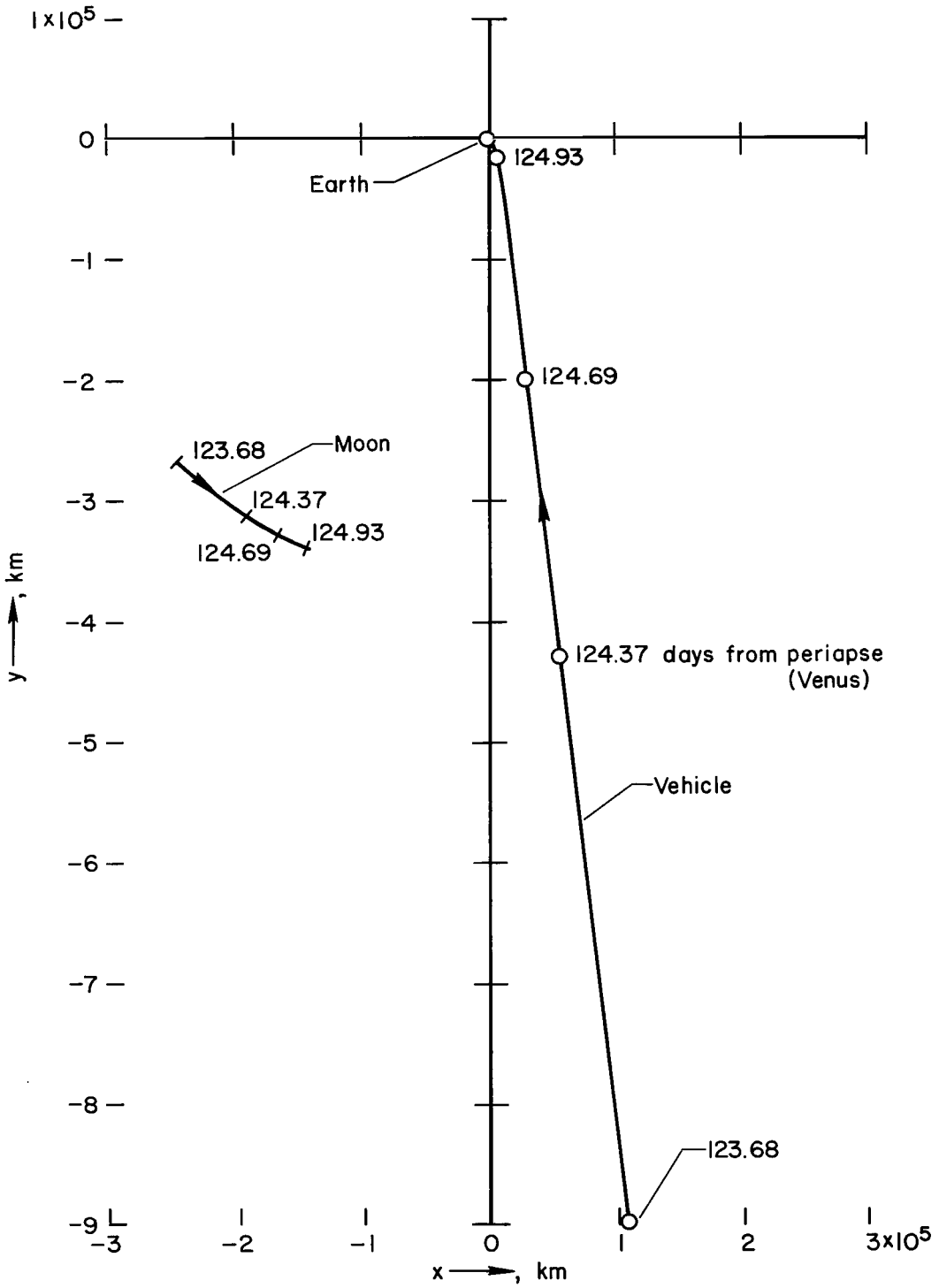

(f) Earth arrival phase.

Figure 4.- Concluded.

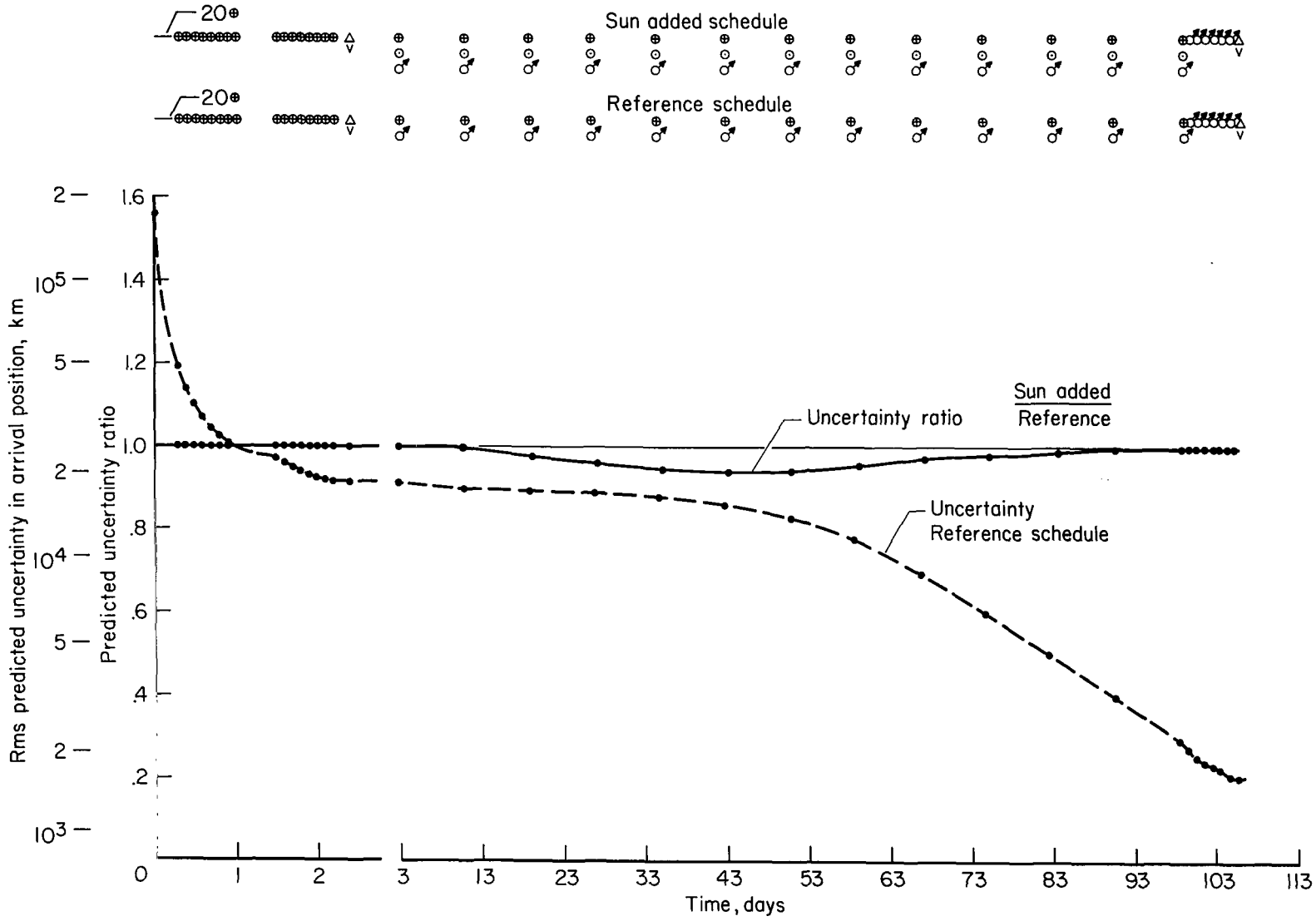

(a) Outbound leg.

Figure 5.- Effect of solar observations - high-speed mission.

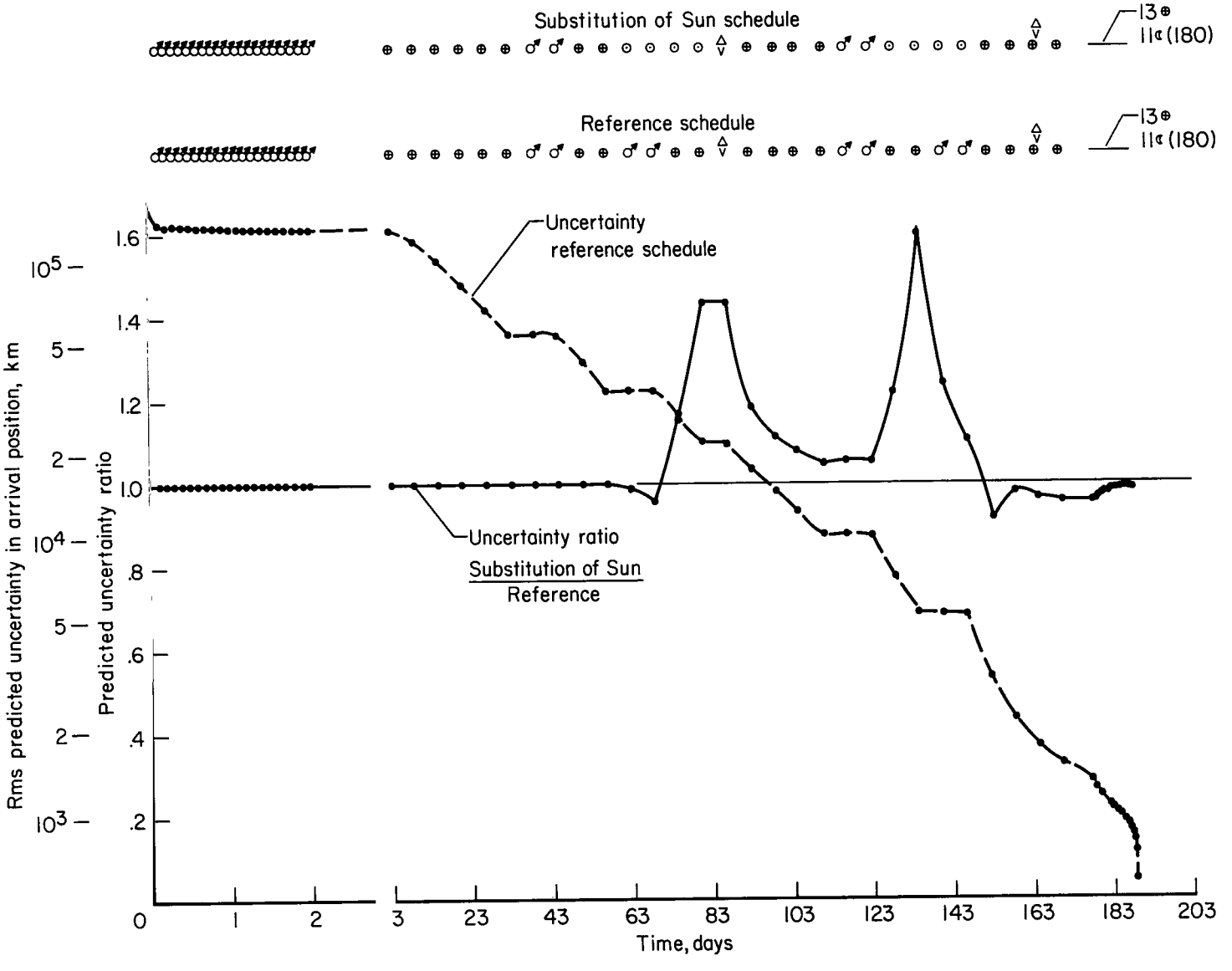

(b) Return leg.

Figure 5.- Concluded.

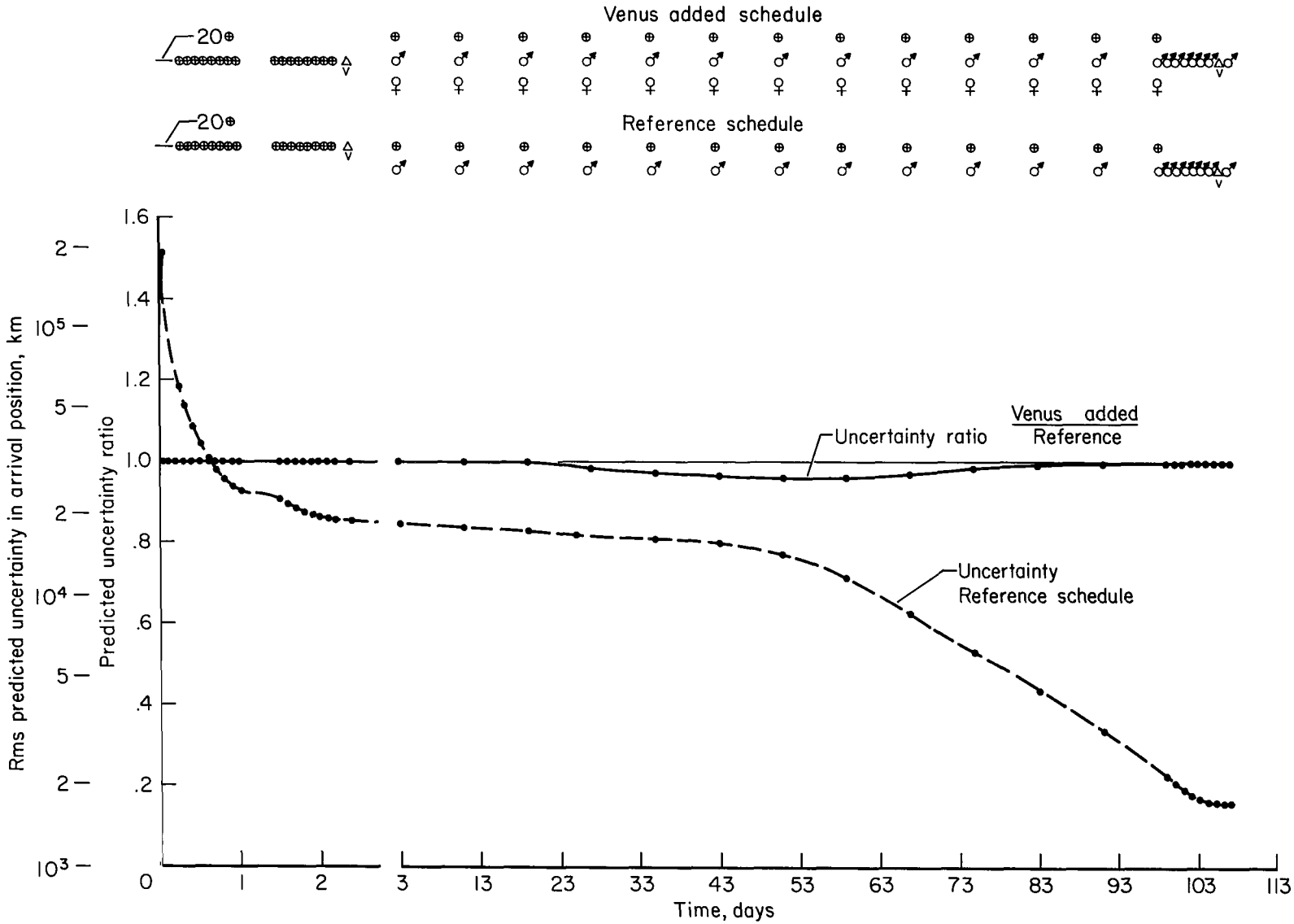

(a) Outbound leg.

Figure 6.- Effect of planetary observations - high-speed mission.

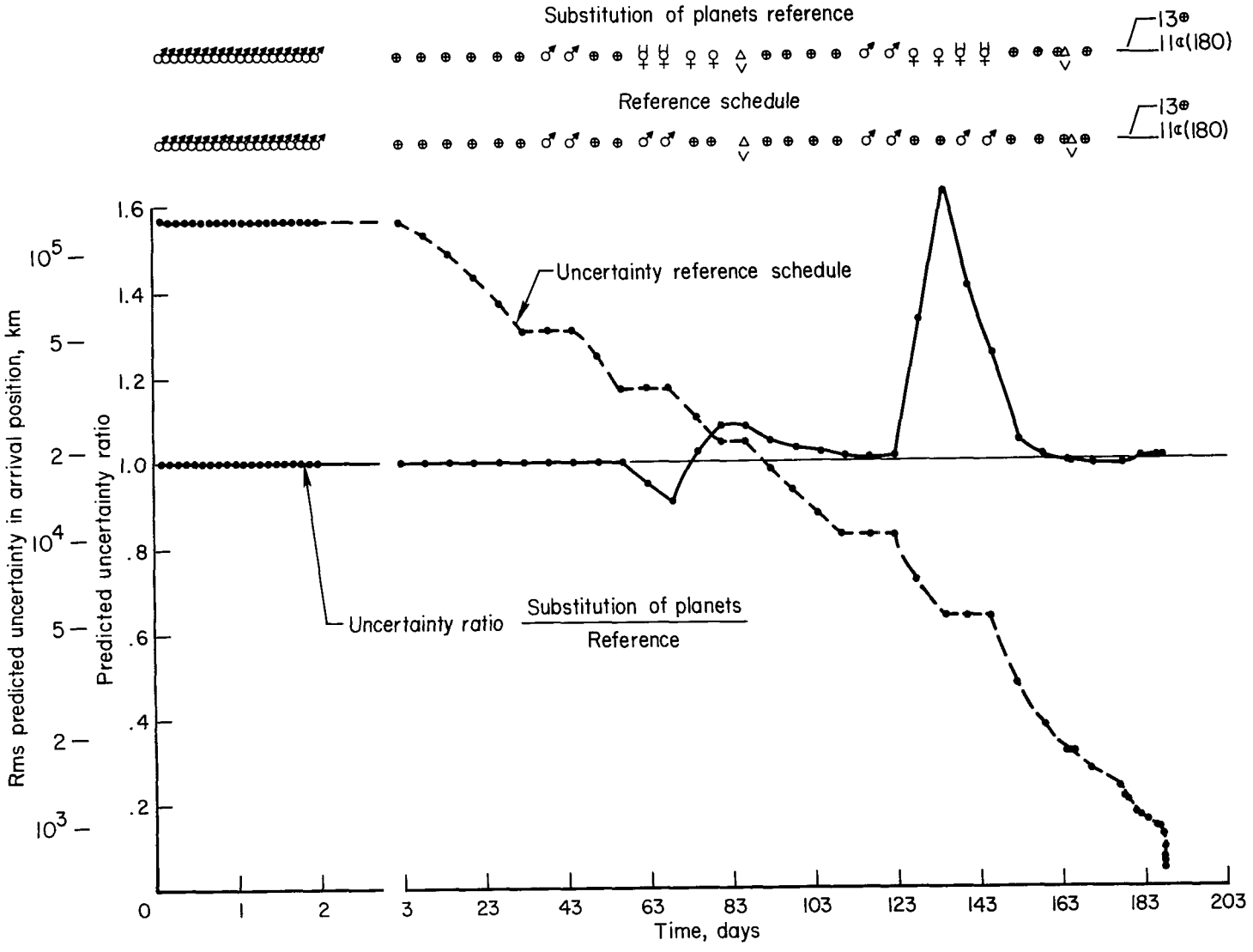

(b) Return leg.

Figure 6.- Concluded.

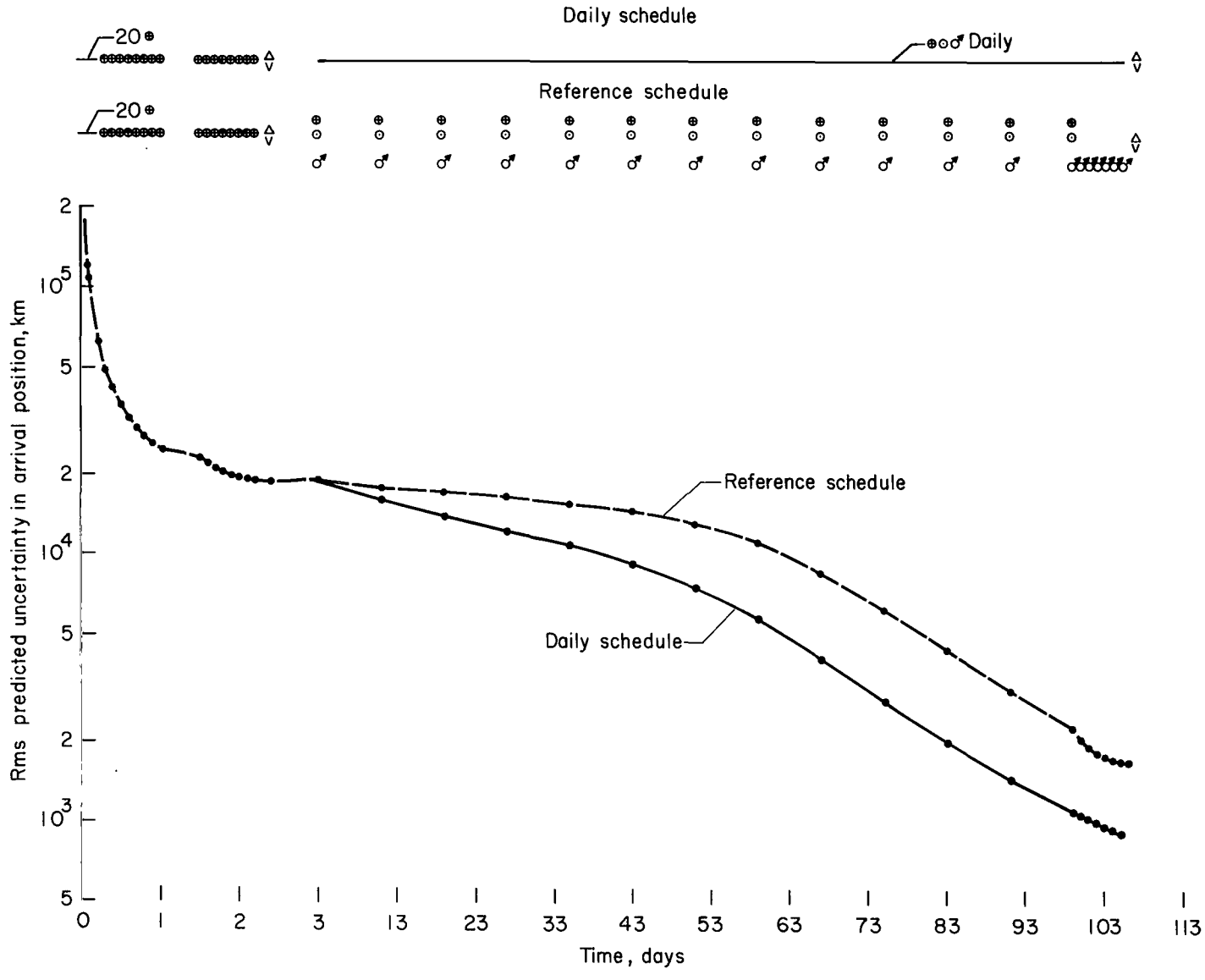

(a) Outbound leg.

Figure 7.- Effect of daily observations - high-speed mission.

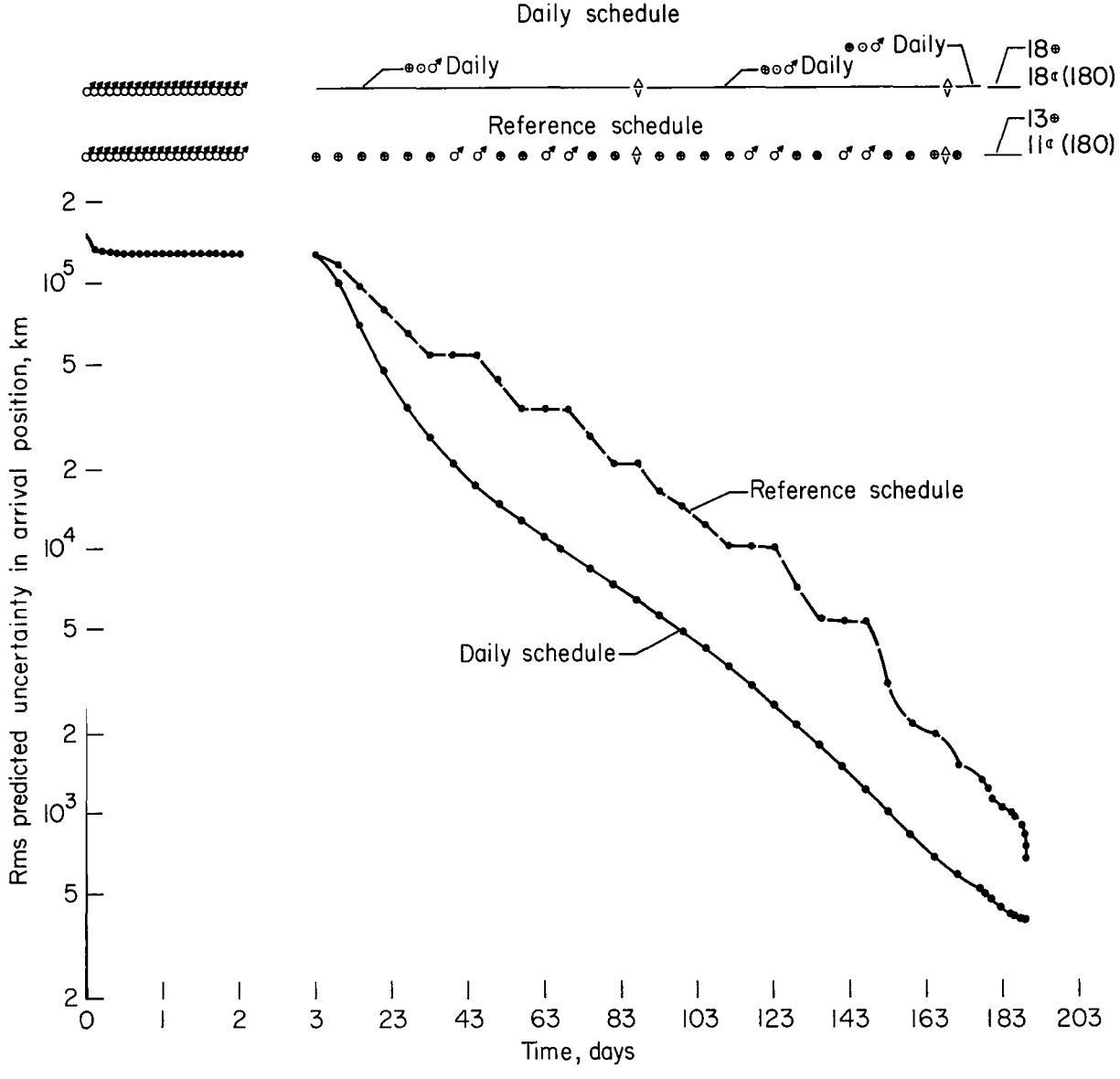

(b) Return leg.

Figure 7.- Concluded.

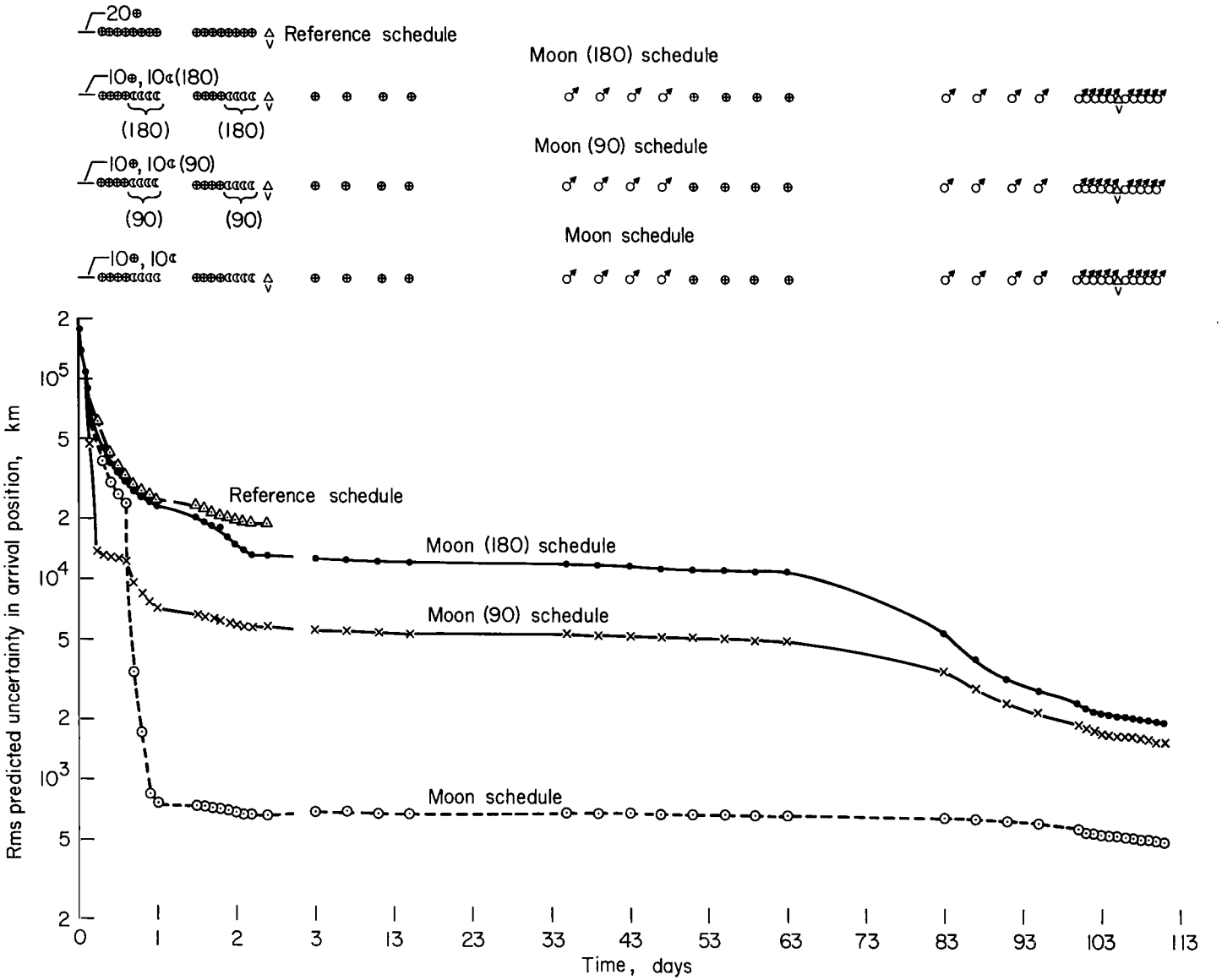

Figure 8.- Effect of Moon observations when leaving Earth - high-speed trajectory.

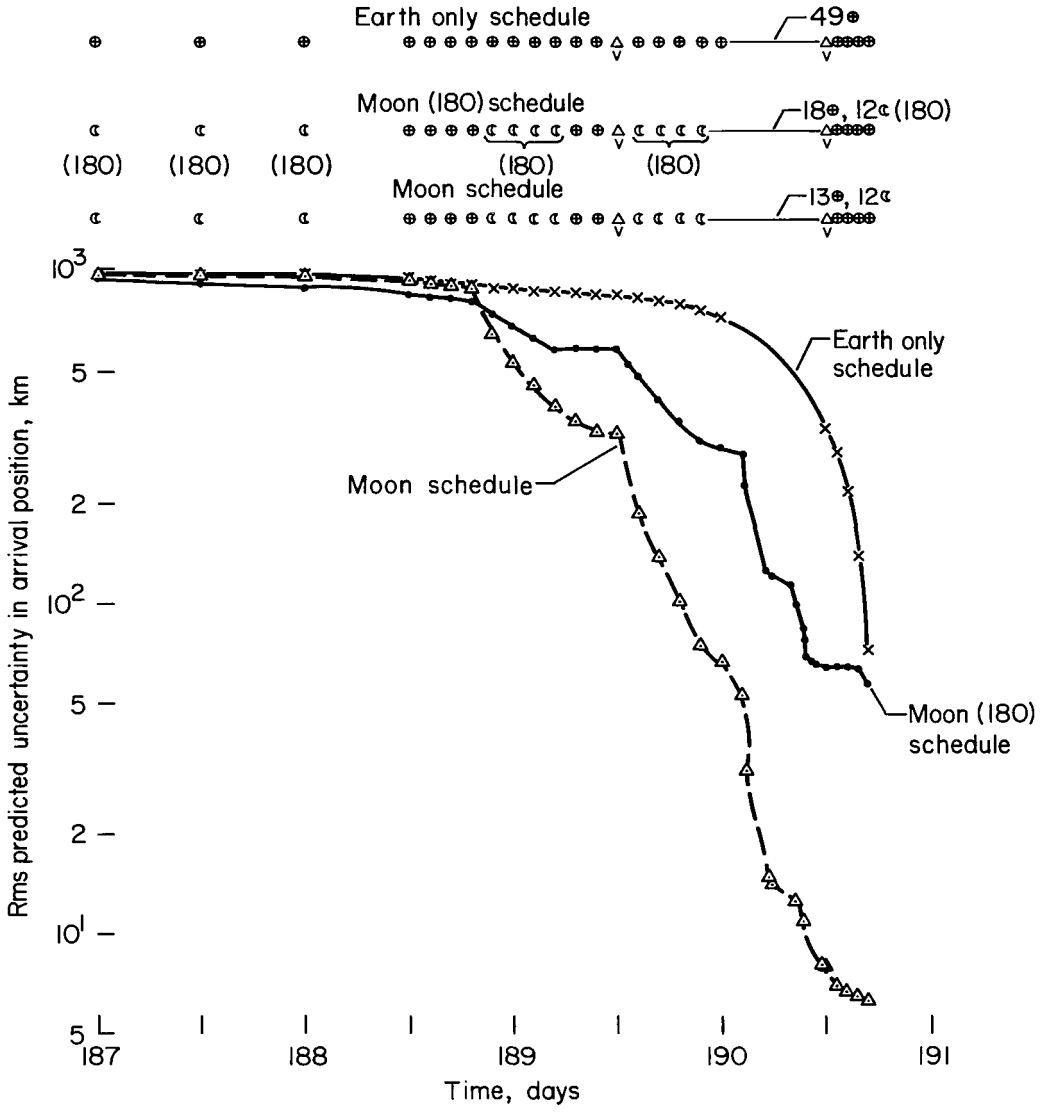

(a) High-speed trajectory.

Figure 9.- Effect of Moon observations on approaching Earth.

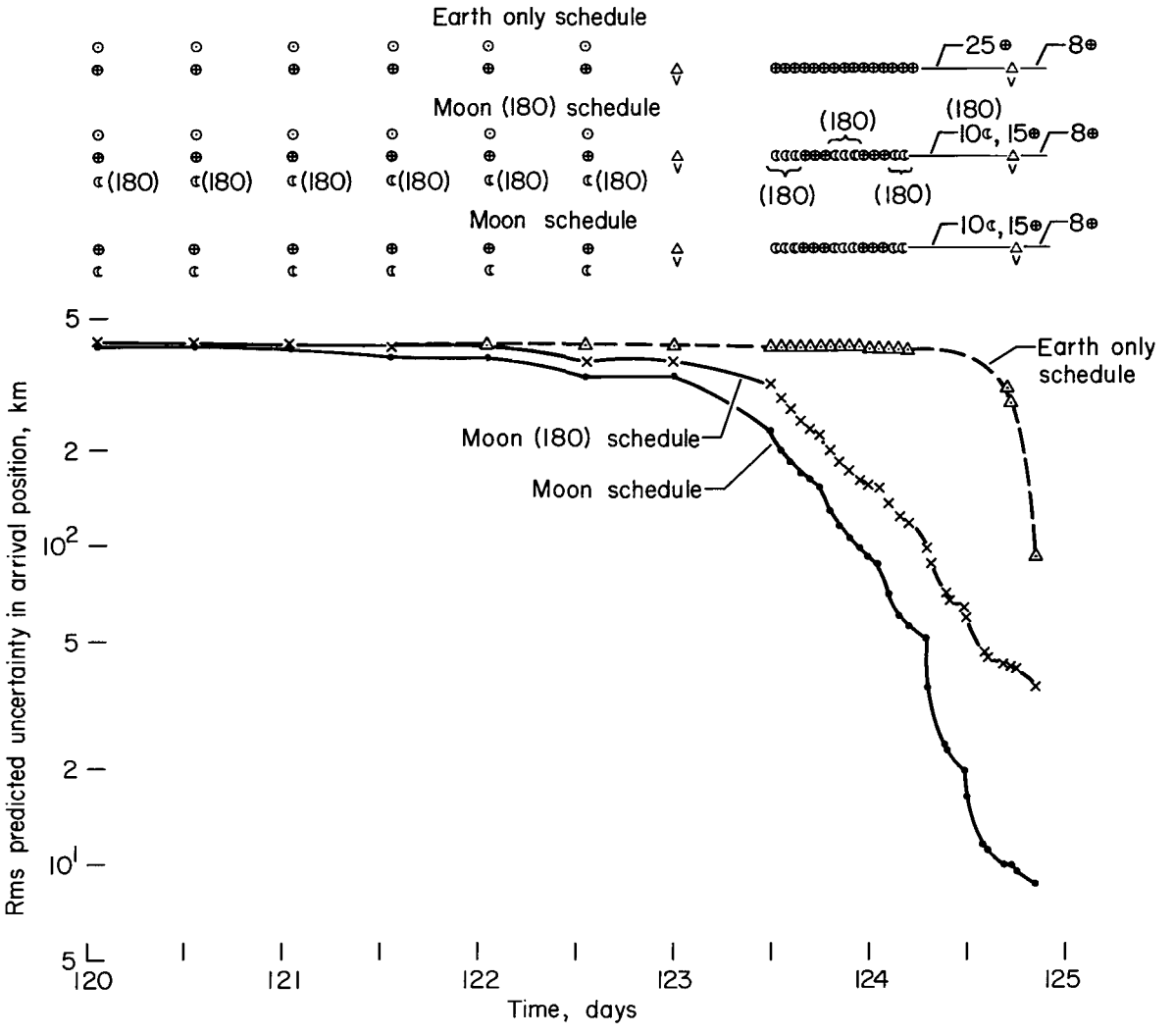

(b) Venus swingby trajectory.

Figure 9.- Concluded.

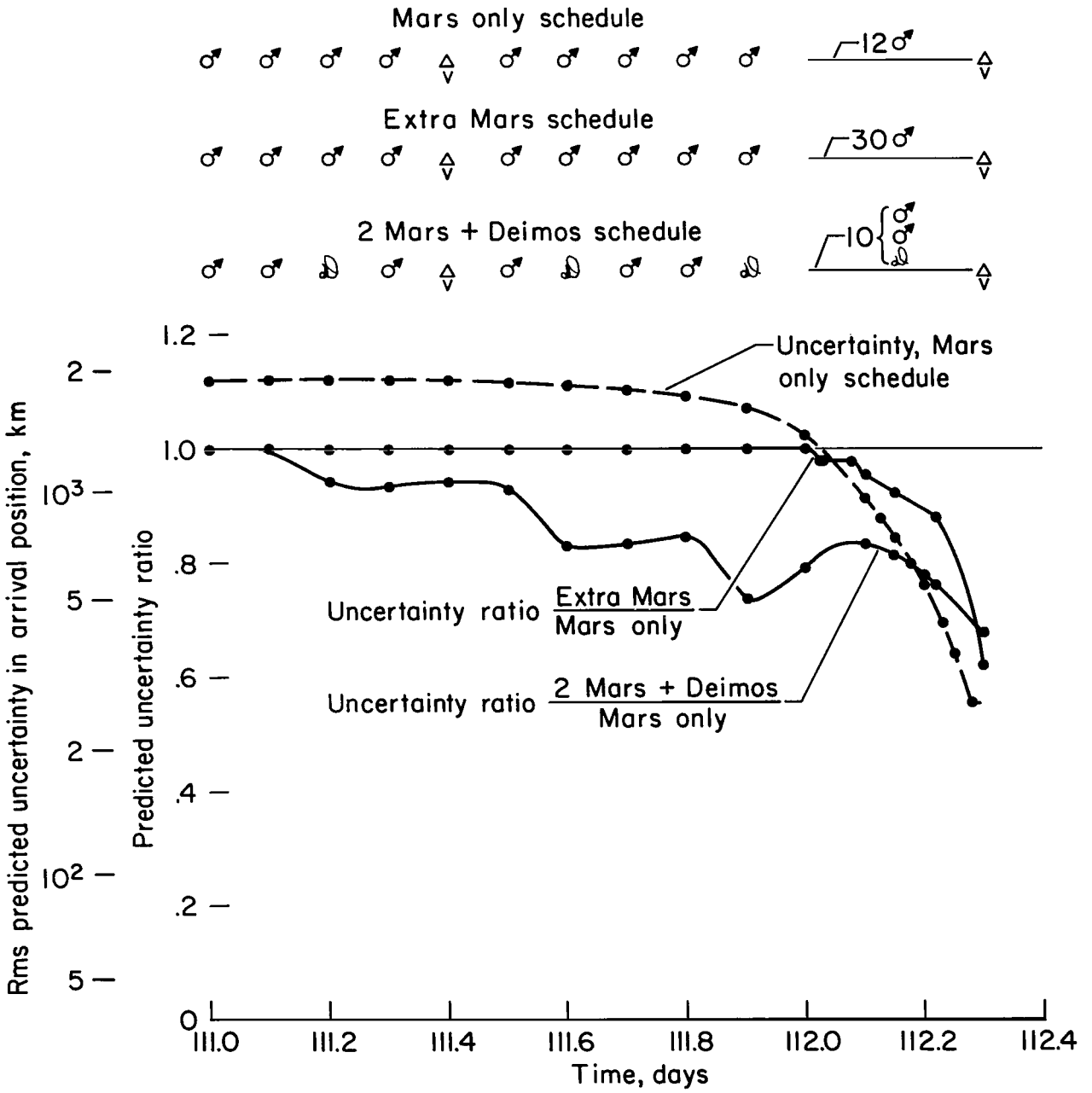

(a) 100 km position uncertainty.

Figure 10.- Effect of observing Deimos and Phobos on approaching Mars - high-speed trajectory.

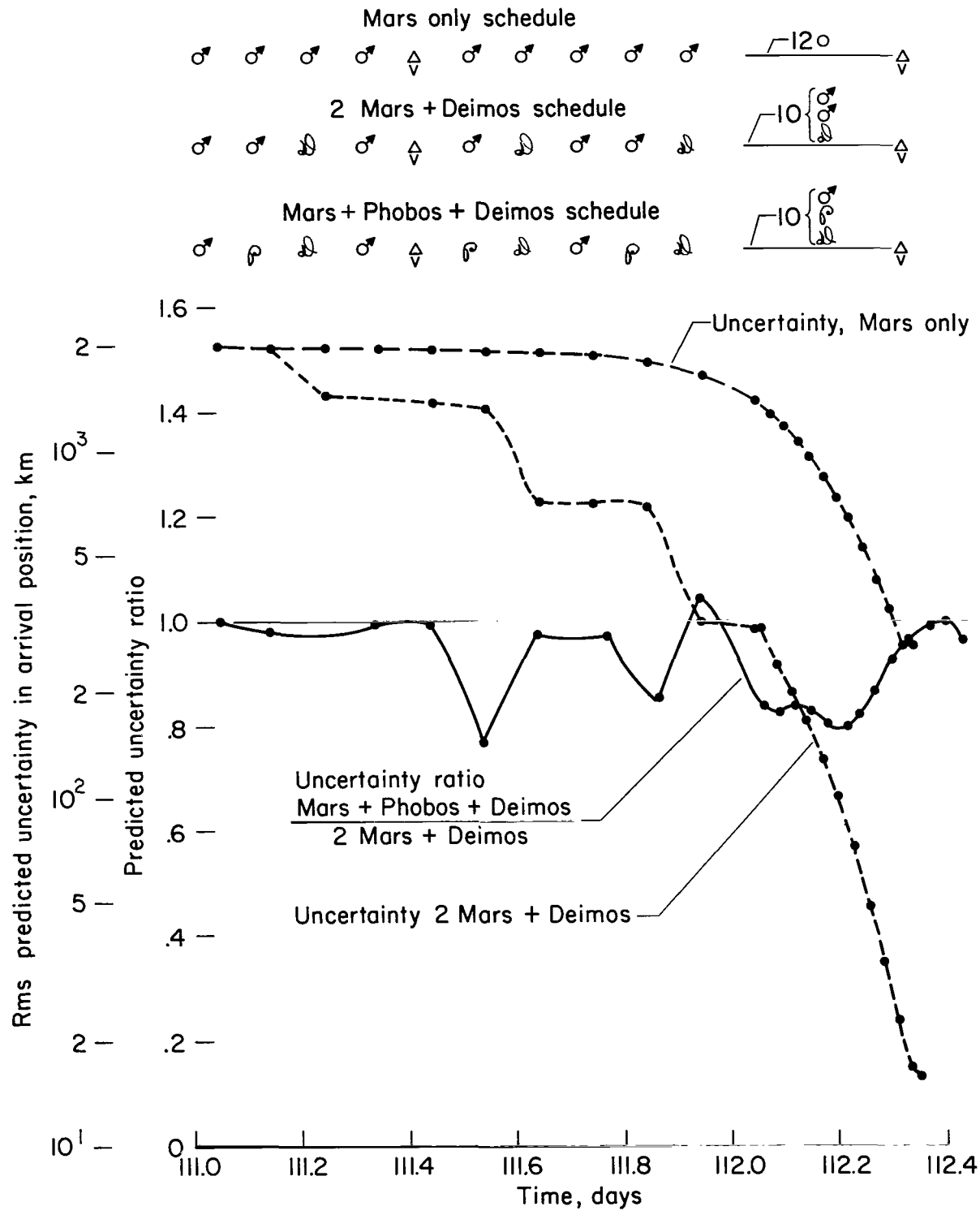

(b) 1 km position uncertainty.

Figure 10.- Concluded.

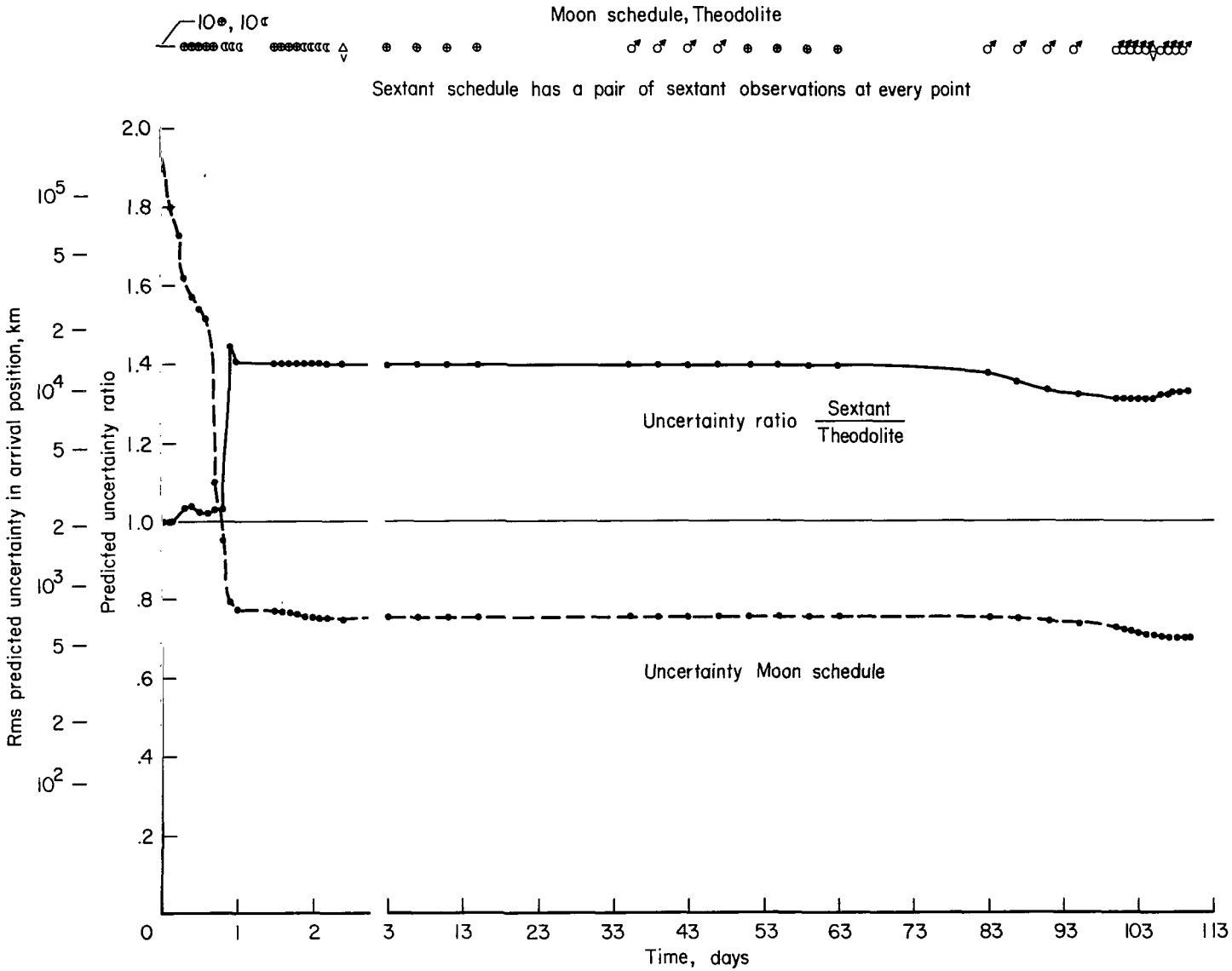

(a) Moon schedule.

Figure 11.- Comparison of theodolite and sextant observations.

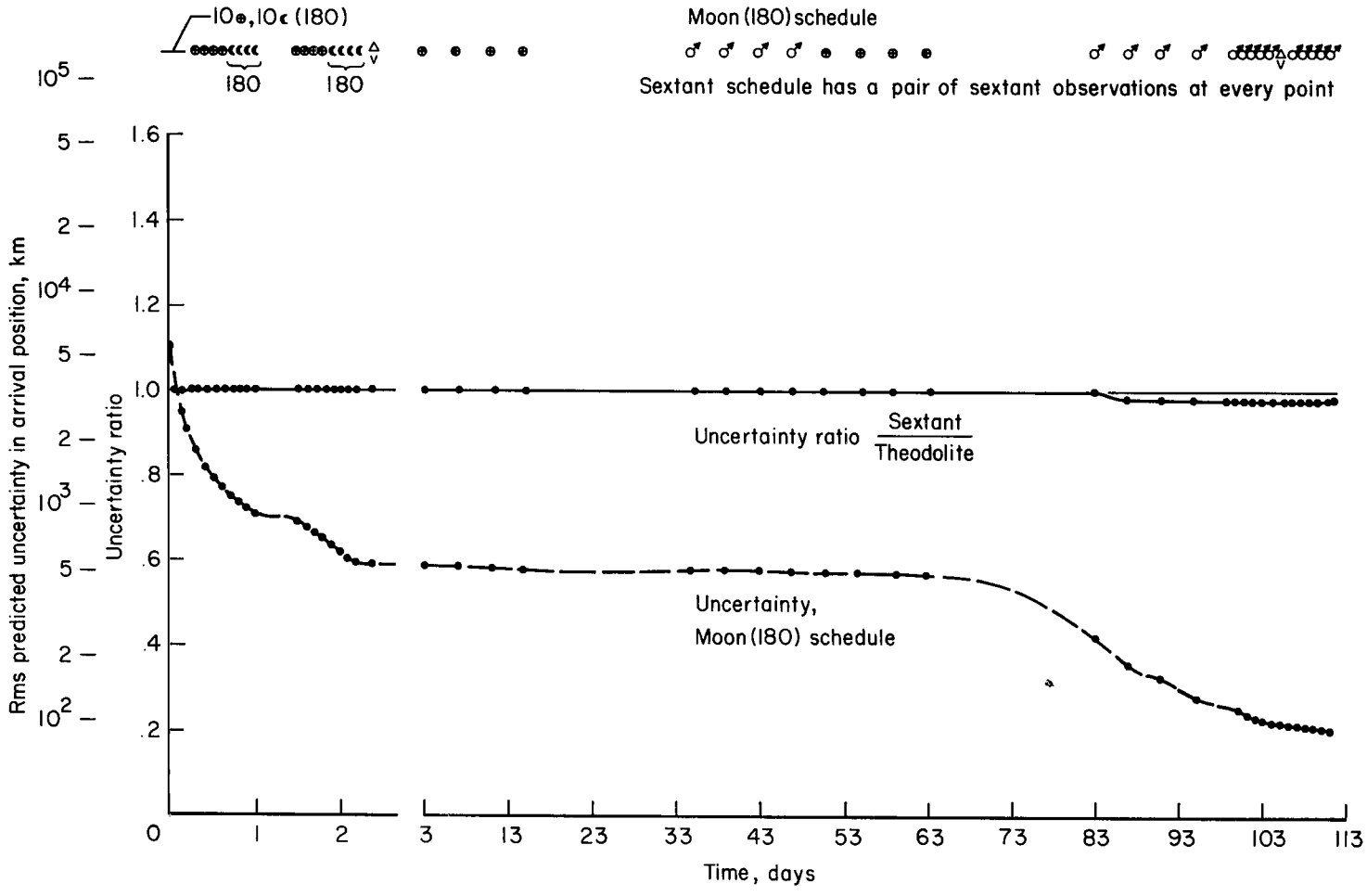

(b) Moon (180) schedule.

Figure 11.- Concluded.

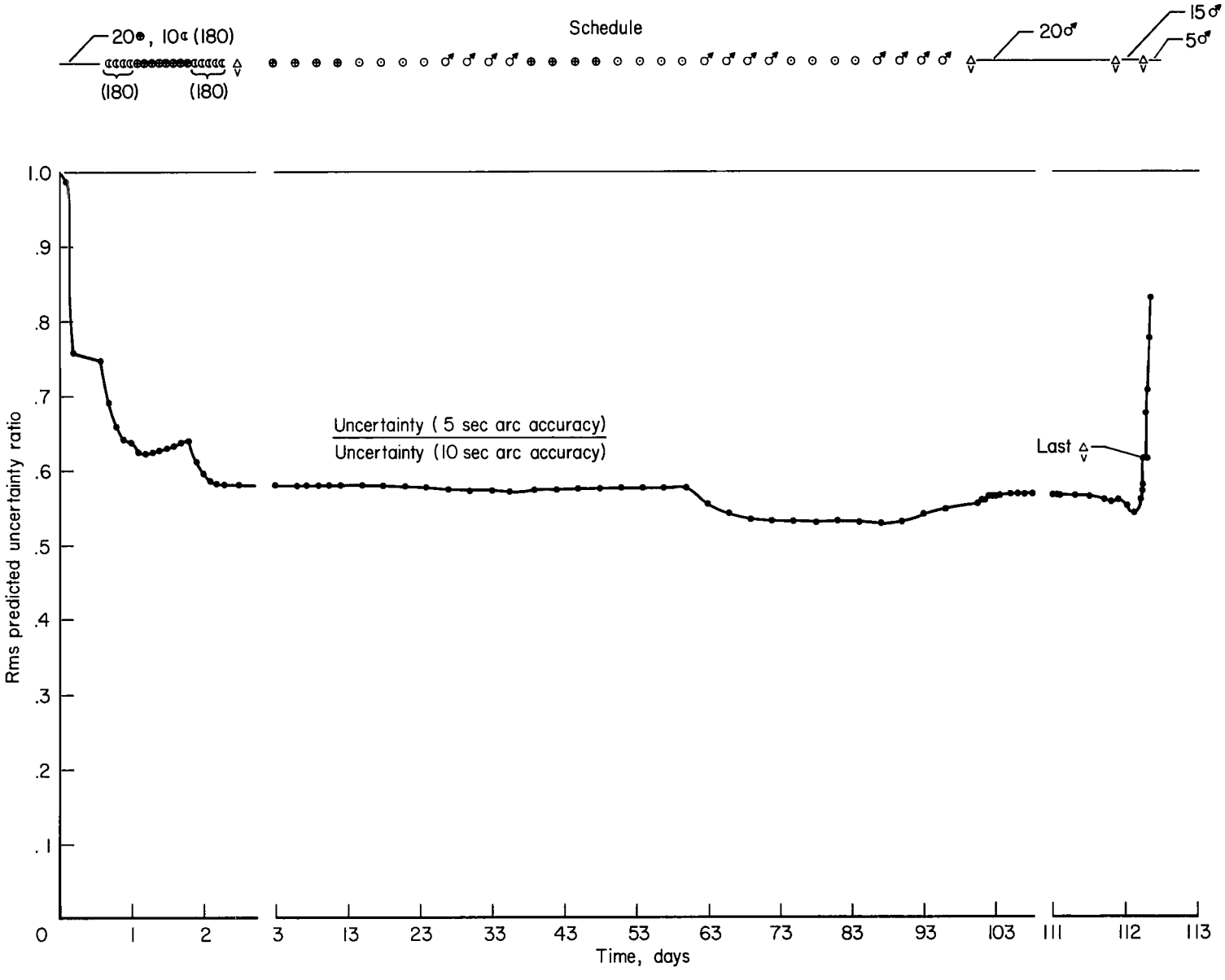

Figure 12.- Effect of sighting accuracy.

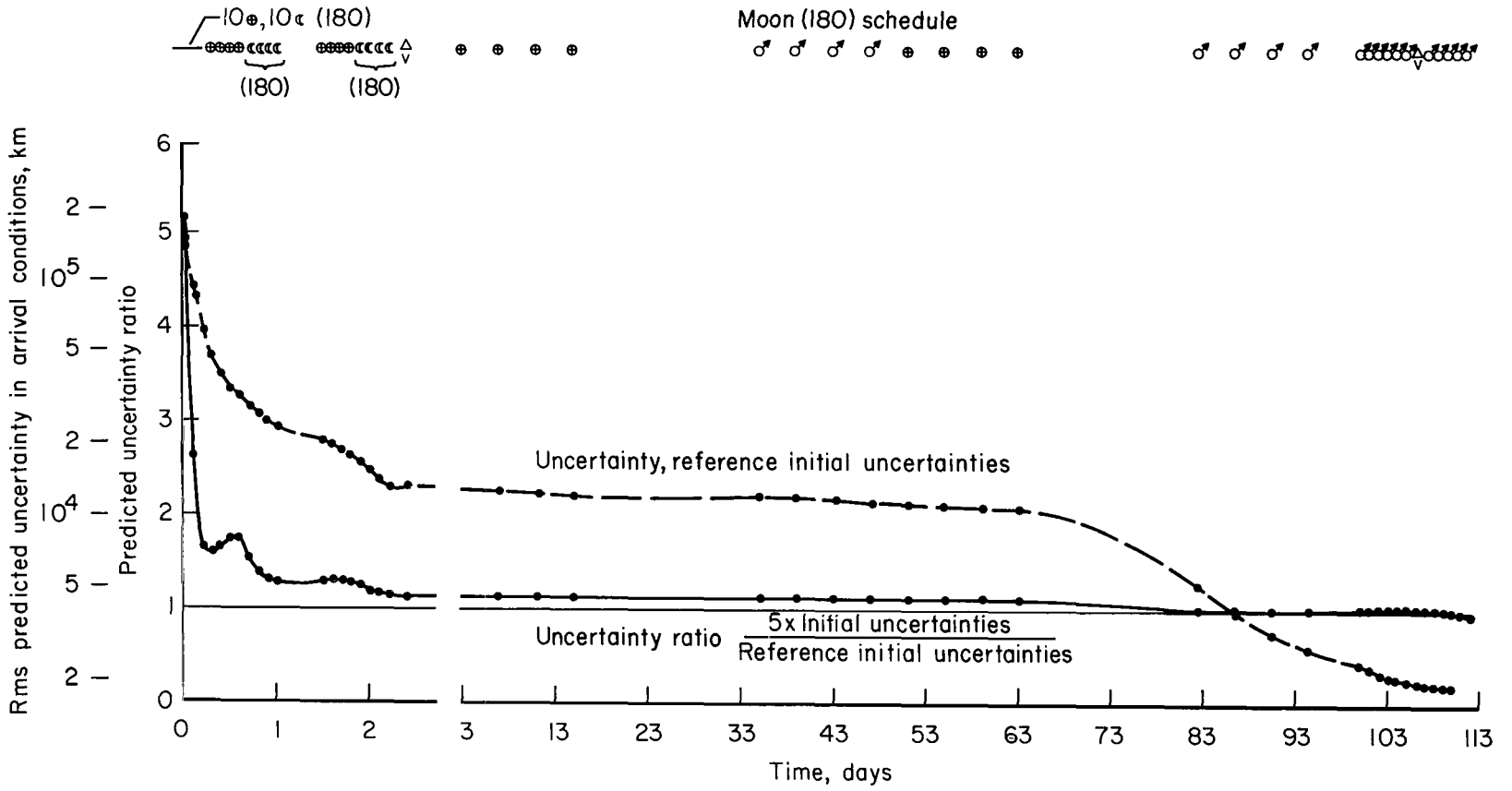

Figure 13.- Effect of varying initial uncertainty.

2/22/85

"The aeronautical and space activities of the United States shall be conducted so as to contribute . . . to the expansion of human knowledge of phenomena in the atmosphere and space. The Administration shall provide for the widest practicable and appropriate dissemination of information concerning its activities and the results thereof."

—NATIONAL AERONAUTICS AND SPACE ACT OF 1958

NASA SCIENTIFIC AND TECHNICAL PUBLICATIONS

TECHNICAL REPORTS: Scientific and technical information considered important, complete, and a lasting contribution to existing knowledge.

TECHNICAL NOTES: Information less broad in scope but nevertheless of importance as a contribution to existing knowledge.

TECHNICAL MEMORANDUMS: Information receiving limited distribution because of preliminary data, security classification, or other reasons.

CONTRACTOR REPORTS: Technical information generated in connection with a NASA contract or grant and released under NASA auspices.

TECHNICAL TRANSLATIONS: Information published in a foreign language considered to merit NASA distribution in English.

TECHNICAL REPRINTS: Information derived from NASA activities and initially published in the form of journal articles.

SPECIAL PUBLICATIONS: Information derived from or of value to NASA activities but not necessarily reporting the results of individual NASA-programmed scientific efforts. Publications include conference proceedings, monographs, data compilations, handbooks, sourcebooks, and special bibliographies.

Details on the availability of these publications may be obtained from:

SCIENTIFIC AND TECHNICAL INFORMATION DIVISION

NATIONAL AERONAUTICS AND SPACE ADMINISTRATION

Washington, D.C. 20546